SOMATIC CANCER-DRIVER MUTATIONS IN ENDOMETRIOSIS: IMPLICATIONS BEYOND MALIGNANCY

by

Vivian Lac

BMSc, The University of Western Ontario, 2016

A THESIS SUBMITTED IN PARTIAL FULFILLMENT OF THE REQUIREMENTS FOR THE DEGREE OF

MASTER OF SCIENCE

in

The Faculty of Graduate and Postdoctoral Studies

(Interdisciplinary Oncology)

THE UNIVERSITY OF BRITISH COLUMBIA

(Vancouver)

October 2018

The following individuals certify that they have read, and recommend to the Faculty of Graduate and Postdoctoral Studies for acceptance, a thesis/dissertation entitled:

Somatic cancer-driver mutations in endometriosis: implications beyond malignancy

submitted by	Vivian Lac	in partial fulfillment of the requirements for
the degree of	Master of Science	
In	Interdisciplinary Oncology	

Examining Committee:

David G. Huntsman

Co-supervisor

Michael S. Anglesio

Co-supervisor

Paul J. Yong

Supervisory Committee Member

Cathie Garnis

Additional Examiner

Additional Supervisory Committee Members:

Kelly McNagny

Supervisory Committee Member

Supervisory Committee Member

Abstract

Introduction: Endometriosis is a chronic, inflammatory gynecological disease characterized by the ectopic growth of endometrial-like tissue. Previous studies have established endometriosis as the precursor to clear cell and endometrioid ovarian carcinomas. The presence of somatic driver mutations in endometriosis is believed to represent early events in transformation, however our group has recently described the presence of such mutations in nearly one-quarter of cases of deep infiltrating endometriosis (DE) – a form of endometriosis that rarely progresses to malignancy. These mutations may play a fundamental role in the pathogenesis of endometriosis outside of the context of cancer, however it is unclear whether they occur in other forms of endometriosis or the eutopic endometrium – the likely tissue of origin for endometriosis. The purpose of my study is to: 1) analyze and compare the mutational profiles of DE and incisional (iatrogenic; IE) endometriosis and 2) characterize somatic cancer-drivers that exist in the eutopic endometrium and determine whether the presence of such mutations reflect the aging of this tissue.

Methods: I macrodissected endometriosis tissue from women with IE or DE. Extracted DNA was analyzed by targeted sequencing and mutations were orthogonally validated by droplet digital PCR. PTEN and ARID1A immunohistochemistry was also performed for each specimen. Using the same protocol, I also analyzed hysterectomy and endometrial biopsy specimens obtained from cancer-free women.

Results: Overall, we detected the presence of somatic alterations in 27.5% and 36.1% of IE and DE cases respectively. These events affected canonical components of RAS/MAPK or PI3K-Akt signaling pathways. Furthermore, over 50% of cancer-free women also harboured similar somatic alterations in their eutopic endometrial tissue. The presence of somatic cancer-drivers in the eutopic endometrium are likely regional and are correlated with age (p = 0.048).

Conclusions: My findings are consistent with a uterine origin of endometriosis. Somatic cancer-driver alterations are commonly found in both endometriosis and the eutopic endometrium of cancer-free women and may reflect the accumulation of DNA damage

over time. These somatic alterations alone are insufficient for malignant transformation and should be interpreted with caution in the early diagnosis of gynecologic malignancies given their common occurrence in cancer-free women.

Lay Summary

Endometriosis is a common disease defined by the growth of endometrial tissue outside of the uterus. Although endometriosis can develop into cancer, this is extremely rare. We recently identified mutations commonly linked to cancer in deep infiltrating endometriosis – a form of endometriosis which virtually never progresses to cancer. This finding suggests that mutations may play a fundamental role in the development of endometriosis itself. However, it remains unclear if these mutations exist in other forms of endometriosis. The main goals of this study were to determine whether mutations commonly linked to cancer exist in incisional endometriosis (another form of endometriosis) as well as the endometrium. Through DNA sequencing we found that mutations are commonly found in both endometriosis and the endometrium of women and may be associated with aging. Consequently, such mutations may be useful targets for endometriosis treatment yet should not be cause for concern for future cancer development.

Preface

This thesis was largely motivated by the findings published in Anglesio et al. (2017) in *The New England Journal of Medicine*, of which I am a contributing author. A subset of samples from the work by Anglesio et al. were subject to more thorough mutational analysis in Chapter 3 of my thesis. Collection of local specimens was approved by the UBC BC Cancer Agency Research Ethics Board [H05-60119] and the UBC Children's and Women's Research Ethics Board [H13-02563; H14-03040]. International specimens from The Referral Centre for Gynecopathology, University Hospital Tuebingen, and VU University Medical Centre were provided by our collaborators for Chapter 3. Institutional review boards at these respective hospital sites approved specimen collection. Experimental work including immunohistochemical experiments and next generation sequencing was approved by UBC BC Cancer Agency Research Ethics Board [H02-61375; H08-01411].

Chapter 3:

A version of Chapter 3 along with methodology detailed in Chapter 2 has been submitted and is currently under review. I was the lead investigator for this work and along with Dr. Michael Anglesio, Dr. David Huntsman, and Dr. Paul Yong, I was responsible for study design. I was also responsible for macrodissection, laser-capture microdissection, DNA processing, mutation calling based on targeted sequencing, orthogonal validation of mutations by droplet digital polymerase-chain-reaction (PCR), analyzing and interpreting the data, and writing the manuscript. Dr. Leah Prentice, Dr. Jaswinder Khattra, and Amy Lum performed targeted sequencing of all samples in this study. Dr. Rosalia Aguirre-Hernandez performed bioinformatics analysis of all targeted sequencing data. Dr. Tayyebeh Nazeran and Dr. Basile Tessier-Cloutier reviewed cases and scored immunohistochemically stained slides. Teresa Praetorius and Danielle Co provided assistance in sectioning and DNA extraction. Dr. Martin Koebel from the University of Calgary (Calgary, AB) and the staff at the Genetic Pathology Evaluation Centre (Vancouver, BC) performed immunohistochemical staining. Teresa Praetorius, Natasha

Orr, Heather Noga, Dr. Anna Lee, Dr. Jana Pasternak, Dr. Bernhard Kraemer, Dr. Sara Brucker, Dr. Friedrich Kommoss, and Dr. Stefan Kommoss were involved in the retrieval of specimens.

It is important to note that Chapter 3 represents a collaborative effort between our lab and the lab of Dr. Hugo Horlings at the National Cancer Institute (Amsterdam, The Netherlands) and co-led by Lisanne Verhoef (a subset of samples from her own master's thesis have been included in our study). Lisanne Verhoef, Dr. Hugo Horlings, Dr. Velja Mijatovic, and Dr. Maaike Bleeker conducted all data collection related to specimens from the VU Univeristy Medical Centre (Amsterdam, The Netherlands) aside from targeted sequencing analysis. Targeted sequencing of these samples was performed at Contextual Genomics (Vancouver, BC) by Dr. Leah Prentice and Dr. Jaswinder Khattra. All authors mentioned above provided manuscript edits.

Chapter 4:

Chapter 4 represents original, unpublished work involving specimens retrieved solely from the local pathology archives at the Vancouver General Hospital (Vancouver, BC). I am the lead investigator of this study and Dr. Michael Anglesio, Dr. David Huntsman, and myself have conceptualized this chapter of the study. Dr. Arianne Albert also provided insight into statistical modelling and estimations of target sample size. Similar to Chapter 3, my roles spanned macrodissection, laser-capture microdissection, DNA processing, mutation calling based on targeted sequencing, orthogonal validation of mutations by droplet digital polymerase-chain-reaction, data analysis, in addition to designing the statistical model. Many of the authors mentioned in the contributions to work in Chapter 3 were also involved to similar capacities to the work in Chapter 4.

Appendix I:

Appendix I represents original, unpublished work involving specimens retrieved solely from the local pathology archives at the Vancouver General Hospital or BC Women's Hospital (Vancouver, BC). This work involves further exploratory analysis of a subset of endometriosis specimens analyzed in Chapter 3 along with several additional cases. I am the lead investigator of this study and Dr. Paul Yong, Dr. Michael Anglesio, and myself have conceptualized this chapter of the study. My roles in this sub-analysis are identical to those outlined in Chapter 3. Many of the contributing authors mentioned in Chapter 3 were also involved to similar capacities to the work in Appendix I. In addition, Natasha Orr and Heather Noga were greatly involved in the identification and selection of cases for this study.

Table of Contents

Abstract iii
Lay Summary v
Preface vi
Table of Contents ix
List of Tables xii
List of Figures xiii
List of Abbreviations xiv
Acknowledgements xvi
1. Introduction 1
1.1 Overview 1
1.2 Classification 1
1.3 Pathogenesis 4
1.3.1 Pathology of Endometriosis 4
1.3.2 Etiology 6
1.3.3 Genetic Risk 7
1.3.4 Environmental Risk 7
1.4 Endometriosis and Cancer 7
1.4.1 Observations and Epidemiological Findings 7
1.4.2 Genetic Risk for EAOCs 8
1.4.3 Loss of Heterozygosity in Endometriosis 9
1.4.4 Somatic Mutations in Cancer and Concurrent Endometriosis 9
1.4.5 Somatic Mutations in Endometriosis without Cancer 10
1.5 Goals of Current Study 12
2. Methodology 14
2.1 DNA collection and extraction 15
2.1.1 Tissue Fixation 15
2.1.2 Needle Macrodissection 16
2.1.2 Laser-Capture Microdissection 18
2.1.3 DNA Extraction and Quantification 19
2.2 Targeted panel sequencing 19
2.2.1 Library Construction 21

2.2.2 Mutation Calling 21
2.3 Orthogonal Validation by ddPCR 21
2.3.1 ddPCR Primers, Assays, and Optimal Temperatures 22
2.3.2 Pre-Amplification 25
2.3.3 Droplet Generation and Quantification 25
2.3.4 ddPCR Controls 26
2.4 Technical Validation 27
2.4.1 *KRAS* G12 Variant Screening 27
2.5 Immunohistochemistry 34
2.5.1 ARID1A immunohistochemistry 34
2.5.1 PTEN immunohistochemistry 34
3. Somatic Cancer-Driver Mutations in Incisional Endometriosis 36
3.1 Patient Specimen Collection 36
3.1.1 Overview of Incisional Endometriosis Specimens 36
3.1.2 Overview of Deep Infiltrating Endometriosis Specimens 37
3.1.3 Ethics Approval 37
3.1.4 Vancouver General Hospital Cohort 38
3.1.5 The Referral Centre for Gynecopathology Cohort 38
3.1.6 University Hospital Tuebingen Cohort 38
3.1.8 British Columbia Women's Centre for Pelvic Pain and Endometriosis Cohort 39
3.2 Additional Details on Methods 40
3.2.1 Tissue Fixation 40
3.2.2 Tissue Microarray Construction 40
3.2.3 DNA Collection and Extraction 40
3.2.4 Targeted Panel Sequencing 41
3.2.5 ddPCR 41
3.2.6 ARID1A IHC 41
3.2.7 PTEN IHC 42
3.2 Results 43
3.2.1 Sample Description 43
3.2.2 Targeted Panel Sequencing 45
3.2.3 Immunohistochemistry 47
3.2.4 Total Mutation Rates 48

3.3 Discussion 51
4. Somatic Cancer-Driver Mutations in Eutopic Endometrium 52
4.1 Patient Specimen Collection 53
4.1.1 Overview of Hysterectomy Cohort 53
4.1.2 Overview of Biopsy Cohort 54
4.1.3 Ethics Approval 54
4.2 Additional Details on Methods 54
4.3 Results 54
4.3.1 Sample Description for Hysterectomy Cases 54
4.3.2 Sample Description for Endometrial Biopsy Cases 55
4.3.3 Overview of Somatic Cancer-Driver Events 57
4.3.4 Multiple Sampling Analysis in Hysterectomy Cases 61
4.3.5 Relationship Between Age and Presence of Somatic Cancer-Driver Events in Endometrial Biopsy Cases 64
4.4 Discussion 67
5. Concluding Chapter 69
5.1 Overview of Findings 69
5.2 Limitations 72
5.3 Future Directions 73
5.4 Significance of Study 75
References 77
Appendices 93
Appendix A: Summary of clinical data for women with IE. 93
Appendix B: Summary of clinical data for women with DE. 96
Appendix C: Summary of somatic cancer-driver events in women with IE. 99
Appendix D: Summary of somatic cancer-driver events in women with DE. 102
Appendix E: Summary of clinical data for women in Hx cohort. 105
Appendix F: Summary of clinical data for women in Bx cohort. 107
Appendix G: Summary of somatic cancer-driver events in Hx patients. 112
Appendix H: Summary of somatic cancer-driver events in Bx patients. 115
Appendix I: Is the Presence of Somatic Cancer-Driver Events in Deep Infiltrating Endometriosis Associated with Deep Dyspareunia? 118
Appendix J: Pelvic Pain Assessment Form 129

List of Tables

Table 1.1: Major and minor forms of endometriosis. 4
Table 2.1: Gene hotspots and exons analyzed by FIND IT™ version 3.4 assay. 20
Table 2.2: Primers designed for ddPCR experiments. 23
Table 2.3: ddPCR assay details and optimal extension temperatures. 24
Table 2.4: Positive controls used for ddPCR experiments. 26
Table 2.5: KRAS G12/G13 variant calling by targeted sequencing and droplet digital PCR. 29
Table 3.1: Overview of clinical characteristics of women in IE cohort. 43
Table 3.2: Overview of clinical characteristics of women in DE cohort. 44
Table 3.3: Somatic cancer-driver mutations detected in endometriosis specimens from women with IE or DE. 46
Table 3.4: Reported P-values for pairwise comparisons of somatic events affecting specific genes. 50
Table 3.5: Reported P-values for pairwise comparisons of somatic events affecting canonical pathways. 50
Table 4.1: Overview of clinical characteristics of women in Hx cohort. 55
Table 4.2: Overview of clinical characteristics of women in Bx cohort. 56
Table 4.3: Reported P-values for pairwise comparisons of somatic events in Hx patients and Bx patients. 61
Table 4.4: Specific point mutations observed in samplings obtained from Hx patients. 63
Table 4.5: Somatic cancer-driver mutations detected in Bx patients. 66

List of Figures

Figure 1.1: The r-ASRM classification of endometriosis. 3
Figure 1.2: The gross presentation of the major forms of endometriosis. 5
Figure 2.1**:** Overview of workflow for this study. 15
Figure 2.2**:** Light staining procedure for needle macrodissection of endometriosis. 17
Figure 2.3: Laser-capture microdissection (LCM) of endometriosis for epithelial and stromal cell fractions. 18
Figure 3.1**:** Boxplot comparison of age of IE and DE patients. 44
Figure 3.2**.** ddPCR validation of ERRB2 c.929C>T (p.S310F) mutation in the epithelial component of endometriosis in Patient IE_16. 47
Figure 3.3**:** IHC studies of endometriosis specimens showing (A) loss of ARID1a in epithelial endometriosis cells in a case of DE and (B) matching H&E staining. 48
Figure 3.4**:** Overview of somatic cancer-driver events in incisional endometriosis and deep infiltrating endometriosis. 49
Figure 4.1**:** Theoretical and simplified model of the pathogenesis of endometriosis. 52
Figure 4.2: Boxplot comparison of age of Hx and Bx patients. 56
Figure 4.3: Overview of somatic cancer-driver events in endometrial tissue from women in the A) Hx cohort and B) Bx cohort. 58
Figure 4.4: Proportion of Hx and Bx cases affected by somatic cancer-driver events. 59
Figure 4.5: PTEN IHC studies of Hx specimens showing (A,C,E) regional loss/heterogeneous expression of PTEN in epithelial endometriosis cells and (B,D,F) matching H&E stain. 60
Figure 4.6**:** Concordance and discordance of point mutations observed among both samplings obtained from Hx patients. 62
Figure 4.7: Logistic regression model depicting the correlation between age and presence of somatic cancer-driver events in Bx patients. 64
Figure 4.8: Logistic regression model depicting the correlation between age and presence of somatic cancer-driver events in Bx patients with endometrium samplings with respect to the phase of the endometrium. 65
Figure 5.1**:** A revised model of the pathogenesis of endometriosis lesions. 72
Figure 5.2: Schematic of the BaseScope assay. 74

List of Abbreviations

BDNF – brain-derived neurotrophic factor

Bx – biopsy

CCOC – clear cell ovarian carcinoma

CI – confidence interval

COSMIC – Catalogue of Somatic Mutations in Cancer

ddPCR – droplet digital PCR

DE – deep (infiltrating) endometriosis

EAOC – endometriosis-associated ovarian cancer

ENOC – endometrioid ovarian carcinoma

EPHect – World Endometriosis Research Foundation Endometriosis Phenome and Biobanking Harmonization Project

FFPE – formalin-fixed and paraffin-embedded

GWAS – genome-wide association study

H&E – hematoxylin-eosin

Hx – hysterectomy

IE – incisional endometriosis

IHC – immunohistochemistry

IL - interleukin

LCM – laser-capture microdissection

LOH – loss of heterozygosity

MFPE – molecular-fixed and paraffin-bedded

NGS – next-generation sequencing

OCP – oral contraceptive pill

OR – odds ratio

Pap – Papanicolaou

r-ASRM – revised scoring system of the American Society for Reproductive Medicine

SD – standard deviation

TMA – tissue microarray

VAF – variant allele frequency

VGH – Vancouver General Hospital

VUMC – VU University Medical Center

Acknowledgements

I would like to express my deepest gratitude and appreciation towards my co-supervisors, Dr. David Huntsman and Dr. Michael Anglesio. Without their ongoing guidance and encouragement, this study would not have been possible. Dr. Huntsman has challenged me to think critically about my research and he continues to inspire me with his excitement regarding this research in this field. Dr. Anglesio has been both an incredible supervisor and teacher and has provided me endless advice for success in the lab and beyond.

I would also like to thank my committee members, Dr. Paul Yong and Dr. Kelly McNagny, both of whom have provided key insight in the development of this study and have helped me set realistic goals for success as a graduate student.

This work would have been impossible without the assistance of my fellow colleagues in the Huntsman and Anglesio labs. In particular, Dr. Tayyebeh Mehrane Nazeran and Dr. Basile Tessier-Cloutier, have helped me review all the cases included in this study. I am extremely grateful for Amy Lum for her assistance and training for various laboratory techniques crucial to my research.

I am thankful for the Canadian Institutes of Health Research for providing me with financial support as a graduate student as well as support for the study itself. I would also like to thank the Canadian Cancer Society and BC Cancer Foundation for providing the funding essential to perform the experimental work involved in this study.

Finally, I would like to thank my brother for providing me emotional support and wisdom over the course of my graduate studies.

1. Introduction

1.1 Overview

Characterized by the growth of endometrial-like glands and stroma outside of the uterus, endometriosis is an estrogen-dependent, chronic, inflammatory gynecological disease affecting roughly 10% of reproductive-aged women and up to 50% of those with infertility or chronic pelvic pain[1-3]. Clinical symptoms of endometriosis overlap with other gynecological conditions and can include: chronic (often cyclical) pain, dyspareunia (painful intercourse), dysmenorrhea, infertility, nausea, dyschezia (difficult or painful defecation), and dysuria[2,3]. An estimated 176 million women are affected by endometriosis globally[4], yet despite the prevalence of endometriosis, it is an underdiagnosed and poorly managed condition. Firstly, there are currently no reliable biomarkers for the non-invasive detection of endometriosis and a definitive diagnosis requires surgery[2,3], contributing to a mean latency period of 6.7 years from initial onset of symptoms to diagnosis with endometriosis. Secondly, recurrence rates of endometriosis following surgical resection are high; the estimated recurrence rate of endometriosis is 40-50% at 5-year follow-up[5]. Consequently, many women continue to live with endometriosis for years and thus the condition represents a major burden to both affected individuals and society at large.

1.2 Classification

First described by Carl Freiherr von Rokitansky in 1860[6], endometriosis is primarily found on the ovaries, surrounding pelvic peritoneum, and uterine ligaments, however it is not restricted to affecting sites in the pelvic region[3,7,8]. Rare cases of extra-pelvic endometriosis have been reported to affect the lungs, liver, pericardium, central nervous system[9,10], and even the site of surgical incisions[7,8,11]. Pelvic endometriotic lesions can be further divided into three subtypes: ovarian endometriosis (also known as endometriomas, which appear as cystic masses of the ovary), superficial peritoneal endometriosis, and deep infiltrating endometriosis (which is surgically defined as lesions that penetrate >5mm into pelvic structures)[2,12].

There are numerous ways that endometriosis can present itself clinically with respect to its histological appearance and potential anatomical sites affected. Professional organizations have developed a multitude of classification systems for endometriosis in efforts to stratify disease burden and guide disease management. The revised scoring system of the American Society for Reproductive Medicine (r-ASRM) is one of the most widely used classification system for endometriosis[13,14]. In the r-ASRM, a weighted point system based on the type, location, depth of invasion, and histologic appearance of endometriosis lesions, the extent of disease, and the presence of adhesions are used to determine the stage of endometriosis from Stage I (minimal disease) to Stage IV (severe disease)[3]. Other classification systems exist such as the Enzian classification for deep infiltrating endometriosis[15] and the endometriosis fertility index[16], however none of the current classifications systems correlate well with severity of pain[17] and they do not prognosticate for critical endpoints such as response to treatment, recurrence, or risk for malignant transformation[14].

AMERICAN SOCIETY FOR REPRODUCTIVE MEDICINE
REVISED CLASSIFICATION OF ENDOMETRIOSIS

Patient's Name _____ Date _____

Stage I (Minimal) - 1-5
Stage II (Mild) - 6-15
Stage III (Moderate) - 16-40
Stage IV (Severe) - >40
Total _____

Laparoscopy _____ Laparotomy _____ Photography _____
Recommended Treatment _____
_____
Prognosis _____

PERITONEUM	ENDOMETRIOSIS	<1cm	1-3cm	>3cm
	Superficial	1	2	4
	Deep	2	4	6
OVARY	R Superficial	1	2	4
	Deep	4	16	20
	L Superficial	1	2	4
	Deep	4	16	20
	POSTERIOR CULDESAC OBLITERATION	Partial	Complete	
		4	40	
OVARY	ADHESIONS	<1/3 Enclosure	1/3-2/3 Enclosure	>2/3 Enclosure
	R Filmy	1	2	4
	Dense	4	8	16
	L Filmy	1	2	4
	Dense	4	8	16
TUBE	R Filmy	1	2	4
	Dense	4*	8*	16
	L Filmy	1	2	4
	Dense	4*	8*	16

*If the fimbriated end of the fallopian tube is completely enclosed, change the point assignment to 16.

Denote appearance of superficial implant types as red [(R), red, red-pink, flamelike, vesicular blobs, clear vesicles], white [(W), opacifications, peritoneal defects, yellow-brown], or black [(B) black, hemosiderin deposits, blue]. Denote percent of total described as R___%, W___% and B___%. Total should equal 100%.

Additional Endometriosis: _____

Associated Pathology: _____

To Be Used with Normal Tubes and Ovaries

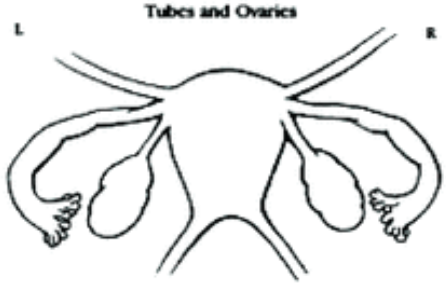

To Be Used with Abnormal Tubes and/or Ovaries

Figure 1.1: The r-ASRM classification of endometriosis. [Figure adapted from American Society for Reproductive Medicine (1997) [13]*.]*

1.3 Pathogenesis

1.3.1 Pathology of Endometriosis

Endometriosis is a multi-factorial disease and its pathogenesis is not fully understood. As mentioned in Section 1.2, endometriosis typically presents itself in three distinct forms: superficial peritoneal endometriosis, ovarian endometriotic cysts, or deep infiltrating endometriosis (Table 1.1; Fig. 1.2). These major forms of endometriosis as well as several minor forms (including iatrogenic, mass-forming, and extrapelvic endometriosis) are described in Table 1.1. It is important to note that occurrences are not mutually exclusive and affected patients may have several lesions of different forms simultaneously.

Table 1.1: Major and minor forms of endometriosis.

Type of Endometriosis	**Brief Description**
superficial peritoneal	lesions existing on the surface of pelvic peritoneum and ovaries[2]
ovarian (endometrioma)	ovarian cysts lined by endometrioid mucosa[2]
deep infiltrating	lesions that locally invade into pelvic structures[2]
iatrogenic	occurs following surgical scars of obstetric or gynecological procedures such as caesarean sections and laparoscopies[18]
mass-forming	benign-appearing endometriotic glands and stroma forming mass lesions and infiltrating organs, mimicking a malignant neoplasm[19]
extrapelvic	lesions found outside of the pelvic cavity, including: lungs, liver, pericardium, the central nervous system, etc.[8-11]

Histologically and by definition, endometriotic lesions are comprised of epithelial and stromal components and consist of normal-appearing cells that closely resemble the eutopic endometrium. Unlike the eutopic endometrium however, endometriotic lesions are characteristically progesterone resistant and locally produce estrogen, prostaglandins, and cytokines[20,21]. These alterations contribute to increased cell survival (and thus the persistence of endometriotic tissue over many menstrual cycles) and constant, localized inflammation, which may ultimately result in chronic pelvic pain and infertility experienced by women with endometriosis[20-23].

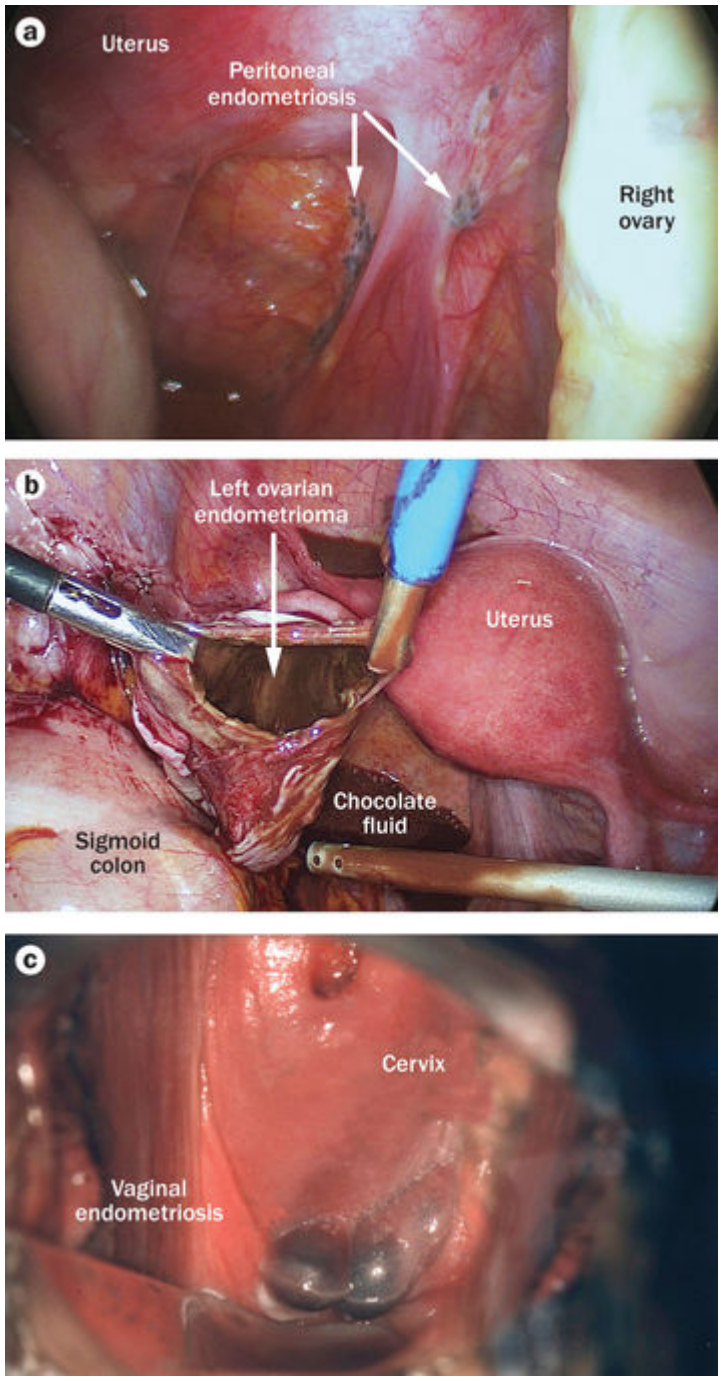

Figure 1.2: The gross presentation of the major forms of endometriosis. The three most prevalent forms of endometriosis – (A) superficial peritoneal endometriosis, (B) ovarian endometriosis (endometrioma), and (C) deep infiltrating endometriosis are shown. [Figure adapted from Vercellini et al. (2014) [2]*.]*

1.3.2 Etiology

The origin of endometriosis is contentious and several theories on its etiology have been proposed. Such theories include retrograde menstruation (the reflux of endometrial fragments through the fallopian tubes during menstruation), coelomic metaplasia, Müllerian remnants, and lymphatic or vascular dissemination[2,20]. Although each theory is supported by at least circumstantial evidence, each theory has its limitations and no single theory can fully explain every incident case of endometriosis.

The most popular theory, retrograde menstruation theory, posits that the development of endometriosis is attributed to the sloughing/reflux of eutopic endometrium through the fallopian tubes and into the peritoneal cavity during menstruation[24]. This theory is supported by the high prevalence of endometriosis in females with congenital outflow obstruction[25] as well as the anatomic distribution of endometriotic lesions[24]. Although up to 90% of women exhibit this reflux of endometrial tissue[24], a far smaller percentage of women (approximately 10%) have endometriosis – this may be explained by: 1) the impaired capacity of immune cells to mediate the clearance of refluxed endometrial cells and 2) other alterations in the cell-mediated and humoral immunity leading to increased levels of a variety of cytokines and growth factors, which may promote the implantation and growth of refluxed endometrial cells[26]. However, this theory fails to explain why endometriosis has been observed in distant/extra-pelvic regions such as the lungs and pericardium.

In contrast a second theory, coelomic metaplasia theory, posits that endometriosis arises from the transformation of normal peritoneal tissue to ectopic endometrial tissue[24]. Metaplasia can explain why endometriosis can develop at distant sites that cannot physically contact refluxed endometrial tissue or why endometriosis can develop in males[27,28]. This theory is supported by experimental models such as the mouse model developed by Dinulescu et al. (2004), wherein the expression of oncogenic *KRAS* or conditional deletion of *PTEN* within the ovarian surface epithelium was observed to give rise to preneoplastic lesions resembling endometriosis[29]. However, causative agents of such transformation of normal peritoneal (or other bodily tissues) remain poorly defined[24].

1.3.3 Genetic Risk

Family and twin studies demonstrate the important contribution of genetic factors to the development of endometriosis. The incidence of endometriosis in the first-degree relatives of women affected with endometriosis is nearly seven times greater than women lacking such family history[30]. Furthermore, based on a study on the concordance of endometriosis among 3096 Australian twins, the heritability component of endometriosis is estimated to be 51%[31]. A genome-wide linkage study of 1,176 families with two or more sister pairs affected by endometriosis has implicated a susceptibility locus for endometriosis on chromosome 10q26[32]. More recent genome-wide association (GWAS) studies have revealed *WNT4* (rs12037376)[33,34,35], *CDKN2BAS* (rs10965235)[33,34], rs12700667 on chromosome 7p15.2 (an intergenic region upstream of *NFE2L3* and *HOXA10*)[36,35], *ESR1* (rs2206949)[37], *SYNE1* (rs17803970)[37], *FN1* (rs1250241)[33,36,37], *VEZT* (rs10859871)[35], and *GREB1* (rs13394619)[35] among others as susceptibility loci for endometriosis.

1.3.4 Environmental Risk

Lifestyle and environmental factors may also contribute to the development of endometriosis. Consumption of red meat and trans-unsaturated fats is associated with an increased risk, whereas consumption of green vegetables and long-chain omega-3 fatty acid consumption is associated with decreased risk for endometriosis[38,39]. Additionally, dioxin exposure as well as *in utero* diethylstibestrol exposure may also increase the incidence of endometriosis[40,41].

1.4 Endometriosis and Cancer

1.4.1 Observations and Epidemiological Findings

One of the more well-studied areas of endometriosis research focuses on its relationship with ovarian cancer. Endometriosis and ovarian cancer share several risk factors including early menarche and late menopause, nulliparity, and short intervals between menses, thereby hinting at a possible relationship between endometriosis and ovarian cancer[42]. In 1925, Sampson first proposed a theory wherein endometriosis (specifically ovarian endometrioma) can transform into ovarian cancer[43]. This theory has

been supported by epidemiological studies, which demonstrate an association between endometriosis and ovarian cancers[44-46]. It is important to note that epithelial ovarian carcinomas are comprised of five major histological subtypes: high-grade serous, low-grade serous, mucinous, clear cell (CCOC), and endometrioid (ENOC) ovarian carcinomas – the association between endometriosis and ovarian cancer is restricted to the CCOC and ENOC subtypes (known as the endometriosis-associated ovarian cancers; EAOCs). In particular, women suffering from (surgically-confirmed) endometriosis have a 3 to 5-fold greater risk of developing CCOC and ENOC, wherein ovarian endometriomas are associated with the highest risk for EAOC development followed by superficial peritoneal endometriosis and then deep infiltrating endometriosis[47]. Although the study by Pearce et al. (2012) shows a weak association between endometriosis and low-grade serous ovarian cancer[45] , a smaller study by Merritt et al. (2013) does not[46] . Moreover, this association remains unexplained as low-grade serous ovarian cancers have not been found contiguous with endometriosis as with CCOCs and ENOCs. Data pooled from 13 population-based case-control studies of over 10,000 women with ovarian cancer revealed that tubal ligation preferentially protects against CCOC and ENOC among ovarian cancer histotypes[48], a finding which further suggests that retrograde menstruation may be a key factor in the genesis of these cancers or their precursor lesions.

1.4.2 Genetic Risk for EAOCs

A limited number of studies have explored the subtype-specific genetic risk factors associated with the different ovarian cancer histotypes. Epigenetic analysis has led to the identification of *HNF1B* as a susceptibility gene for CCOC[49] , whereas a recent GWAS study identified rs555025179 on 5q12.3 as a susceptibility loci for ENOC[50]. Interestingly, there is little overlap in susceptibility loci between endometriosis and EAOCs – the closest match appears to be around the *ESR1/SYNE*1 loci (rs2295190)[43] (two genes involved in sex steroid hormone pathways), however this association does not reach genome-wide significance for either CCOC nor ENOC and the specific risk loci differs for endometriosis[37,51] (see section 1.3.3).

1.4.3 Loss of Heterozygosity in Endometriosis

Despite the classification of endometriosis as a benign disease, endometriotic lesions can harbor genetic aberrations. Loss of heterozygosity (LOH) was one of the first genomic abnormalities observed in endometriosis[52]. Microsatellite analysis studies revealed LOH in endometriosis affecting regions commonly lost in ovarian neoplasms including 1q, 9p, 11q, 17p, and 22q[52,53]. Providing molecular evidence for the progression of endometriosis to EAOCs, Sato et al. (2000) found that 3/5 ENOC cases and 3/7 CCOC cases with concurrent endometriosis displayed LOH events on 10q23.3 (a region encoding *PTEN*) common to both the carcinoma and the endometriosis[54]. Moreover, a separate study analyzing 82 microsatellite markers spanning the genome detected 63 LOH events among 10 EAOC samples, wherein 22 LOH events were subsequently detected in the corresponding endometriosis samples (yet LOH events were never detected in the endometriosis only)[55]. This data further suggests the selection for/accumulation of LOH events as endometriosis progresses to malignancy. It is important to note, however, that although these LOH events provide support for clonality between endometriosis and concurrent EAOCs, they are insufficient to conclude a clonal origin between the two since common LOH events may instead indicate that similar pathway aberrations are involved in endometriosis and cancer.

1.4.4 Somatic Mutations in Cancer and Concurrent Endometriosis

Molecular studies focusing on somatic mutations found in EAOCs and contiguous endometriosis lesions have established endometriosis as the precursor of EAOCs. Both CCOC and ENOC are characterized by a high prevalence of *ARID1A* mutations and frequent activation of the PIK3CA-mTOR pathway[56,57] – such aberrations have been found in endometriosis, therefore implicating such events as early markers in malignant transformation. Wiegand et al. described *ARID1A* mutations in 55 of 119 CCOC cases (46%) and 10 of 33 ENOC cases (30%)[58]. Moreover, identical *ARID1A* mutations were found in the ovarian carcinoma and contiguous atypical endometriosis but not in distant lesions of endometriosis[58]. Similarly, Anglesio et al. consistently observed *ARID1A* and *PIK3CA* mutations in concurrent endometriosis when present in primary CCOCs[59]. Whole-genome shotgun sequencing in this study also revealed the presence of ancestral mutations in both distant and tumour-adjacent endometriotic lesions, with generally

increasing mutational burden the more central to the tumour site the endometriotic lesions were located[59].

In short, recent molecular studies focusing on somatic mutations in EAOCs and concurrent endometriosis have led to the following observations regarding the nature of endometriosis:

1. Endometriotic lesions found adjacent to or contiguous with CCOC or ENOC harbour many of the same mutations, therefore **some endometriotic lesions share origins with the cancer (i.e. a clonal relationship exists).**
2. Both distant and adjacent endometriosis can share common mutations, therefore **some endometriotic lesions (even without cytologic atypia) are capable of dissemination/metastasis.**
3. Endometriosis contiguous with CCOC/ENOC typically share a larger number of mutations than more distant lesions, thereby supporting of a progression model wherein **endometriosis is the direct precursor to CCOC/ENOC.**

1.4.5 Somatic Mutations in Endometriosis without Cancer

Although the studies outlined above have provided us with much insight into the relationship between endometriosis and EAOCs, it is crucial to also study the somatic mutations in endometriosis outside of the context of cancer. Endometriosis is far more prevalent in the population than ovarian cancer (particularly CCOC and ENOC) and is estimated to progress to cancer in only approximately 1% of affected women[2]. Furthermore, despite being considered a benign disease, endometriosis shares many notable features with cancer. Unlike the eutopic endometrium, cells from endometriotic lesions are resistant to apoptosis and can stimulate angiogenesis[20,60]. Particularly in deep infiltrating endometriosis, endometriosis is also capable of invading local tissue[61].

A small number of studies have identified somatic cancer-driver mutations in endometriotic lesions in patients without cancer. Immunohistochemistry studies showed loss of ARID1A in a small percentage of benign ovarian endometriosis and deep infiltrating endometriosis cases[62,63]. Sato et al. (2000) reported somatic *PTEN* mutations in 7/34 (20.6%) endometriomas in cases without cancer through the sequencing of laser-

captured endometriotic lesions[54]. The study of somatic mutations in endometriosis remains technically challenging since endometriotic lesions are often small and scattered among reactive and fibrotic (non-endometriotic) tissue. Without specific enrichment of endometriotic cells (such as by laser-capture microdissection), mutations – particularly those at low allelic frequencies – may not be detectable among DNA contributed by surrounding, normal/non-endometriotic cells. The dilution of the endometriotic cell fraction of interest (in whole-excised surgical specimens) is especially problematic combined with low-resolution detection methods (such as Sanger sequencing), which generally detect variant allelic frequencies as low as only 10-20%[64]. Such challenges may explain the extremely low rates of somatic *KRAS* mutations reported by two separate groups (1/23 patients and 0/19 patients)[65,66], as well as the identification of somatic driver mutations in only 3/101 Chinese patients with ovarian endometriosis[67] . In stark contrast, a whole-exome sequencing study by Li et al. (2014) reported on extremely high rates of somatic mutations (averaging over 1000 somatic mutations per case) within both endometriotic cells and eutopic endometrial cells[68] , however no orthogonal validation was performed, and specimen curation, collection, and sequencing methods were ambiguously described. It remains likely that many of the reported mutations represent sequencing artifacts, poor technical and/or analytical methods, or background noise and this study cannot be considered credible. Compiling the findings of these studies, there has been little consensus on the extent to which somatic mutations exist in endometriosis outside of the context of cancer and the general belief maintains that such events are directly linked to malignant transformation[69].

In a recent study by our group along with collaborators at John Hopkins University, deep infiltrating endometriotic (DE) lesions were analyzed by lesions by means of exome-wide sequencing (24 cases), cancer-driver targeted sequencing (3 cases), and droplet digital PCR assay (12 cases)[59]. Ten of 39 (26%) cases of DE harboured somatic mutations including known cancer-driver hotspots in *KRAS*, *PIK3CA*, and *PPP2RIA* as well as loss of function mutations in *ARID1A*[59]. Since DE virtually never undergoes malignant transformation[47], the function of these somatic mutations is unclear. It is possible such mutations may contribute to the development and pathogenesis of DE unrelated to oncogenic change. Another possibility is that the somatic mutation of one

allele of a given oncogene or tumour suppressor gene is insufficient for malignant transformation of endometriosis and further DNA damage rarely occurs in cases of DE compared to ovarian endometriomas. Nonetheless, it is difficult to speculate on the functional role of somatic cancer-driver mutations in endometriosis found without associated cancer without elucidating the extent in which such mutations exist in other forms of endometriosis (to date, no equivalent analysis has been conducted on superficial peritoneal endometriosis, ovarian endometriomas, or even rarer forms of endometriosis). Moreover, do such mutations already pre-exist in the eutopic endometrium (the presumed site of origin of endometriosis)? To date, a limited number of studies have been published on the possible existence of somatic mutations in non-diseased (normal) eutopic endometrium, yet such studies have been largely restricted to immunohistochemistry studies of PTEN and PAX2[70-73].

1.5 Goals of Current Study

The goal of my current research study is to explore the prevalence of somatic cancer-driver mutations among benign tissue types involved in EAOC pathogenesis (assuming the retrograde menstruation theory), particularly endometriosis and the eutopic endometrium. I will seek to address the following questions:

1. **"Do benign forms of endometriosis aside from DE harbour somatic cancer-driver mutations?"** In regards to Question 1, I hypothesize that other benign forms of endometriosis (i.e. forms of endometriosis with an exceptionally low likelihood of malignant transformation) harbour somatic cancer-driver mutations. To test this hypothesis, I will compare the mutational profiles of DE to incisional endometriosis (IE – a rare, iatrogenic form of endometriosis) by means of targeted sequencing. This comparison between DE and IE also serves to address a secondary question: does the mutational spectrum of iatrogenically-occurring endometriosis (IE) differ from endogenous forms of endometriosis (DE)? I will compare the proportion of cases affected as well as the specific genes/signalling pathways involved in somatic mutations in both forms of endometriosis.

2. **“Does the eutopic endometrium harbour somatic cancer-driver mutations? If so, does the presence of somatic mutations reflecting aging of this tissue?”** In regards to Question 2, I hypothesize that the eutopic endometrium harbours somatic cancer-driver mutations and that age is associated with an increased likelihood of observing these somatic mutations. To test this hypothesis, I will assess the presence of somatic cancer-drivers in the eutopic endometrium of women without evidence of gynecologic malignancy by means of targeted sequencing. I will examine the presence of mutation and age of women studied to generate a logistic regression model to determine the effect of age on the likelihood of observing a somatic driver mutation in the eutopic endometrium (odds ratio).

2. Methodology

This chapter provides an overview of the common methods used throughout this work, specifically in the analysis of somatic alterations in benign forms of endometriosis (Chapter 3) and eutopic endometrium (Chapter 4). Note that because of the small size of lesions and non-specific symptomology, the pathological confirmation and subsequent identification of endometriosis often requires formalin fixation of specimens. Consequently, this work focuses on the analysis of archival endometriosis specimens since these are the most readily accessible endometriotic material.

Fig. 2.1 below illustrates a simplified version of the workflow. The remainder of the chapter provides further details on the methodology. Patient collection information and any deviations from the common methods presented here will be discussed in the relevant chapters.

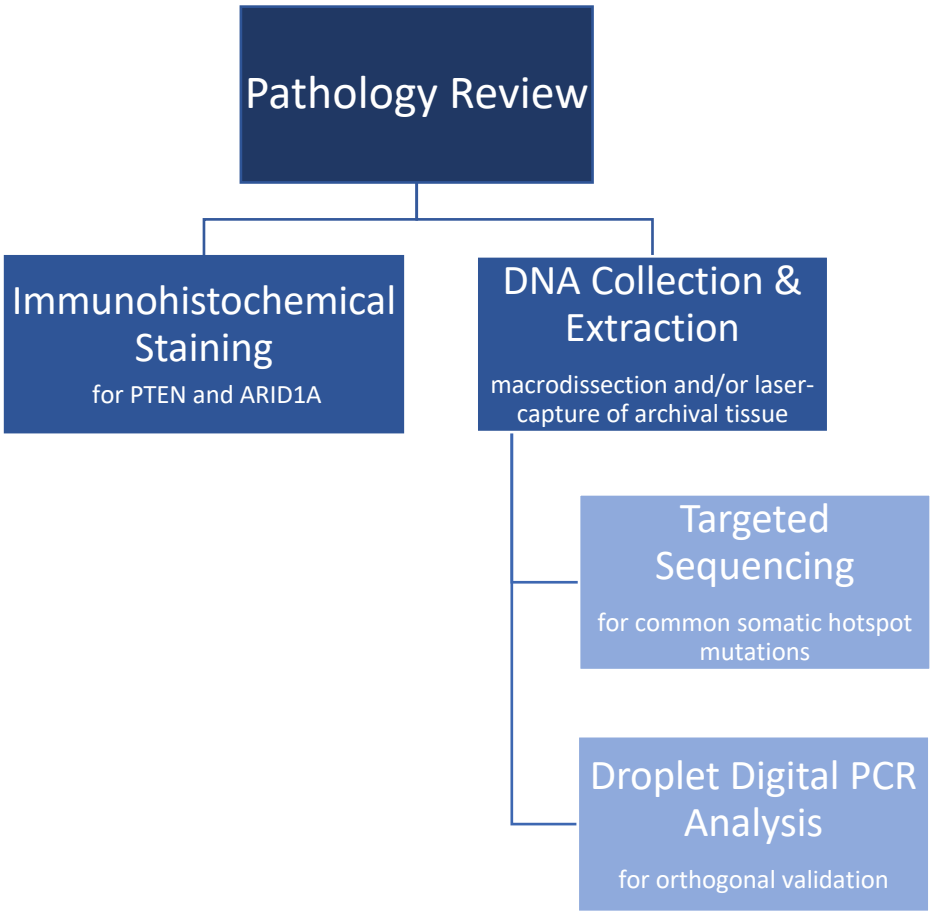

Figure 2.1: Overview of workflow for this study. Endometriosis and eutopic endometrium cases undergo pathology review to ensure lack of evidence of cancer or dysplasia and sufficient tissue for analysis. Suitable cases undergo PTEN and ARID1A immunohistochemistry and are also macrodissected (in some cases laser-captured) to enrich for DNA of interest. Extracted DNA is used in targeted sequencing and subsequently in orthogonal validation by means of droplet digital polymerase-chain-reaction.

2.1 DNA collection and extraction

2.1.1 Tissue Fixation

Most endometriosis and all endometrial tissue specimens were formalin-fixed and paraffin-embedded (FFPE) tissues, which were fixed in (10%) neutral-buffered formalin and paraffin-embedded following standard methods. A subset of endometriosis cases were molecular-fixed and paraffin-embedded (MFPE) tissues – endometriosis lesions from these cases were surgically removed and fixed in Tissue-Tek molecular fixative

(Sakura Finetek, USA), processed, and embedded using the Tissue-Tek microwave rapid processing system (Sakura Finetek, USA)[74].

2.1.2 Needle Macrodissection

As defined, endometriosis tissue exists ectopically within other tissues. Moreover, glands present are variable in number, shape, and size (although often miniscule compared to cancers) within a given tissue section. Consequently, standard macrodissection or coring would result in collecting proportionally more cells from the surrounding, normal tissue than the endometriotic lesion itself and therefore poor resolution for the detection of mutations affecting endometriotic cells. We have instead developed a protocol for stereo microscope-guided needle macrodissection of tissue specimens. Firstly, specimens were sectioned at 8μm onto standard glass slides and baked at 60°C for 1 hour. Next, slides were deparaffinized with xylene and stained with 10% diluted hematoxylin and eosin (which we will refer to as “light staining”) following the protocol below:

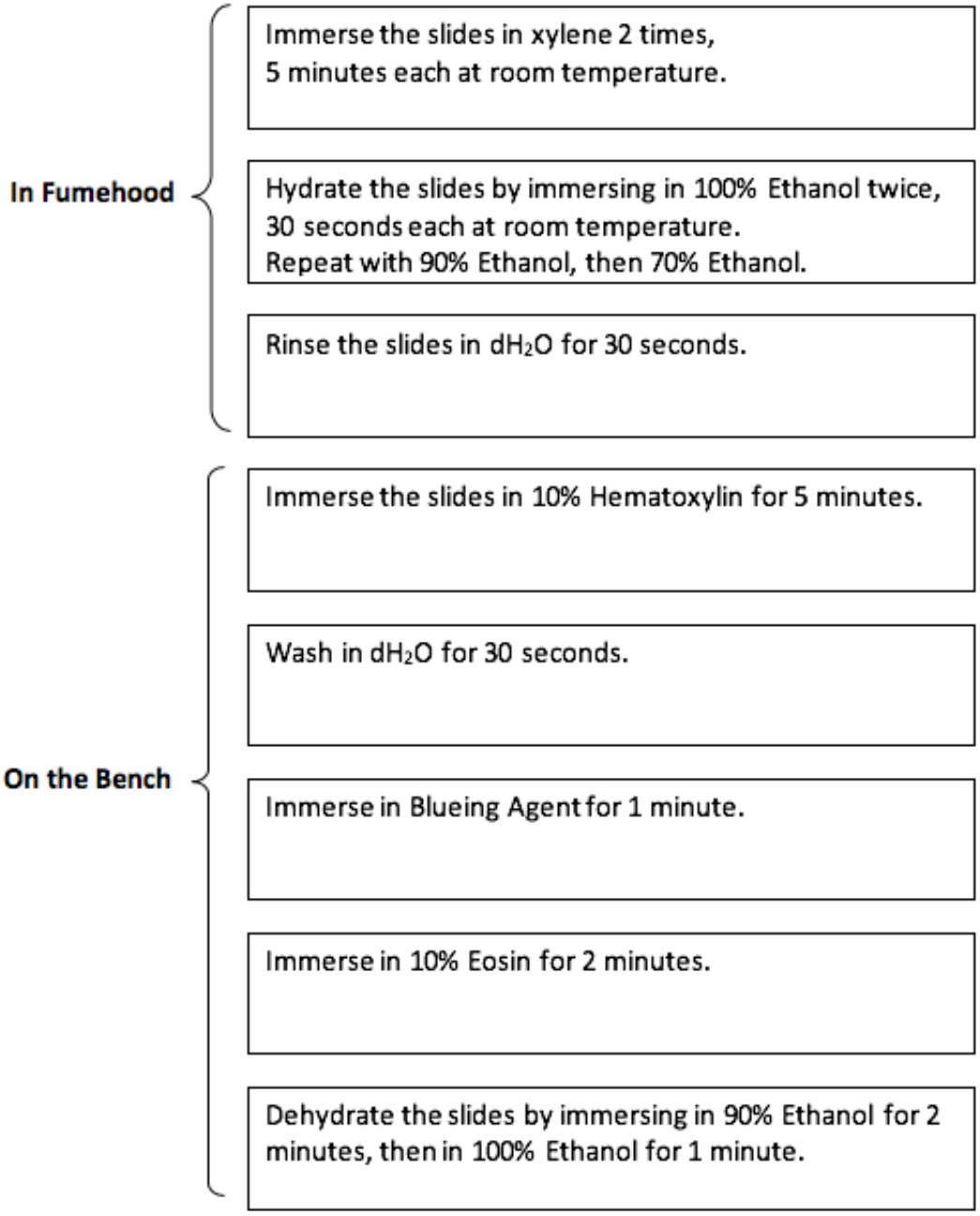

Figure 2.2: Light staining procedure for needle macrodissection of endometriosis. Note that this protocol can be adapted for dissection of larger areas of interest such as endometrial tissue.

After light staining, using a standard hematoxylin-eosin (H&E) slide as a guide, I manually macrodissected tissue of interest (endometriosis or eutopic endometrium) under a stereo microscope using the tip of a 20-guage, bevel-tip needle.

2.1.2 Laser-Capture Microdissection (LCM)

For technical validation of our targeted sequencing assay (see section 2.2) as well as orthogonal validation of mutations called by this assay, I collected laser-captured material for many of the cases we studied. Samples were sectioned at 8μm onto PEN membrane slides (Leica Microsystems Inc., Switzerland). Laser-captured specimens were also stained with the same light staining protocol as defined above for macrodissected specimens (Fig. 2.2). I used serial H&E slides to identify areas of interest and performed LCM using the LMD7000 Laser Microdissection system (Leica Microsystems Inc., Switzerland).

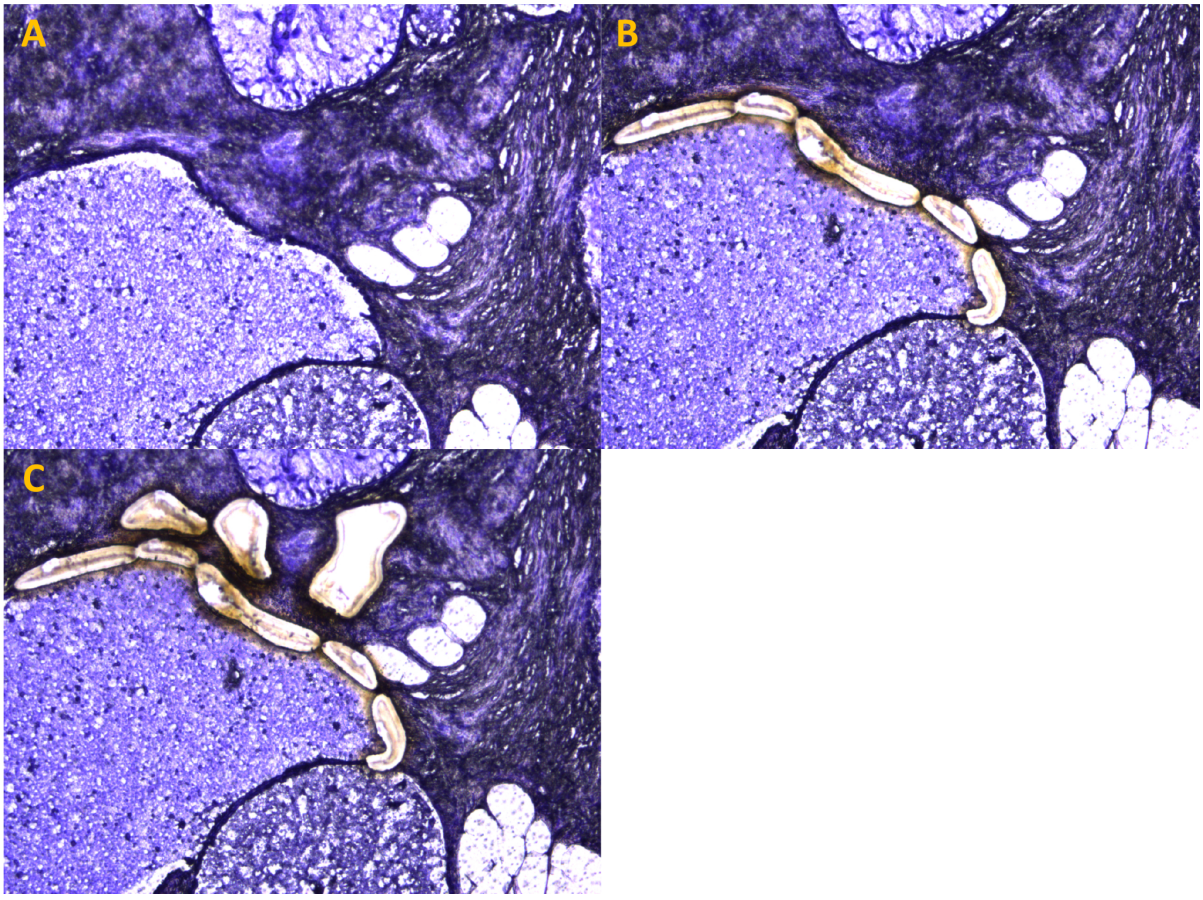

Figure 2.3: Laser-capture microdissection (LCM) of endometriosis for epithelial and stromal cell fractions. An area of endometriosis is shown (A) before LCM, (B) after separation of endometriotic epithelium, and (C) after subsequent separation of endometriotic stroma.

2.1.3 DNA Extraction and Quantification

For all macrodissected and laser-captured tissue, I performed DNA extraction using the ARCTURUS® PicoPure® DNA Extraction Kit (ThermoFisher Scientific, USA). Quantification of extracted DNA was performed using the Qubit 2.0 Fluorometer (ThermoFisher Scientific, USA).

2.2 Targeted panel sequencing

We performed next-generation sequencing (NGS) of DNA extracted from macrodissected specimens using the FIND IT^{TM} version 3.4 (Contextual Genomics, Canada) assay. The FIND IT^{TM} version 3.4 assay is an Illumina-based, targeted sequencing assay which focuses on the detection of known mutations found in many solid tumour cancers (many of which are treatable with current therapies). The assay can be performed on FFPE tissue to detect mutations at very low variant allele frequencies (VAFs) (< 1%). Currently, over 120 hotspots and 17 exons in 33 known cancer genes are analyzed in the FIND IT^{TM} panel. These gene regions are outlined below in Table 2.1.

Table 2.1: Gene hotspots and exons analyzed by FIND IT™ version 3.4 assay.

Gene	Position
AKT1	E17
ALK	T1151, L1152, C1156, F1174, L1196, L1198, G1202, D1203, S1206, R1275, G1269
AR	H875, F877, T878, S741, W742, V716
BRAF	G466, F468, G469, Y472, D594, G596, L597, V600, K601, Q201
CTNNB1	D32, S33, G34, S37, T41, S45
DDR2	I638,L239,S768
EGFR	Exon18,Exon19,Exon20,Exon21
ERBB2	Exon20,G309,S310,L755
ESR1	K303, S463, V534, P535, L536, Y537, D538
FGFR1	N546, K656
FGFR2	S252, P253, N549, K659
GNA11	Q209
GNAQ	Q209
GNAS	R201
HRAS	G12,G13,Q61
IDH1	R132
IDH2	R140,R172
JAK1	V658, S703
KIT	Exon9, Exon11, Exon13, T670, D816, D820, N822, Y823, A829
KRAS	G12, G13, A59, Q61, K117, A146
MAP2K1	Q56, K57, K59, D67, P387
MAP2K2	F57, Q60, K61, L119
MET	Exon13, Exon 14-50+25, Exon18, Y1253
NRAS	G12, G13, A59, Q61, K117, A146
PDGFRA	N659, R560-E571, D842, L839-Y849
PIK3CA	R88, E542, E545, Q546, D549, M1043, N1044, A1046, H1047, G1049
PTCH1	W844, G1093
PTEN	R130, R173, I122_M134, S170_Y188, Y225_F243, K254_K267
RET	C634, V804, M918
ROS1	L2026, G2032
SMO	D473, S533, W535
STK11	Q37, P281
TP53	Exon4, Exon5, Exon6, Exon7, Exon8, Exon9

2.2.1 Library Construction

Libraries were constructed for panel-based sequencing for hotspot mutations in 33 genes (Table 2.1) using 45-75 ng of DNA input from endometriosis specimens. DNA samples were barcoded and run using the 300-cyle MiSeq Reagent Kit v2 (Illumina Inc., USA). Proprietary quality assurance methods based on DNA sequence barcodes, that were incorporated into the assay and the bioinformatics pipeline, were used to increase the sensitivity of called mutations. The bioinformatics pipeline first removed poor quality reads based on sequence length and base mismatches in the primer region. Good quality reads were then aligned to a reference genome.

2.2.2 Mutation Calling

Mutations were called with a supervised classification method that returned the probability that a variant belongs to the mutation class (as opposed to the artifact class) based on the alignment, sequence composition and barcode information of the variant. Germline mutations were removed from the list. Candidate variants for orthogonal validation by ddPCR were selected as the ones with probability scores ≥ 0.8 and variant allele frequency (VAF) ≥ 0.8% for macrodissected samples (or VAF ≥ 5.0% for laser-captured samples). Note that these VAF cut-offs were determined empirically following mutation calling thresholds for *KRAS* mutations I have established for macrodissected samples (see Chapter 2.4.1), since mutations (even if real) at lower VAFs would not be able to be orthogonally validated by droplet digital PCR (note that other mutations were reported far less often than *KRAS* and I assumed that such mutations would have similar detection thresholds). Additionally, variants must have also been reported in the Catalogue of Somatic Mutations in Cancer (COSMIC) as somatic, hotspot driver mutations[75].

2.3 Orthogonal Validation by ddPCR

DNA extracted from FFPE tissues is comparatively poor in quality. Not only is DNA fragmented, but the process of this fixation results in the introduction of DNA lesions, which result in sequencing artifacts (most notably C>T changes)[76]. Consequently, I used droplet digital PCR (ddPCR) to orthogonally validate mutations called by targeted

sequencing to determine whether mutations were real (true positives) or sequencing artifacts (false positives). Macrodissected, and/or laser-captured, material was used to orthogonally validate hotspot mutations – in most cases, the same aliquot of DNA collected and extracted for targeted sequencing was used in these validations.

2.3.1 ddPCR Primers, Assays, and Optimal Temperatures

Overall, I performed ddPCR for *KRAS* G12 hotspot mutations (G12S, G12A, G12V, G12D, G12R, and G12C) (technical validation purposes – see section 2.4) as well as mutations identified by targeted sequencing. These included mutations in the following genes: *PIK3CA* (R88Q, H1047R), *ERRB2* (S310F), *CTNNB1* (G34V), *FGFR2* (K659E) *NRAS* (G13D), as well as other mutations affecting *KRAS* (G13D).

The list of primers used for our ddPCR assays are provided in Table 2.2, whereas the specific details on each ddPCR assay and their corresponding optimal annealing/extension temperature are provided in Table 2.3.

Table 2.2: Primers designed for ddPCR experiments.

Assay	Description	Primer Sequence	Source
KRAS G12/G13 (all)	forward	5'-GCCTGCTGAAAATGACTGAATATAAACT-3'	Applied Biosystems, Inc., USA
	reverse	5'-GCTGTATCGTCAAGGCACTCTT -3'	Applied Biosystems, Inc., USA
PIK3CA R88Q	forward	pre-designed; included in assay (see Table 2.3)	Bio-Rad Laboratories, USA
	reverse	pre-designed; included in assay (see Table 2.3)	Bio-Rad Laboratories, USA
PIK3CA H1047R	forward	pre-designed; included in assay (see Table 2.3)	Bio-Rad Laboratories, USA
	reverse	pre-designed; included in assay (see Table 2.3)	Bio-Rad Laboratories, USA
ERBB2 S310F	forward	pre-designed; included in assay (see Table 2.3)	Bio-Rad Laboratories, USA
	reverse	pre-designed; included in assay (see Table 2.3)	Bio-Rad Laboratories, USA
CTNNB1 G34V	forward	pre-designed; included in assay (see Table 2.3)	Bio-Rad Laboratories, USA
	reverse	pre-designed; included in assay (see Table 2.3)	Bio-Rad Laboratories, USA
FGFR2 K659E	forward	5'-GCCAGAGATATCAACAATATAGACTATT -3'	Integrated DNA Technologies, Inc., USA
	reverse	5'-CTGTGTTACTGCCATCGACTTA -3'	Integrated DNA Technologies, Inc., USA
NRAS G13D	forward	pre-designed; included in assay (see Table 2.3)	Bio-Rad Laboratories, USA
	reverse	pre-designed; included in assay (see Table 2.3)	Bio-Rad Laboratories, USA

Table 2.3: ddPCR assay details and optimal extension temperatures.

Assay	Description	Probe Details	Source	Extension Temp. (°C)	Assay Specifications
KRAS G12S (c.34G>A)	Wildtype	5'-Yak Yellow-CGCC+A+C+CA+GCT-IABkFQ-3'	Integrated DNA Technologies, Inc., USA	60	500nM primer + 200nM probe
	Mutant	5'-FAM-CGC+CA+C+T+AGC-IABkFQ-3'	Integrated DNA Technologies, Inc., USA		
KRAS G12A (c.35G>C)	Wildtype	5'-Yak Yellow-CGCC+A+C+CA+GCT-IABkFQ-3'	Integrated DNA Technologies, Inc., USA	60	500nM primer + 200nM probe
	Mutant	5'-FAM-CGCC+A+G+CA+GCT-IABkFQ-3'	Integrated DNA Technologies, Inc., USA		
KRAS G12V (c.35G>T)	Wildtype	5'-Yak Yellow-CGCC+A+C+CA+GCT-IABkFQ-3'	Integrated DNA Technologies, Inc., USA	60	500nM primer + 200nM probe
	Mutant	5'-FAM-CG+CC+A+A+CAGC+TC-IABkFQ-3'	Integrated DNA Technologies, Inc., USA		
KRAS G12D (c.35G>A)	Wildtype	5'-VIC-TTGGAGCTGGTGGCGTA-NFQ-3'	Applied Biosystems, Inc., USA	60	assay at 40X - use 1x primer/probe mix
	Mutant	5'-FAM-TTGGAGCTGATGGCGTA-NFQ-3'	Applied Biosystems, Inc., USA		
KRAS G12R (c.34G>C)	Wildtype	5'-VIC-TTGGAGCTGGTGGCGTA-NFQ-3'	Applied Biosystems, Inc., USA	60	assay at 40X - use 1x primer/probe mix
	Mutant	5'-FAM-TTGGAGCTCGTGGCGTA-NFQ-3'	Applied Biosystems, Inc., USA		
KRAS G12C (C.34G>T)	Wildtype	5'-VIC-TTGGAGCTGGTGGCGTA-NFQ-3'	Applied Biosystems, Inc., USA	60	assay at 40X - use 1x primer/probe mix
	Mutant	5'-FAM-TTGGAGCTTGTGGCGTA-NFQ-3'	Applied Biosystems, Inc., USA		
KRAS G13D (c.38G>A)	Wildtype	5'-Yak Yellow-TA+CG+C+C+ACCA-IABkFQ-3'	Integrated DNA Technologies, Inc., USA	60	500nM primer + 200nM probe
	Mutant	5'-FAM-CTA+C+G+T+CAC+CA-IABkFQ-3'	Integrated DNA Technologies, Inc., USA		
PIK3CA R88Q (c.263G>A)	Wildtype	PIK3CA WT for p.R88Q, Human (dHsaCP2500559)	Bio-Rad Laboratories, USA	55	450nM primer + 250nM probe
	Mutant	PIK3CA p.R88Q, Human (dHsaCP2500558)	Bio-Rad Laboratories, USA		

Assay	Description	Probe Details	Source	Extension Temp. (°C)	Assay Specifications
PIK3CA H1047R (c.3140A>G)	Wildtype	PIK3CA WT for p.H1047R, Human (dHsaCP2000078)	Bio-Rad Laboratories, USA	55	450nM primer + 250nM probe
	Mutant	PIK3CA p.H1047R, Human (dHsaCP2000077)	Bio-Rad Laboratories, USA		
ERBB2 S310F (c.929C>T)	Wildtype	ERBB2 WT for p.S310F, Human (dHsaIS2501415)	Bio-Rad Laboratories, USA	54	900nM primer + 450nM probe
	Mutant	ERBB2 p.S310F, Human (dHsaIS250141)	Bio-Rad Laboratories, USA		
CTNNB1 G34V (c.101G>T)	Wildtype	CTNNB1 WT for p.G34V, Human (dHsaCP2500551)	Bio-Rad Laboratories, USA	55	450nM primer + 250nM probe
	Mutant	CTNNB1 p.G34V, Human (dHsaCP2500550)	Bio-Rad Laboratories, USA		
FGFR2 K659E (c.1975A>G)	Wildtype	5'-HEX-CAA+A+A+AGA+C+C+ACC-IABkFQ-3'	Integrated DNA Technologies, Inc., USA	53	500nM primer + 200nM probe
	Mutant	5'-FAM-CAA+A+G+AGA+C+CA-IABkFQ-3'	Integrated DNA Technologies, Inc., USA		
NRAS G13D (c.38G>A)	Wildtype	NRAS WT for p.G13D, Human (dHsaCP2500527)	Bio-Rad Laboratories, USA	55	450nM primer + 250nM probe
	Mutant	NRAS p.G13D, Human (dHsaCP2500526)	Bio-Rad Laboratories, USA		

2.3.2 Pre-Amplification

Since targeted sequencing requires a DNA input of 45-75 ng, DNA remaining for ddPCR validation was often limited. Therefore, I performed DNA pre-amplification for 10 cycles. Thermocycler conditions for pre-amplification were as follows: polymerase activation at 95ºC for 10 minutes followed by 10 cycles of 94ºC for 30 seconds and annealing/extension at an optimal temperature (for the specific ddPCR assay used) (see Table 2.3) for 4 minutes.

2.3.3 Droplet Generation and Quantification

Using the QX200 Droplet Generator (Bio-Rad Laboratories, USA), droplets were generated in a 25uL reaction consisting of ddPCR™ Supermix for Probes (no dUTP) (Bio-Rad Laboratories, USA), diluted pre-amplification PCR product, and PrimePCR™ ddPCR™ Mutation Assays (Bio-Rad Laboratories, USA) for mutations of interest at primer/probe concentrations according to the manufacturer's protocol (see Table 2.3).

The following conditions were used for PCR cycle amplification for ddPCR analysis: initial polymerase activation at 95ºC for 10 minutes, then 40 cycles of denaturation at 94ºC for 30 seconds followed by annealing/extension at an optimal temperature for the specific ddPCR assay used (see Table 2.2) for 90 seconds (with ramp of 2.5ºC per second to reach temperature), and final denaturation of 98ºC for 10 minutes. After thermal cycling, the QX200 Droplet Reader (Bio-Rad Laboratories, USA) was used to quantify droplets.

2.3.4 ddPCR Controls

For each assay, I ran the following controls alongside samples of interest:

Positive control: Sheared DNA from the sources listed in Table 2.4 below

Negative/wild type-only control: macrodissected, normal tissue

No-Template control: ddH_20

Table 2.4: Positive controls used for ddPCR experiments. The wildtype DNA was supplied from Promega Corporation, USA. All custom-designed oligos were designed by Integrated DNA Technologies, Inc., USA.

Assay	Description of Positive Control
KRAS G12S	1:1 mix of A549 cell line and wildtype DNA
KRAS G12A	H2009 cell line
KRAS G12V	1:1 mix of OvCar5 cell line and wildtype DNA
KRAS G12D	HEY cell line
KRAS G12R	PK-8 cell line
KRAS G12C	MIA PaCa-2 cell line
KRAS G13D	HCT116 cell line
PIK3CA R88Q	1:1 mix of custom-designed oligo and wildtype DNA
PIK3CA H1047R	HCT116 cell line
ERBB2 S310F	1:1 mix of custom-designed oligo and wildtype DNA
CTNNB1 G34V	1:1 mix of custom-designed oligo and wildtype DNA
FGFR2 K659E	1:1 mix of custom-designed oligo and wildtype DNA
NRAS G13D	1:1 mix of custom-designed oligo and wildtype DNA

Mutations were determined to be “real” if the VAFs determined by ddPCR were at least 3X higher than the average background mutation rate determined from three different negative control specimens (macrodissected, normal tissue).

2.4 Technical Validation

In our previous paper, we identified mutations by targeted sequencing (TruSeq Amplicon Cancer Panel and TruSeq Amplicon Custom Panel) using laser-captured tissue[59]. LCM-based enrichment was necessary to achieve high enough VAFs for possible mutations in endometriosis lesions to be detected by TruSeq panel sequencing. Laser-capturing tissue for every sample analyzed is a time-consuming, costly (due to labour and operation costs) task that may take up to a few days per sample. Furthermore, the amount of sections required to obtain enough DNA for sequencing was high – most cases required 15-25 slides of 8μm tissue sections. For these reasons, we performed targeted panel sequencing in this study using the FIND IT^{TM} version 3.4 assay (Contextual Genomics, Canada). Because this assay is capable of detecting mutations at very low frequencies (1% and possibly lower), I sought to determine whether FIND IT^{TM} would be able to detect somatic mutations in macrodissected tissue (which is far less time consuming to collect and usually requires between 2-14 8μm sections only). Among DE cases analyzed in our previous study, the most commonly observed mutations were *KRAS* G12 mutations (6 of 39 cases)[59]. Therefore, I sought to perform technical validation of the analysis of macrodissected FFPE tissue by FIND IT^{TM} by comparing *KRAS* mutations detected by the FIND IT^{TM} to ddPCR (the gold standard for quantitative mutation detection).

2.4.1 *KRAS* G12 Variant Screening

My technical validations were performed on endometriosis specimens from the IE and DE cases studied in Chapter 3. Independent of mutation calling from targeted sequencing, one block containing endometriosis from each patient was tested for *KRAS* G12 (G12S, G12A, G12V, G12D, G12R, G12C) variants (a subset of cases were also tested for G13D) (see Table 2.5). To be conservative on reporting *KRAS* mutations in macrodissected samples and to reflect mutation calling VAF thresholds by targeted sequencing, I set a cut-off of 0.80% VAF for all KRAS G12 variants. This cut-off is above the empirically determined positive thresholds (defined as 3X the average background mutation rate) for all KRAS G12 variants as indicated below:

KRAS G12S (c.34G>S) assay > 0.673%

KRAS G12A (c.35G>C) assay > 0.0243%

KRAS G12V (c.35G>T) assay > undetermined (only positive control specimens recorded mutant droplet counts)

KRAS G12D (c.35G>A) assay > 0.392%

KRAS G12R (c.34G>C) assay > *undetermined*

KRAS G12C (C.34G>T) assay > undetermined

Table 2.5 summarizes all *KRAS* G12 (and G13D) calls by both targeted sequencing and ddPCR. True positive calls were considered those that were positive via targeted sequencing AND ddPCR assay, whereas false positive calls were considered those that were positive via targeted sequencing but not ddPCR. Overall, with these thresholds, I observed a sensitivity of 88.9% (95% CI: 51.7% - 99.7%) and specificity of 97.0% (95% CI: 89.6% - 99.6%) for the detection of *KRAS* G12/G13 mutations by FIND IT™ version 3.4 (Contextual Genomics, Canada).

Table 2.5: KRAS G12/G13 variant calling by targeted sequencing and droplet digital PCR. For readability purposes, variant allele frequencies (VAFs) are not stated in this table unless they surpassed the KRAS mutation calling threshold (VAF of 0.80%).

Patient ID	Block ID and Descriptor	Targeted Sequencing		Droplet Digital PCR			Annotation
		Collection Method and Specimen Descriptor	Mutation Identified and VAF (%)	Collection Method and Specimen Descriptor	ddPCR KRAS assay performed	Mutation Identified and VAF (%)	
IE_1	A: index	macrodissected - mixed		macrodissected - mixed	G12A, G12C, G12D, G12V, G12R, G12S		
IE_2	A: index	macrodissected - mixed		macrodissected - mixed	G12A, G12C, G12D, G12V, G12R, G12S		
IE_3	A: index	macrodissected - mixed		macrodissected - mixed	G12A, G12C, G12D, G12V, G12R, G12S		
IE_4	A: index	macrodissected - mixed		macrodissected - mixed	G12A, G12C, G12D, G12V, G12R, G12S		
IE_5	A: index	macrodissected - mixed		macrodissected - mixed	G12A, G12C, G12D, G12V, G12R, G12S		
IE_6	A: index	macrodissected - mixed		macrodissected - mixed	G12A, G12C, G12D, G12V, G12R, G12S		
IE_7	A: index	macrodissected - mixed		macrodissected - mixed	G12A, G12C, G12D, G12V, G12R, G12S		
IE_8	A: index	macrodissected - mixed	KRAS G12V (3.04%)	macrodissected - mixed	G12A, G12C, G12D, G12V, G12R, G12S	KRAS G12V (2.53%)	true positive for KRAS G12V
IE_9	A: index	macrodissected - mixed		macrodissected - mixed	G12A, G12C, G12D, G12V, G12R, G12S		
IE_10	A: index	macrodissected - mixed		macrodissected - mixed	G12A, G12C, G12D, G12V, G12R, G12S		
IE_11	A: index	macrodissected - mixed		macrodissected - mixed	G12A, G12C, G12D, G12V, G12R, G12S		
IE_12	A: index	macrodissected - mixed		macrodissected - mixed	G12A, G12C, G12D, G12V, G12R, G12S		
IE_13	A: index	macrodissected - mixed		macrodissected - mixed	G12A, G12C, G12D, G12V, G12R, G12S		
IE_14	A: index	macrodissected - mixed		macrodissected - mixed	G12A, G12C, G12D, G12V, G12R, G12S		
IE_15	A: index	macrodissected - mixed	KRAS G12V (6.407)	macrodissected - mixed	G12A, G12C, G12D, G12V, G12R, G12S		false positive for KRAS G12V

Patient ID	Block ID and Descriptor	Targeted Sequencing		Droplet Digital PCR			Annotation
		Collection Method and Specimen Descriptor	Mutation Identified and VAF (%)	Collection Method and Specimen Descriptor	ddPCR KRAS assay performed	Mutation Identified and VAF (%)	
IE_16	A: index	macrodissected - mixed		macrodissected - mixed	G12A, G12C, G12D, G12V, G12R, G12S		
IE_17	A: index	macrodissected - mixed		macrodissected - mixed	G12A, G12C, G12D, G12V, G12R, G12S		
IE_18	A: index	macrodissected - mixed		macrodissected - mixed	G12A, G12C, G12D, G12V, G12R, G12S		
IE_19	A: index	macrodissected - mixed	KRAS G12C (4.833%)	macrodissected - mixed	G12A, G12C, G12D, G12V, G12R, G12S	KRAS G12C (4.19%)	true positive for KRAS G12C
IE_20	A: index	macrodissected - mixed		macrodissected - mixed	G12A, G12C, G12D, G12V, G12R, G12S		
IE_21	A: index	macrodissected - mixed		macrodissected - mixed	G12A, G12C, G12D, G12V, G12R, G12S		
IE_22	A: index	macrodissected - mixed		macrodissected - mixed	G12A, G12C, G12D, G12V, G12R, G12S		
IE_23	A: index	macrodissected - mixed		macrodissected - mixed	G12A, G12C, G12D, G12V, G12R, G12S		
IE_24	A: index	macrodissected - mixed		macrodissected - mixed	G12A, G12C, G12D, G12V, G12R, G12S		
IE_25	A: index	macrodissected - mixed		macrodissected - mixed	G12A, G12C, G12D, G12V, G12R, G12S		
IE_26	A: index	macrodissected - mixed		macrodissected - mixed	G12A, G12C, G12D, G12V, G12R, G12S		
IE_27	A: index	macrodissected - mixed		macrodissected - mixed	G12A, G12C, G12D, G12V, G12R, G12S		
IE_28	A: index	macrodissected - mixed		macrodissected - mixed	G12A, G12C, G12D, G12V, G12R, G12S		
IE_29	A: index	macrodissected - mixed		macrodissected - mixed	G12A, G12C, G12D, G12V, G12R, G12S		
IE_30	A: index	macrodissected - mixed		macrodissected - mixed	G12A, G12C, G12D, G12V, G12R, G12S		
IE_31	A: index	macrodissected - mixed		macrodissected - mixed	G12A, G12C, G12D, G12V, G12R, G12S		
IE_32	A: index	macrodissected - mixed		macrodissected - mixed	G12A, G12C, G12D, G12V, G12R, G12S		

Patient ID	Block ID and Descriptor	Targeted Sequencing		Droplet Digital PCR			Annotation
		Collection Method and Specimen Descriptor	Mutation Identified and VAF (%)	Collection Method and Specimen Descriptor	ddPCR KRAS assay performed	Mutation Identified and VAF (%)	
IE_33	A: index	macrodissected - mixed		macrodissected - mixed	G12A, G12C, G12D, G12V, G12R, G12S		
IE_34	A: index	macrodissected - mixed		macrodissected - mixed	G12A, G12C, G12D, G12V, G12R, G12S		
IE_35	A: index	macrodissected - mixed		macrodissected - mixed	G12A, G12C, G12D, G12V, G12R, G12S		
IE_36	A: index	macrodissected - mixed		macrodissected - mixed	G12A, G12C, G12D, G12V, G12R, G12S		
IE_37	A: index	macrodissected - mixed		macrodissected - mixed	G12A, G12C, G12D, G12V, G12R, G12S		
IE_38	A: index	LCM - mixed		LCM - mixed	multiplex (G12A, G12C, G12D, G12V, G12R, G12S, G13D)		
IE_39	A: index	LCM - mixed		LCM - mixed	multiplex (G12A, G12C, G12D, G12V, G12R, G12S, G13D)		
IE_40	A: index	LCM - mixed		LCM - mixed	multiplex (G12A, G12C, G12D, G12V, G12R, G12S, G13D)		
DE_1	A: index	macrodissected - mixed		LCM - mixed	G12A, G12C, G12D, G12V, G12R		
DE_2	A: index	macrodissected - mixed	KRAS G12D (2.807%)	macrodissected - mixed	G12A, G12C, G12D, G12V, G12R, G12S	KRAS G12D (2.14%)	true positive for KRAS G12D
DE_3	A: index	macrodissected - mixed		LCM - mixed	G12A, G12C, G12D, G12V, G12R		
DE_4	A: index	macrodissected - mixed		macrodissected - mixed	G12A, G12C, G12D, G12V, G12R		
DE_5	A: index	macrodissected - mixed	KRAS G12D (0.932%)	LCM - mixed	G12A, G12C, G12D, G12V, G12R	KRAS G12D (2.065%)	true positive for KRAS G12D
DE_6	A: index	macrodissected - mixed		macrodissected - mixed	G12A, G12C, G12D, G12V, G12R		
DE_7	A: index	macrodissected – mixed		LCM - mixed	G12A, G12C, G12D, G12V, G12R		

Patient ID	Block ID and Descriptor	Targeted Sequencing		Droplet Digital PCR			Annotation
		Collection Method and Specimen Descriptor	Mutation Identified and VAF (%)	Collection Method and Specimen Descriptor	ddPCR KRAS assay performed	Mutation Identified and VAF (%)	
DE_8	A: index	macrodissected – mixed		LCM - mixed	G12A, G12C, G12D, G12V, G12R		
DE_9	A: index	macrodissected – mixed		LCM - mixed	G12A, G12C, G12D, G12V, G12R		
DE_10	A: index	macrodissected – mixed		LCM - mixed	G12A, G12C, G12D, G12V, G12R	KRAS G12V (3.589%)	false negative for KRAS G12V
DE_11	A: index	macrodissected – mixed	KRAS G12D (1.108%)	macrodissected - mixed	G12A, G12C, G12D, G12V, G12R, G12S	KRAS G12D (1.03%)	true positive for KRAS G12D
DE_12	A: index	macrodissected – mixed		macrodissected - mixed	G12A, G12C, G12D, G12V, G12R, G12S		
DE_13	A: index	macrodissected – mixed		macrodissected - mixed	G12A, G12C, G12D, G12V, G12R, G12S		
DE_14	A: index	macrodissected – mixed	KRAS G12C (1.05%)	macrodissected - mixed	G12A, G12C, G12D, G12V, G12R, G12S	KRAS G12C (1.19%)	true positive for KRAS G12C
DE_15	A: index	macrodissected – mixed		macrodissected - mixed	G12A, G12C, G12D, G12V, G12R, G12S		
DE_16	A: index	macrodissected – mixed		macrodissected - mixed	G12A, G12C, G12D, G12V, G12R, G12S		
DE_17	A: index	macrodissected – mixed		macrodissected - mixed	G12A, G12C, G12D, G12V, G12R, G12S		
DE_18	A: index	macrodissected – mixed	KRAS G13D (2.158%)	macrodissected - mixed	G12A, G12C, G12D, G12V, G12R, G12S, G13D		false postive for KRAS G13D
DE_19	B: separate	macrodissected – mixed		macrodissected - mixed	G12A, G12C, G12D, G12V, G12R, G12S		
DE_20	A: index	macrodissected – mixed		macrodissected - mixed	G12A, G12C, G12D, G12V, G12R, G12S		
DE_21	B: separate	macrodissected – mixed	KRAS G12V (2.627%)	macrodissected - mixed	G12A, G12C, G12D, G12V, G12R, G12S	KRAS G12V (2.81%)	true positive for KRAS G12V
DE_22	A: index	macrodissected – mixed		macrodissected - mixed	G12A, G12C, G12D, G12V, G12R, G12S		

Patient ID	Block ID and Descriptor	Targeted Sequencing		Droplet Digital PCR			Annotation
		Collection Method and Specimen Descriptor	Mutation Identified and VAF (%)	Collection Method and Specimen Descriptor	ddPCR KRAS assay performed	Mutation Identified and VAF (%)	
DE_23	A: index	macrodissected – mixed		macrodissected - mixed	G12A, G12C, G12D, G12V, G12R, G12S		
DE_24	A: index	LCM - mixed		LCM - mixed	multiplex - G12A, G12C, G12D, G12V, G12R, G12S, G13D		
DE_25	A: index	LCM - mixed		LCM - mixed	multiplex - G12A, G12C, G12D, G12V, G12R, G12S, G13D		
DE_26	A: index	LCM - mixed		LCM - mixed	multiplex - G12A, G12C, G12D, G12V, G12R, G12S, G13D		
DE_27	A: index	LCM - mixed		LCM - mixed	multiplex - G12A, G12C, G12D, G12V, G12R, G12S, G13D		
DE_28	A: index	LCM - mixed		LCM - mixed	multiplex - G12A, G12C, G12D, G12V, G12R, G12S, G13D		
DE_29	A: index	LCM - mixed		LCM - mixed	multiplex - G12A, G12C, G12D, G12V, G12R, G12S, G13D		
DE_30	A: index	LCM - mixed		LCM - mixed	multiplex - G12A, G12C, G12D, G12V, G12R, G12S, G13D		
DE_31	A: index	LCM - mixed		LCM - mixed	multiplex - G12A, G12C, G12D, G12V, G12R, G12S, G13D		
DE_32	A: index	LCM - mixed	KRAS G12A (10.749%)	LCM - mixed	multiplex - G12A, G12C, G12D, G12V, G12R, G12S, G13D	KRAS G12 (10.41%)	true postive for KRAS G12A
DE_33	A: index	LCM - mixed		LCM - mixed	multiplex - G12A, G12C, G12D, G12V, G12R, G12S, G13D		
DE_34	A: index	LCM - mixed		LCM - mixed	multiplex - G12A, G12C, G12D, G12V, G12R, G12S, G13D		
DE_35	A: index	LCM - mixed		LCM - mixed	multiplex - G12A, G12C, G12D, G12V, G12R, G12S, G13D		

Patient ID	Block ID and Descriptor	Targeted Sequencing		Droplet Digital PCR			Annotation
		Collection Method and Specimen Descriptor	Mutation Identified and VAF (%)	Collection Method and Specimen Descriptor	ddPCR KRAS assay performed	Mutation Identified and VAF (%)	
DE_36	A: index	LCM - mixed		LCM - mixed	multiplex - G12A, G12C, G12D, G12V, G12R, G12S, G13D		

2.5 Immunohistochemistry

2.5.1 ARID1A immunohistochemistry

Loss of ARID1A is implicated as an early event in the malignant transformation of cancer and has been observed in endometriosis lesions both within and outside of the context of cancer[58,77]. Especially since the FIND IT™ version 3.4 assay does not cover the *ARID1A* gene, we performed ARID1A immunohistochemistry (IHC) on endometriosis and eutopic endometrium cases analyzed in this study. In particular, loss of nuclear ARID1A immunoreactivity was used as a surrogate for *ARID1A* inactivating mutations – studies suggest that there is good concordance between ARID1A IHC findings and *ARID1A* mutational status[78]. Archival tissue sections were stained on the Dako Omnis (Agilent Technologies, USA) automated immunostainer with the use of a 1:150 dilution of ARID1A rabbit polyclonal antibody (HPA005456, Sigma-Aldrich, USA) for batch at 0.1mg/ml or 1:200 for batch at 0.2 mg/ml[59]. Slides underwent a 10-X-10 incubation and detection was HRP based using 3,3'-diaminobenzidine (DAB). A pathologist, Dr. Tayyebeh M. Nazeran, and a pathology resident, Dr. Basile Tessier-Cloutier, scored ARID1A immunostained slides.

2.5.1 PTEN immunohistochemistry

PTEN mutations occur commonly in EAOCs and have also been observed in endometriosis[54]. Furthermore, PTEN loss by IHC has been observed in normal, eutopic endometrial glands in nearly half of cases studied by Monte et al. (2010)[73]. Although the FIND IT™ version 3.4 assay has partial coverage of *PTEN,* inactivating mutations in regions not covered by the assay (as well as loss of PTEN by other means such as large-scale deletion or epigenetic mechanisms) would not be detected[79]. Therefore, as with

ARID1A, we performed PTEN IHC on endometriosis and eutopic endometrium cases analyzed in this study. PTEN immunoreactivity was used as a surrogate for *PTEN* inactivating mutations as described in previous work[80]. Immunostains were performed on the Ventana Discovery Ultra (Ventana Medical Systems, USA) immunostainer. Slides underwent antigen retrieval with Cell Conditioning 1 (CC1, Ventana Medical Systems, USA) followed by 60 minutes of primary antibody incubation at room temperature and detected using UltraMap DAB anti-Rb Detection Kit (Ventana Medical Systems, USA). PTEN antibody (rabbit clone 138G6, Cell Signaling, USA) was applied at dilution of 1:25. Dr. Tayyebeh M. Nazeran and Dr. Basile Tessier-Cloutier, scored PTEN immunostained slides.

3. Somatic Cancer-Driver Mutations in Incisional Endometriosis

In this chapter, I sought to investigate the prevalence of somatic cancer-driver mutations in endometriosis by comparing DE to another form that is unlikely to undergo malignant transformation. Specifically, I examined IE, an iatrogenic form of endometriosis that occurs in the resulting surgical scars of obstetric or gynecological procedures[18]. Unlike other forms of endometriosis, the uterine origin of cells is well accepted for incisional endometriosis: endometrial cells, both stroma and epithelium, are mechanically transferred to the abdominal fascia or subcutaneous tissue around sites of incision following procedures such as caesarean sections, hysterectomies, myomectomies appendectomies, tubal ligations, and episiotomies[11,81,82]. I compared somatic driver mutation profiles between deep infiltrating endometriosis and incisional endometriosis to determine whether there were differences in mutation profile between these two types of endometriosis with unique differences in their etiologies.

3.1 Patient Specimen Collection

We obtained archival tissue specimens from four independent cohorts of women with IE and two independent cohorts of women with DE.

3.1.1 Overview of Incisional Endometriosis Specimens

The Vancouver General Hospital in Vancouver, BC, Canada contributed tissue samples from 12 IE patients. The Referral Centre for Gynecopathology in Mannheim, Germany contributed endometriotic tissue samples from 10 IE patients. The University Hospital Tuebingen in Tuebingen, Germany contributed tissue samples from 15 IE patients. Lastly, the VU University Medical Center (VUMC) in Amsterdam, The Netherlands contributed tissue samples from three IE patients. Inclusion criteria for the IE cohort were diagnosis with incisional, umbilical, or post C-sectional endometriosis lesions containing both epithelial and stromal components by extensive pathology review, the absence of cancer or dysplasia, and a lesion size sufficient for tissue coring, macrodissection, and/or

laser-capture microdissection. Details of prior surgery and the time interval between suspected inciting surgery and subsequent diagnosis with IE were available for most but not all patients (Appendix A). Note that a few cases included in our IE cohort lacked surgical history or only had a history of surgical abortion and a diagnosis of spontaneous abdominal wall or subcutaneous endometriosis (rather than iatrogenic disease) cannot be ruled out. Adjacent tissue blocks of endometriosis (same anatomical site) were available for sampling for some IE patients (Appendix A).

3.1.2 Overview of Deep Infiltrating Endometriosis Specimens

We obtained FFPE or MFPE (Sakura Finetek, USA) tissue specimens from two independent cohorts of women with deep infiltrating endometriosis (DE). Endometriotic tissue samples from 23 DE patients were retrieved from local pathology archives and the prospective tissue bank at BC Women's Centre for Pelvic Pain and Endometriosis in Vancouver, BC, Canada. Ten cases (Patients DE_1 to DE_10) overlap with our previous study (Appendix B) wherein they were analyzed by droplet digital PCR for *KRAS* mutations alone[59]. Here we include them with a broader genomic analysis as noted below. The VUMC contributed tissue samples from an additional 13 DE patients. Inclusion criteria for the DE cohort were local invasion > 5mm, pathologist-confirmed endometriosis, the absence of cancer or dysplasia, and a lesion size sufficient for tissue coring, macrodissection, and/or laser-capture microdissection. Blocks of tissue representing DE at distant/anatomically distinct sites were available for several cases (Appendix B).

3.1.3 Ethics Approval

Institutional review boards at each respective hospital approved tissue collection and collection of clinical data. Detailed description of specimens collected from each hospital site are provided in sections 3.1.4 – 3.1.8.

3.1.4 Vancouver General Hospital (VGH) Cohort

Tissue specimens from 12 women were obtained from the Department of Anatomical Pathology at the Vancouver General Hospital in Vancouver, Canada. These cases were identified using the search terms “endometriosis”, “scar”, “incisional”, “C-section” and “laparoscopic” between January 2004 and 2017. Inclusion criteria were limited to the pathologic diagnosis of endometriosis in a laparoscopic or a C-section scar. Patient were excluded if a malignancy was diagnosed in the same specimen. Specimen collection and retrieval of clinical data was approved by the UBC BC Cancer Agency Research Ethics Board [H05-60119]. We also obtained ethics approval for immunohistochemical experiments and next generation sequencing to be performed on these specimens [H02-61375; H08-01411].

3.1.5 The Referral Centre for Gynecopathology (Mannheim) Cohort

Tissue specimens from 10 women with IE were obtained from the Referral Centre for Gynecopathology in Mannheim, Germany. These cases were identified using the search terms equivalent to “endometriosis”, “scar”, “incisional”, “C-section” and “laparoscopic” between January 2010 and 2016. Most patients presented with painful nodules in C-section scars which were then surgically removed. No clinical data aside from age and site of endometriosis have been provided for these cases.

3.1.6 University Hospital Tuebingen (Tuebingen) Cohort

Tissue specimens from 15 women with IE were obtained from the University Hospital Tuebingen in Tuebingen, Germany. These cases were identified using the search terms equivalent to “endometriosis”, “scar”, “incisional”, and “C-section” between January 2007 and June 2017. Inclusion criteria were limited to the pathologic diagnosis of endometriosis in a laparoscopic or a C-section scar. Patient were excluded if a malignancy was diagnosed in the same specimen. Specimen collection and retrieval of clinical data was approved by the institutional research ethics committee.

3.1.7 VU University Medical Center (VUMC) Cohort

Note that the VUMC contributed both IE and DE specimens. Tissue specimens from 13 women with DE and 3 women with IE were retrieved from the Biobank Unit Pathology at the VU University Medical Center in Amsterdam, the Netherlands. All women had histologically proven endometriosis without any known or diagnosed ovarian cancer during follow up. For DE cases, inclusion criteria were deep endometriosis (within the pelvic cavity) and lack of cancer or dysplasia associated with the lesions. Similarly, for IE cases, inclusion criteria were (extra-pelvic) endometriosis in C-section and lack of cancer or dysplasia associated with the lesions. Specimen and data collection for these cases was approved by the Medical Ethical Committee (METc) of the VUMC, Amsterdam, the Netherlands.

3.1.8 British Columbia Women's Centre for Pelvic Pain and Endometriosis (BC Women's) Cohort

Women with DE were seen at the British Columbia Women's Centre for Pelvic Pain and Endometriosis in Vancouver, Canada. Deep infiltrating endometriosis lesions were clinically defined as lesions with depths greater than 5 mm and were surgically excised with histopathological confirmation of endometriosis epithelial and stromal cells by Dr. Nazeran and Dr. Tessier-Cloutier. Tissues were sourced from the OVCARE Tissue bank (banking performed in accordance with the World Endometriosis Research Foundation Endometriosis Phenome and Biobanking Harmonization Project (EPHect)[83]), with ethics approval from the UBC Children's and Women's Research Ethics Board [H13-02563; H14-03040] for the collection of archival tissue specimens. We have obtained a waiver of consent for specimen collection.

Ten women from our previous study (whose DE lesions were analyzed KRAS mutations via ddPCR)[59] were further analyzed in the current study for other potential somatic cancer-driver alterations. Moreover, we identified and retrieved endometriosis specimens from an additional 13 women with DE.

3.2 Additional Details on Methods

The analyses in this chapter follow the methodology described in Chapter 2. Additional details on methodology specific for this chapter are detailed below. In short, a subset of cases were MFPE tissues (see section 3.2.1) and cases from VUMC (Patients IE_38 to IE_40 and Patients DE_24 to DE_36, see Appendix A; Appendix B) underwent separate experimentation from all other cases (this experimental work was led by Ms. Lisanne Verhoef, a graduate student at the National Cancer Institute in Amsterdam, the Netherlands in a collaborative effort) and is described in sections 3.2.2 – 3.2.7.

3.2.1 Tissue Fixation

A subset of endometriosis specimens analyzed in Chapter 3 were MFPE tissues (Patients DE_3 to DE_10, see Appendix B). All other specimens were FFPE tissues.

3.2.2 Tissue Microarray Construction

Cases from VUMC were used to build tissue microarrays (TMAs). Using a tissue microarrayer (TMA) (Grand Master, Sysmex Europe GmbH, Norderstedt, Germany), a median of four cores (range, 1-15) of endometriosis (morphologically representative lesions, as determined by hematoxylin-eosin (H&E) slides from corresponding cases) with a median donor core height of 3.9 mm (range, 3-5), 2.0-mm diameter core biopsy of the area of interest in the donor block were punched and transferred to a recipient paraffin block.

Note: All subsequent analyses of VUMC cases (including targeted sequencing, ddPCR analysis, and IHC staining) were carried out from TMA tissue sections.

3.2.3 DNA Collection and Extraction

DNA collected for VUMC cases were obtained solely by means of LCM. All cases from VUMC were sectioned at 5μm from TMAs and attached to PEN membrane slides (Leica Microsystems Inc., Switzerland). Sections were deparaffinized applying Tuolidin blue staining by using the ST5020 multi-stainer (Leica Microsystems Inc., Switzerland). Using

the Leica LCM laser microdissection system (Leica Microsystems Inc., Switzerland) endometriotic lesions were microdissected according the manufacturer's instructions.

After laser-capture, DNA from VUMC specimens were extracted using the ARCTURUS® PicoPure® DNA Extraction Kit (ThermoFisher Scientific, USA). Quantification of extracted DNA was performed using the Qubit 2.0 Fluorometer (ThermoFisher Scientific, USA).

3.2.4 Targeted Panel Sequencing

Extracted DNA (75ng) from laser-captured VUMC specimens were sent to Contextual Genomics for targeted panel sequencing using the FIND IT™ version 3.4 assay. In 11/16 (68.8%) cases the optimized 75ng input was not available and therefore a range as low as 45ng was used. The expected enrichment for endometriosis tissues is higher for laser-captured samples compared to macrodissected samples, therefore mutations were called in these laser-captured specimens if the VAF determined by targeted sequencing was 5.0% or higher.

3.2.5 ddPCR

Independent of target panel sequencing findings, VUMC specimens were analyzed for potential *KRAS* mutations from laser-captured material using the ddPCR *KRAS* G12/G13 Screening Kit (catalog #1863506, Bio-Rad Laboratories, USA) following manufacturer's instructions. Positive references were from Horizon Discovery (Cambridge, UK) (15:15 wildtype/mutant) and negative control was H_2O. I have reported these results in our technical validation of the FIND IT™ assay in section 2.4 (see Table 2.5).

3.2.6 ARID1A IHC

Archival TMA tissue sections from VUMC were stained on the BenchMark Ultra autostainer (Ventana Medical Systems, USA) with the use of a 1:100 dilution of ARID1A

rabbit polyclonal antibody (HPA005456, Sigma-Aldrich, USA). Heat-induced antigen retrieval was carried out using Cell Conditioning 2 (CC2, Ventana Medical Systems, USA) for BAF250a (ARID1a) followed by 60 minutes primary antibody incubation at room temperature. Pathologist, Dr. Hugo M. Horlings, scored ARID1A immunostained slides from VUMC.

3.2.7 PTEN IHC

PTEN IHC staining of TMA tissue sections from VUMC were executed on the BenchMark Ultra autostainer (Ventana Medical Systems, USA) followed by heat-induced antigen retrieval with Cell Conditioning 1 (Ventana Medical Systems, USA). Slides then underwent primary antibody incubation with a rabbit monoclonal antibody (SP218, Spring Bioscience, USA) for 32 minutes at 36 degrees at a dilution of 1:100). Dr. Horlings scored PTEN immunostained slides from VUMC.

3.2 Results

3.2.1 Sample Description

I examined somatic mutations in common cancer hotspots in 40 women with IE (total of 59 specimens studied), and in 36 women with DE (total of 43 specimens studied). The mean age of women with IE was 36.5 years with a standard deviation (SD) of 5.5 years (Table 3.1; Fig. 3.1; Appendix A). Between one and four tissue blocks from each patient were collected and analyzed. In four patients (Patients IE_5, IE_10, IE_12, and IE_28) eutopic endometrium samples were available for sequencing – we did not detect somatic cancer-driver mutations in the available eutopic endometrium specimens, although heterogeneous loss of PTEN was noted in 2/4 specimens. Of IE cases with obtainable surgical history, the original surgical procedure performed was most often caesarean section and the interval between the most recent gynecological or obstetric surgery and subsequent diagnosis with IE ranged from 1 month to 11 years.

Table 3.1: Overview of clinical characteristics of women in IE cohort.

Patient characteristics	**IE cohort (n = 40)**
Age (years; mean ± SD)	36.5 ± 5.5
Interval (years; mean ± SD)	5.1 ± 4.4
Diagnosis	
incisional endometriosis	20 (50.0%)
post c-section endometriosis	11 (27.5%)
umbilical endometriosis	9 (22.5%)
Surgical History	
c-section	25 (62.5%)
laparascopy	4 (10.0%)
no prior surgery identified	3 (7.5%)
hysterectomy	2 (5.0%)
surgical abortion	2 (5.0%)
umbilical hernia	1 (2.5%)
adnexectomy	1 (2.5%)
n/a	2 (5.0%)

The mean age of women with DE was 33.9 years with SD of 7.0 years (Table 3.2; Fig. 3.1; Appendix B). Although most women were affected with DE at a single anatomical site, several women had multiple DE lesions at distinct anatomical sites, these additional lesions were included when available. The mean age of women in the IE and DE cohorts were not significantly different (p = 0.0765, Student's t-test) (Fig. 3.1).

Table 3.2: Overview of clinical characteristics of women in DE cohort.

Patient characteristics	**DE cohort (n = 36)**
Age (years; mean ± SD)	33.9 ± 7.0
ASRM Clinical Stage	
I	1 (2.8%)
II	5 (13.9%)
III	10 (27.8%)
IV	20 (55.6%)

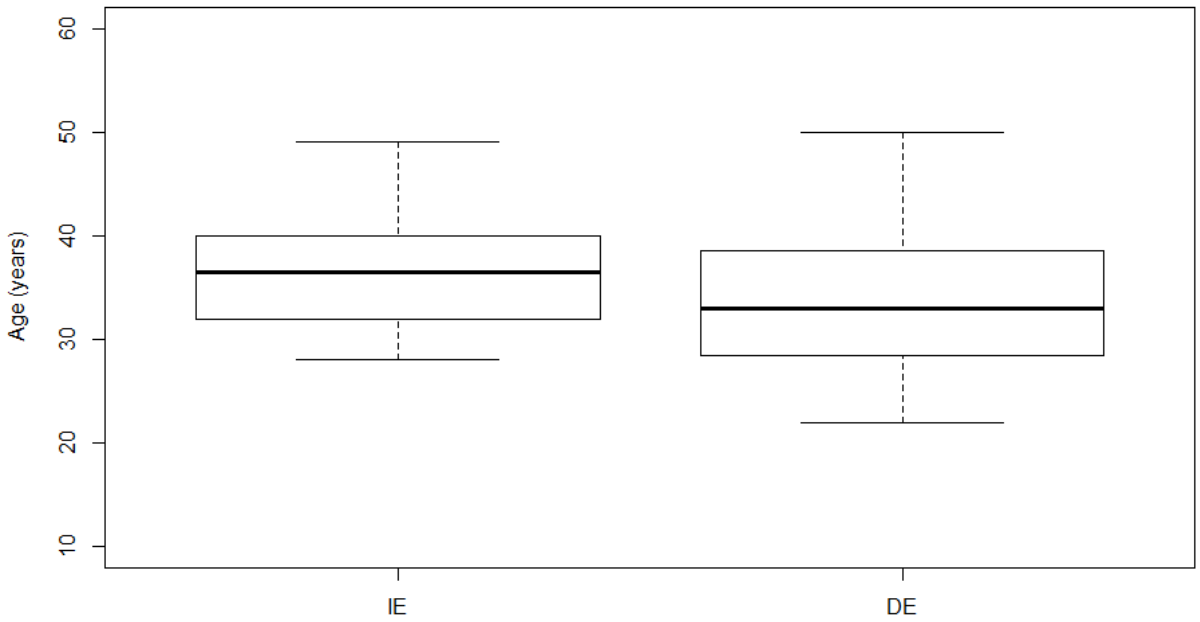

Figure 3.1: Boxplot comparison of age of IE and DE patients. The difference in age of women with IE and women with DE in this study is not statistically significant (p = 0.0765, Student's t-test).

3.2.2 Targeted Panel Sequencing

Of 40 patients with IE, four patients (10.0%) harbored somatic COSMIC hotspot mutations in either *KRAS* (2), *PIK3CA* (1), or *ERBB2* (1) (Table 3.3). Of 36 patients with DE, nine patients (25.0%) harboured somatic cancer-driver mutations in either *KRAS* (7), *CTNNB1* (1), or *PIK3CA* (1) (Table 3.3).

To identify which cells in endometriosis lesions harboured the mutations I detected, I performed epithelial and stromal separation of endometriotic lesions by LCM. We previously determined *KRAS* G12 mutations to be restricted to the epithelial component of endometriotic lesions using ddPCR from laser-captured epithelium and stromal compartments[59] . Similarly, I was able to confirm that *CTNNB1*, *PIK3CA*, and *ERBB2* hotspot mutations were also enriched in the epithelium of endometriotic glands (Table 3.3; Fig. 3.2). Hotspot *KRAS* mutations remained the most common somatic cancer-driver mutations detected in both IE and DE: there were *KRAS* mutations in 2 of 40 patients with IE (5%) compared to 7 of 36 patients with DE (19.4%) (p = 0.076, Fisher's exact test).

Note: I also collected laser-captured tissue in a subset of cases (Patients IE_1 to IE_20 and Patients DE_1 to DE_10) to determine the differences in enrichment between macrodissected and laser-captured specimens when somatic mutations are detected. Overall, I observe an enrichment of 6.7 times in mixed, laser-captured specimens over mixed, macrodissected specimens.

Table 3.3: Somatic cancer-driver mutations detected in endometriosis specimens from women with IE or DE. The VAF of macrodissected or laser-captured specimens as determined by means of targeted panel sequencing and corresponding ddPCR assays are presented below. "Adjacent" refers to tissue specimens obtained from a different archival tissue block yet the same anatomical site as the index block. "Separate" refers to specimens obtained from an anatomically distinct site from the index block.

Patient and Block	Descriptor	Driver Mutation Identified	Collection Method and Component	VAF (%) - Targeted Sequencing	VAF (%) - ddPCR
IE_8A	index	KRAS G12V	macrodissection: mixed	3.04	2.53
		KRAS G12V	LCM: mixed		28.7
IE_8B	adjacent	KRAS G12V	macrodissection: mixed	not detected	3.29
IE_16A	index	ERBB2 S310F	macrodissection: mixed	3.336	3.97
		ERBB2 S310F	LCM: mixed		18.2
		ERBB2 S310F	LCM: epithelium		21.4
		ERBB2 S310F	LCM: stroma		1.36
IE_19A	index	KRAS G12C	macrodissection: mixed	4.833	4.19
		KRAS G12C	LCM: mixed		29.5
IE_25A	index	PIK3CA H1047R	macrodissection: mixed	5.359	5.79
		PIK3CA H1047R	LCM: epithelium		24.9
		PIK3CA H1047R	LCM: stroma		0.567
DE_1A	index	CTNNB1 G34V	macrodissection: mixed	3.933	3.88
		CTNNB1 G34V	LCM: epithelium		19.5
		CTNNB1 G34V	LCM: stroma		0.664
DE_2A	index	KRAS G12D	macrodissection: mixed	2.807	2.14
		KRAS G12D	LCM: epithelium		38.125
		KRAS G12D	LCM: stroma		0.002
DE_5A	index	KRAS G12D	macrodissection: mixed	0.932	n/a
		KRAS G12D	LCM: mixed		2.065
DE_10A	index	KRAS G12V	macrodissection: mixed	not detected	0.941
		KRAS G12V	LCM: mixed		3.589
DE_11A	index	KRAS G12D	macrodissection: mixed	1.108	1.03
DE_14A	index	KRAS G12C	macrodissection: mixed	1.05	1.19
DE_15A	index	PIK3CA E545A	macrodissection: mixed	1.546	n/a
DE_21B	separate	KRAS G12V	macrodissection: mixed	2.627	2.81
DE_32A	index	KRAS G12A	LCM: mixed	10.749	10.41

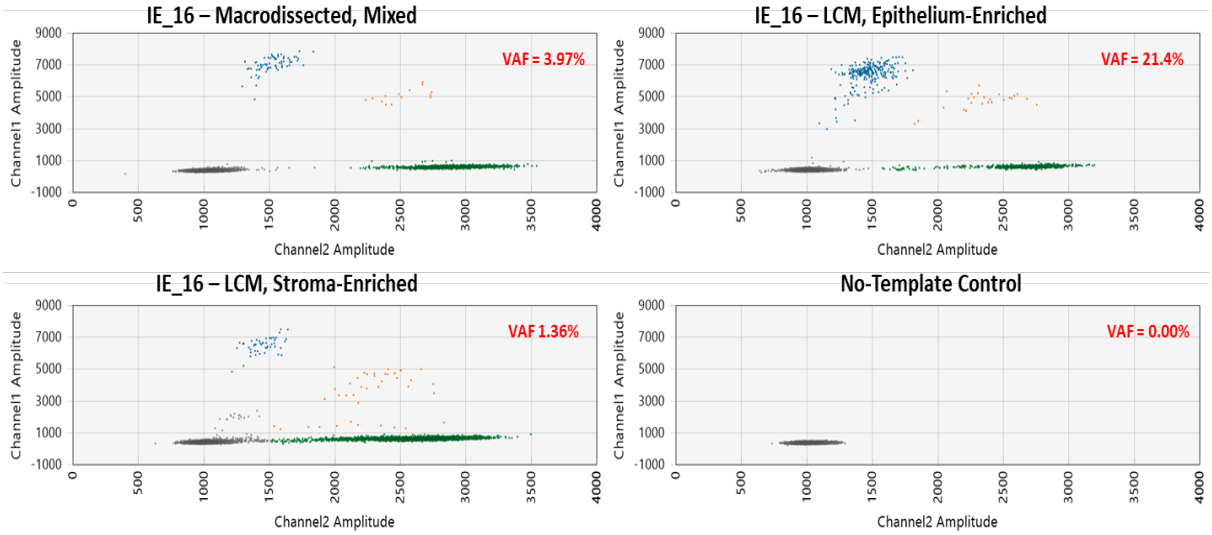

Figure 3.2. ddPCR validation of ERRB2 c.929C>T (p.S310F) mutation in the epithelial component of endometriosis in Patient IE_16. Patient IE_16 harbours an ERBB2 *S310F mutation as detected by ddPCR in a macrodissected endometriosis sample. The VAF in the epithelium-enriched, LCM sample (from the same tissue block) is higher than in the stroma-enriched LCM sample (21.4% versus 1.36% respectively).*

3.2.3 Immunohistochemistry

IHC staining revealed loss of ARID1A protein to be a rare event with only a single case of ARID1A-loss in a DE case (1/36; 2.78%) and no detectable loss in IE cases (Fig. 3.3A-B; Appendix C; Appendix D). Conversely, 7 of 40 patients with IE (17.5%), and 5 of 36 patients with DE, (13.89%) exhibited a heterogeneous pattern on staining for PTEN wherein some, but not all, glands demonstrate loss of PTEN immunoreactivity (Fig. 3.3C-D, Appendix C; Appendix D). As with cancer-driver mutations, we observed ARID1A-loss and PTEN-loss in only the epithelial component of endometriosis.

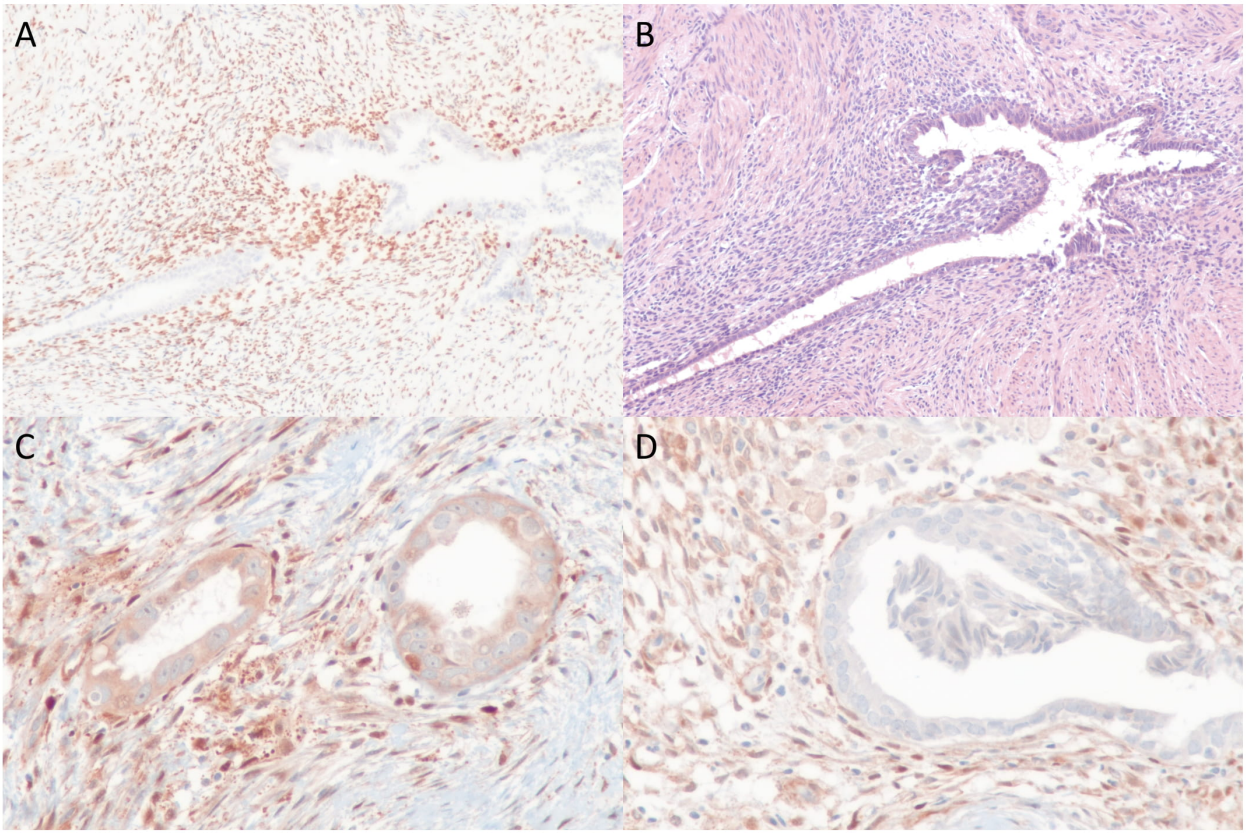

Figure 3.3: IHC studies of endometriosis specimens showing (A) loss of ARID1a in epithelial endometriosis cells in a case of DE and (B) matching H&E staining. A case of IE with heterogeneous expression of PTEN IHC, (C) intermediate expression in some glands and (D) faint expression in others.

3.2.4 Total Mutation Rates

Accounting for both ddPCR-validated somatic COSMIC hotspot mutations and the IHC findings, the overall frequency of somatic cancer-driver events in IE and DE was 27.5% (proportion) and 36.1% (proportion), respectively. The pattern of somatic mutations compared between the IE and DE cases is illustrated in Fig. 3.4.

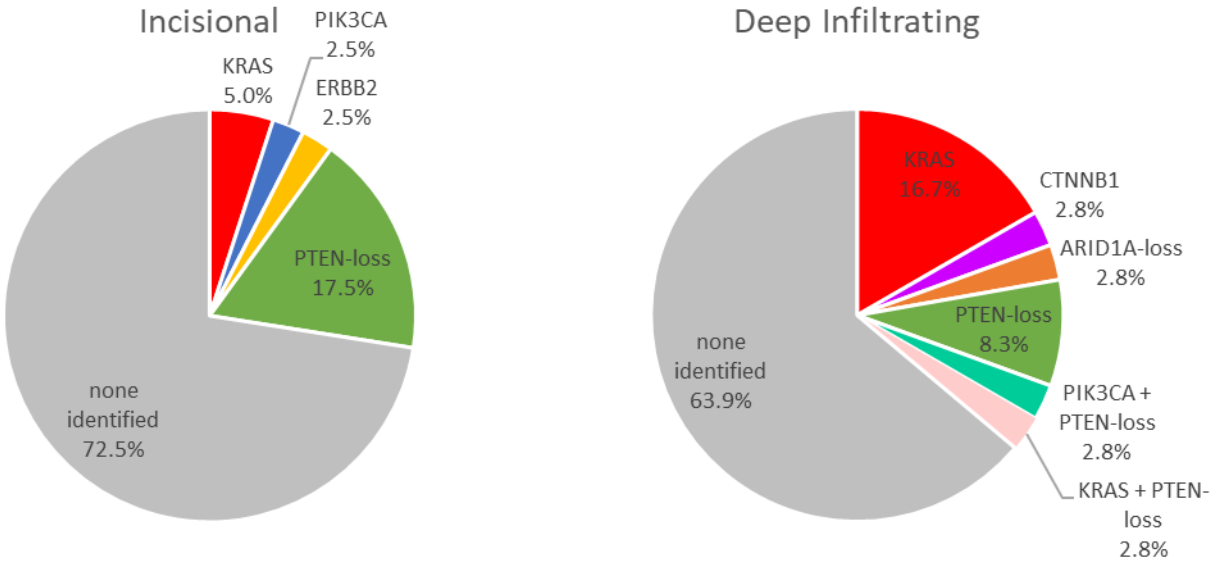

Figure 3.4: Overview of somatic cancer-driver events in incisional endometriosis and deep infiltrating endometriosis.

Somatic cancer-driver events were observed to co-occur in individual specimens and across specimens from the same patient. Consequently, rather than conducting statistical analysis comparing the overall rates of mutation, I performed a Fisher's exact test on each pairwise comparison of presence of a given somatic cancer-driver event in incisional endometriosis versus deep infiltrating endometriosis to assess whether the observed rates of cancer-driver events were significantly different between IE and DE patients. All tests were two-sided, where a *P*-value <0.05 was considered to be statistically significant. The *P*-value for each pairwise comparison is shown below in Table 3.4.

** It is important to note that because I am performing several statistical tests simultaneously (here and in subsequent analyses), it would be intuitive to correct for multiple comparisons (such as through the Bonferroni correction) to reduce the false discovery rate[84]. However, given the exploratory/hypothesis-generating nature of this work and because the number of comparisons made is small, I chose not to formally apply these corrections. Findings from this work should be interpreted with caution and should be validated in a second, independent cohort.

Table 3.4: Reported P-values for pairwise comparisons of somatic events affecting specific genes.

Pairwise Comparison	IE patients affected	DE patients affected	*P* -value
KRAS in IE vs. DE	2/40	7/36	0.0762
CTNNB1 in IE vs. DE	0/40	1/36	0.4737
PIK3CA in IE vs. DE	1/40	1/36	1.0000
ERBB2 in IE vs. DE	1/40	0/36	1.0000
ARID1A-loss in IE vs. DE	0/39	1/34	0.4658
PTEN-loss in IE vs. DE	7/37	5/25	1.0000

Most of the somatic cancer-driver events we observed affected components of the MAPK/RAS signalling pathway (includes *KRAS* and *ERBB2*) and PI3K-Akt signalling pathway (includes *CTNNB1*, *PIK3CA*, and *PTEN*). The proportion of DE samples with activating RAS pathway alterations was higher than that observed for IE, however this difference was not quite significant ($p = 0.0762$). I therefore also examined whether the collective rates of somatic events affecting these pathways differed in women with IE and women with DE. As shown in Table 3.5, all P-values were > 0.05 and therefore the rate of somatic alterations affecting canonical components of the MAPK/RAS and PI3K-Akt pathway mutations are not significantly different.

Table 3.5: Reported P-values for pairwise comparisons of somatic events affecting canonical pathways.

Pairwise Comparison	IE patients affected	DE patients affected	*P* -value
MAPK/RAS in IE vs. DE	3/40	7/36	0.1773
PI3K-Akt in IE vs. DE	8/40	6/36	0.7735

3.3 Discussion

Our previous study revealed the presence of recurrent somatic cancer-driver mutations (particularly *KRAS*) in DE[59]. In the current study, I analyzed the prevalence of somatic cancer-driver events in IE, another form of endometriosis with little malignant potential, using a hypersensitive cancer hotspot assay combined with orthogonal validation by ddPCR or IHC staining. We found that the overall rates of somatic cancer-driver events to be similar for IE and DE, moreover the spectrum of affected pathways was similar. The similarity in the rates of mutation and mutational profile of IE and DE is consistent with endometriotic cells in both forms of endometriosis originating from the same source. Because IE is accepted to originate from endometrial cells in the uterus via iatrogenic transplantation, this may support a uterine origin of deep infiltrating endometriosis as well (e.g. secondary to retrograde menstruation).

Although our sample sizes were insufficiently large to conclude difference in either overall rates of somatic events or enrichment of particular alterations when comparing IE and DE, it is apparent that alterations resulting in upregulation of the MAPK/RAS or PI3K-Akt-mTOR signalling pathways are present in a substantial fraction of endometriosis cases. Aberrant signalling of these pathways is known to affect cell growth/proliferation, differentiation, and apoptosis[85,86] and therefore these mutations might be important in driving the growth and survival of endometriosis in ectopic regions of the body. Interestingly, ddPCR assays and IHC staining revealed that all somatic cancer-driver events observed (hotspot mutations in *KRAS*, *CTNNB1*, and *PIK3CA*, loss of PTEN, or loss of ARID1A) affected only the epithelial compartment of endometriosis lesions. Moreover, visualization of lesions with PTEN-loss or ARID1A-loss revealed that only some glands were affected by these somatic events whereas other glands had normal expression. It is unclear whether the hotspot mutations identified also affect only a few glands in endometriotic lesions or whether these mutations exist at low allelic frequencies throughout the entire lesion – though the prior would be more in line with clonal expansion and observed alterations seen by IHC. If somatic cancer-driver alterations truly affect only certain endometriotic glands within lesions, do such alterations affect the fate of such glands over other glands where somatic events are absent?

4. Somatic Cancer-Driver Mutations in Eutopic Endometrium

As discussed in the previous chapter, I observed somatic cancer-driver alterations in over 25% of women with DE and women with IE studied, including hotspot, gain-of-function mutations in *KRAS*, *CTNNB1*, *ERBB2*, and *PIK3CA* as well as loss of PTEN protein. Since a uterine origin of IE is well accepted, the similarity in mutation rates and spectra is consistent with a uterine origin of DE as well (perhaps through retrograde menstruation). A proposed model for the pathogenesis of endometriosis (based on a uterine origin) is illustrated in Figure 4.1 below:

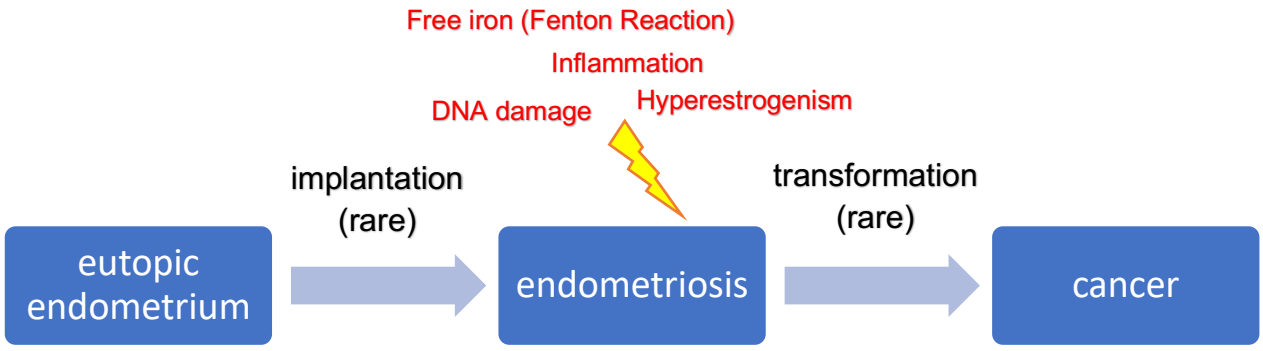

Figure 4.1: Theoretical and simplified model of the pathogenesis of endometriosis. Endometrial cells from their native uterine site are transferred (via mechanical transplantation, retrograde menstruation, or other means) into a secondary site wherein endometriosis implants will establish themselves. Additional DNA damage (such as through the accumulation of mutations), free iron (which results in iron-induced oxidative stress by the Fenton reaction)[87], inflammation[42] and/or hyperestrogenism[42] occasionally lead to malignant transformation.

Although previous studies have documented somatic driver mutations in EAOCs and concurrent endometriotic lesions, our frequent findings of somatic mutations in cases of endometriosis very unlikely to progress to cancer prompt speculation on whether mutations independently arise in implanted endometrial cells or whether they already are already presenting in the originating cells. To be put simply: "Which came first, the chicken (endometriosis) or the egg (somatic mutation)?" Although the origin of

(endogenous) endometriosis remains contentious, assuming a uterine origin of endometriosis and examining uterine tissue serves to potentially identify the originating cells of endometriosis as well as increase our understanding of latent mutations of unknown clinical significance (particularly in eutopic endometrial tissue, which often serves as "normal tissue" for molecular studies on endometriosis). Therefore, are such cancer-driver events naturally present in the eutopic endometrium, perhaps merely reflecting the aging of that tissue[88]? A study analyzing uterine lavage fluid has recently reported cancer-associated mutations, such as driver mutations in *KRAS* and *PIK3CA*, in roughly half of women analyzed (51 of 95) that lacked histopathological evidence of (endometrial) cancer[89]. Likewise, peritoneal washing revealed TP53 mutations in 19 of 20 control women (women unaffected by cancer or reported benign pathology), albeit at ultra-low allelic frequencies (< 0.1%), with an apparent increase in mutational burden correlating with age[90]. These studies suggest that somatic cancer-driver mutations may pre-exist in the eutopic endometrium. To clarify these speculations, in this chapter I assessed the presence of somatic cancer-drivers in the eutopic endometrium of women without evidence of endometrial hyperplasia or gynecologic malignancy and whether the presence of such alterations was associated with age.

4.1 Patient Specimen Collection

4.1.1 Overview of Hysterectomy Cohort

I examined somatic mutations in common cancer hotspots in endometrium specimens obtained from 25 women who underwent hysterectomies at VGH. Hysterectomy (Hx) cases were identified using the search terms "endometrium" and "hysterectomy" between January 2004 and January 2018. Inclusion criteria were limited to unremarkable proliferative or secretory endometrium between the age of 20 and 65 years, excluding malignant or premalignant disease and benign neoplasms. Cases with previous history of endometrial hyperplasia or gynecologic malignancy were also excluded.

4.1.2 Overview of Biopsy Cohort

I examined somatic mutations in common cancer hotspots in endometrium specimens obtained from 66 women who underwent endometrial biopsies at VGH. These cases were identified using the search terms “endometrial” and “biopsy” between January 2015 and 2017. Inclusion criteria were limited to the unremarkable proliferative or secretory endometrium between the age of 20 and 65 years, excluding malignant or premalignant disease and benign neoplasms. Cases with previous history of endometrial hyperplasia or gynecologic malignancy were also excluded.

4.1.3 Ethics Approval

Specimen collection and retrieval of clinical data was approved by the UBC BC Cancer Agency Research Ethics Board [H05-60119]. We also obtained ethics approval for immunohistochemical experiments and next generation sequencing to be performed on these specimens [H02-61375; H08-01411].

4.2 Additional Details on Methods

The analyses in this chapter follow the methodology described in Chapter 2. The following difference should be noted: although Hx patients followed the same protocol for DNA collection by means of needle microdissection, DNA collected from Bx patients were derived from 2 – 4 10μm FFPE scrolls.

4.3 Results

4.3.1 Sample Description for Hysterectomy Cases

The mean age of women in the Hx cohort (Patients Hx_1 to Hx_25) was 37.3 years (Table 4.1). The most common reasons for women in this cohort to undergo hysterectomy was fibroids or pelvic pain (36% and 20% of women respectively). Women noted as having “other/unclear” reasons for undergoing hysterectomy represented patients that were suspected (but not confirmed) to have pathology affecting the uterus, such as leiomyoma or endometrial polyps (Table 4.1; Appendix E). We collected and subsequently analyzed

two blocks presumed to represent endometrial tissue from the posterior uterus and anterior uterus from each patient. Note that in one patient (Patient Hx_25) anatomical distortion of the uterus resulted in the inability to define the location in the uterus in which the two blocks of endometrial tissue collected were sampled from (see Appendix E).

Table 4.1: Overview of clinical characteristics of women in Hx cohort.

Patient characteristics	**Hysterectomy cohort (n = 25)**
Age (years; mean ± SD)	37.3 ± 6.5
Reason for procedure	
fibroids	9 (36.0%)
pelvic pain	5 (20.0%)
leiomyoma	2 (8.0%)
prolapse	1 (4.0%)
sex reassignment	1 (4.0%)
abnormal bleeding	1 (4.0%)
dysmenorrhea	1 (4.0%)
*other/unclear**	5 (20.0%)
Endometrium State	
proliferative	16 (64.0%)
secretory	7 (28.0%)
undetermined	2 (8.0%)

4.3.2 Sample Description for Endometrial Biopsy Cases

The mean age of women in the endometrial biopsy (Bx) cohort (Patients Bx1 – Bx67, note Bx56 was not included in analysis) was 32.9 years (Table 4.2; Appendix F). The difference in age between the Hx and Bx cohorts is not statistically significant ($p = 0.5630$, Student's t-test). The most common reasons for women in this cohort to undergo endometrial biopsy were abnormal uterine bleeding or not otherwise specified (48.5% and 22.7% of women respectively) (Table 4.2).

Table 4.2: Overview of clinical characteristics of women in Bx cohort.

Patient characteristics	**Endometrial Biopsy cohort (n = 66)**
Age (years; mean ± SD)	38.6 ± 10.0
Reason for procedure	
abnormal uterine bleeding	32 (48.5%)
not specified	15 (22.7%)
infertility	6 (9.1%)
rule out hyperplasia	4 (6.1%)
irregular menstrual cycle	3 (4.5%)
recurrent implant failure	2(3.0%)
submucosal fibroid	2 (3.0%)
postcoital spotting	1 (1.5%)
chronic anovulation	1 (1.5%)
Endometrium State	
proliferative	33 (50.0%)
secretory	31 (47.0%)
inactive	2 (3.0%)

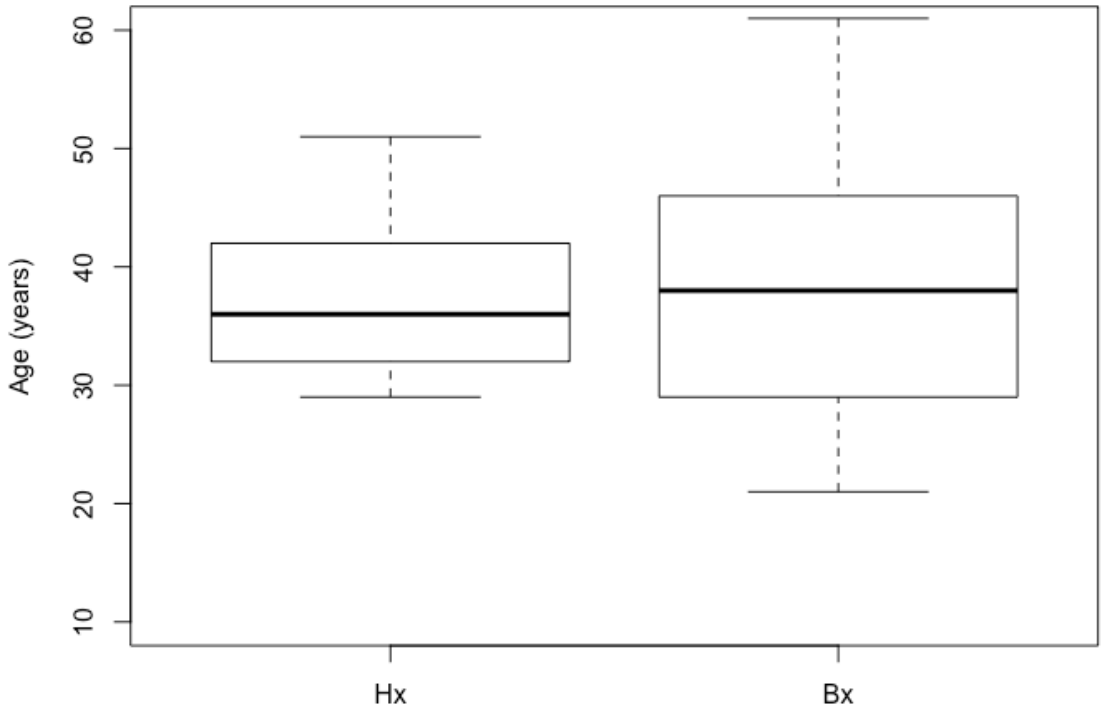

*Figure 4.2: Boxplot comparison of age of Hx and Bx patients. The difference in age between the Hx and Bx cohorts is not statically significant (*p = *0.5630, Student's t-test).*

4.3.3 Overview of Somatic Cancer-Driver Events

Using the FIND IT™ version 3.4 assay, we performed targeted sequencing of macrodissected, endometrial tissue obtained from Hx women and Bx women for hotspots in the 33 genes listed in Table 2.1. We also performed PTEN and ARID1A IHC as surrogates for *PTEN* and *ARID1A* inactivating mutations. Targeted sequencing and IHC findings are summarized in Fig. 4.3.

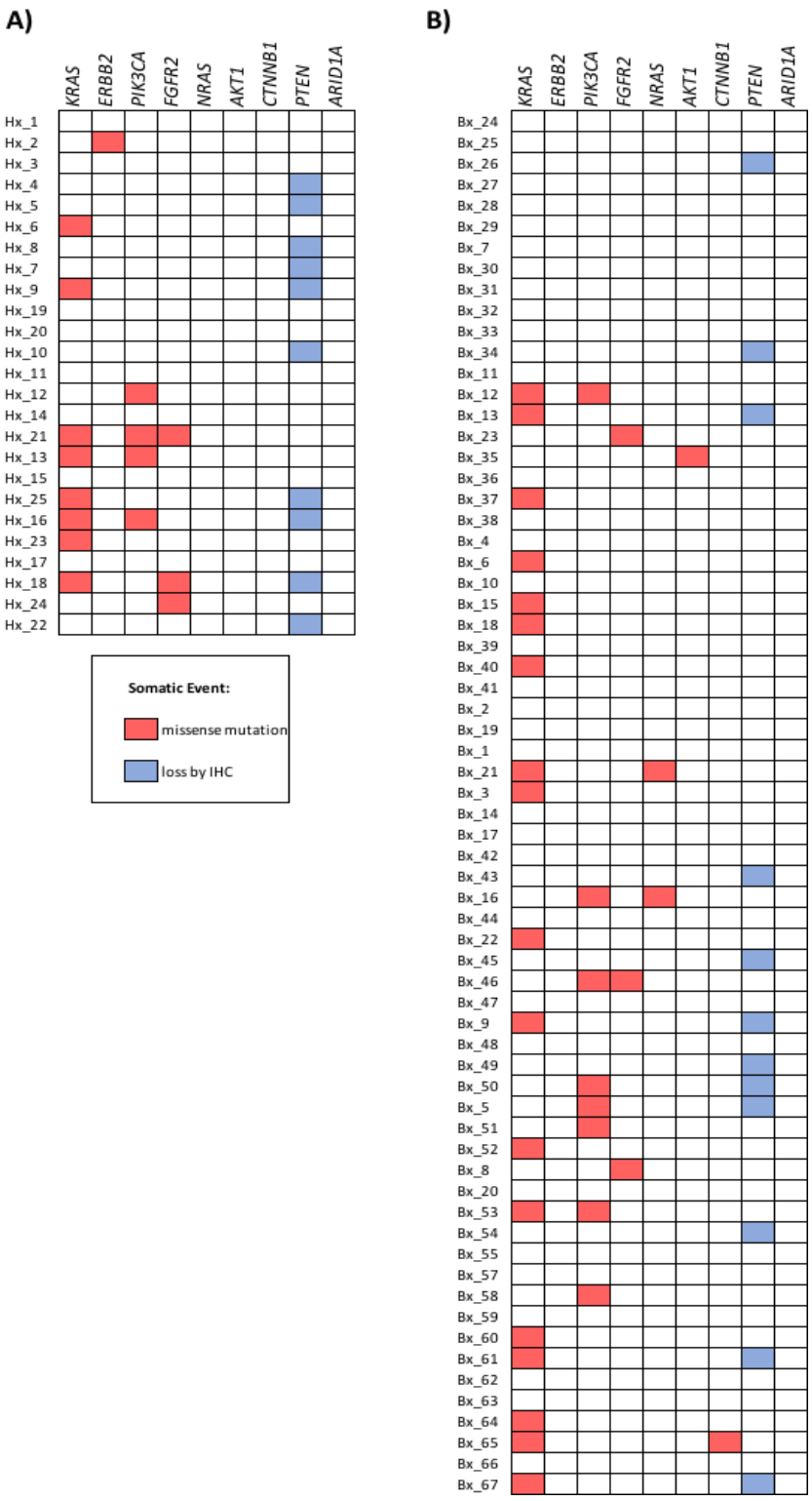

Figure 4.3: Overview of somatic cancer-driver events in endometrial tissue from women in the A) Hx cohort and B) Bx cohort. Cases are arranged by increasing age going downwards. It is important to note that somatic events reported in Hx samples were derived from two specimens/blocks of endometrial tissue whereas Bx samples were

derived from a single biopsy specimen/block. Somatic missense mutations are denoted in red and loss by IHC is denoted in blue.

I observed somatic-cancer driver events in 68.0% (17 of 25) of Hx cases including somatic hotspot, gain-of-function mutations in *KRAS* (8), *ERBB2* (1), *PIK3CA* (4), and *FGFR2* (3) as well as PTEN-loss by IHC (10) (Fig. 4.4; Fig. 4.5, Appendix G). On the other hand, I observed somatic-cancer driver events in 50.0% (33 of 66) of Bx cases (Fig. 4.4, Appendix H). These events included somatic hotspot mutations in *KRAS* (18), *PIK3CA* (8), and *FGFR2* (3) as well as PTEN-loss by IHC (12). I detected 0 – 3 somatic events in each patient, however I observed no abnormalities in ARID1A IHC in any Hx or Bx specimens.

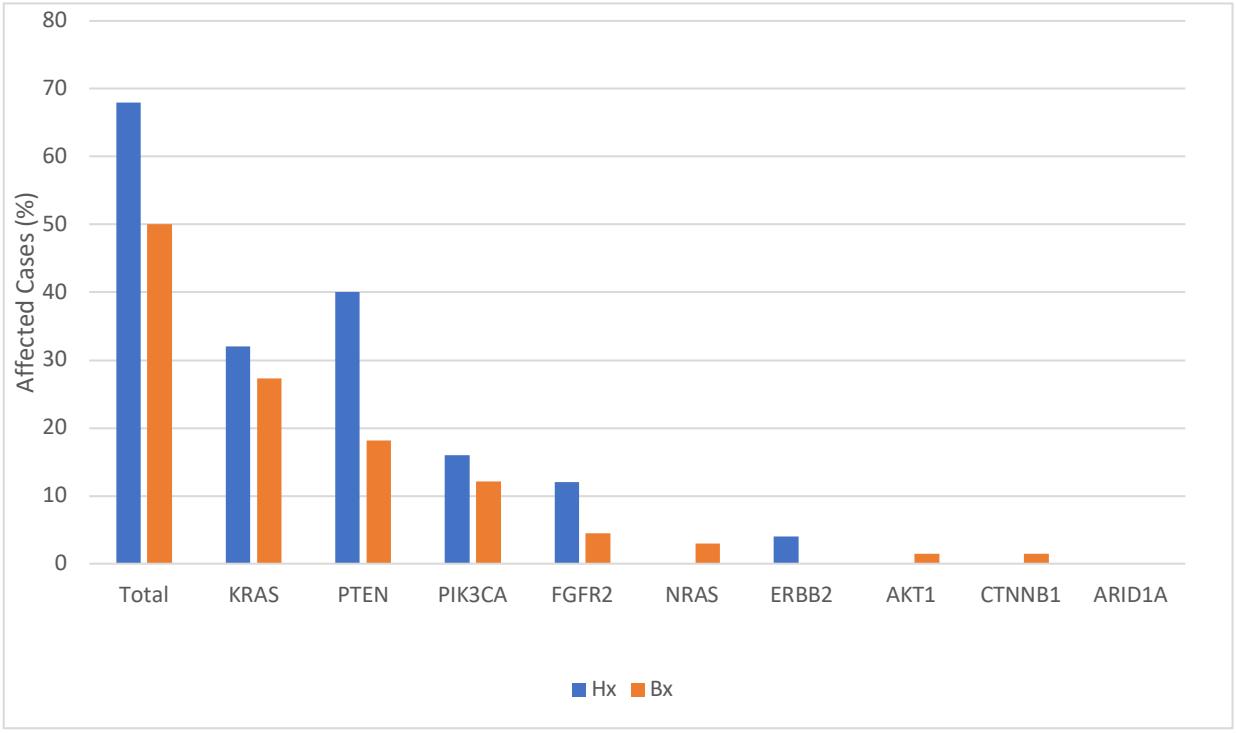

Figure 4.4: Proportion of Hx and Bx cases affected by somatic cancer-driver events.

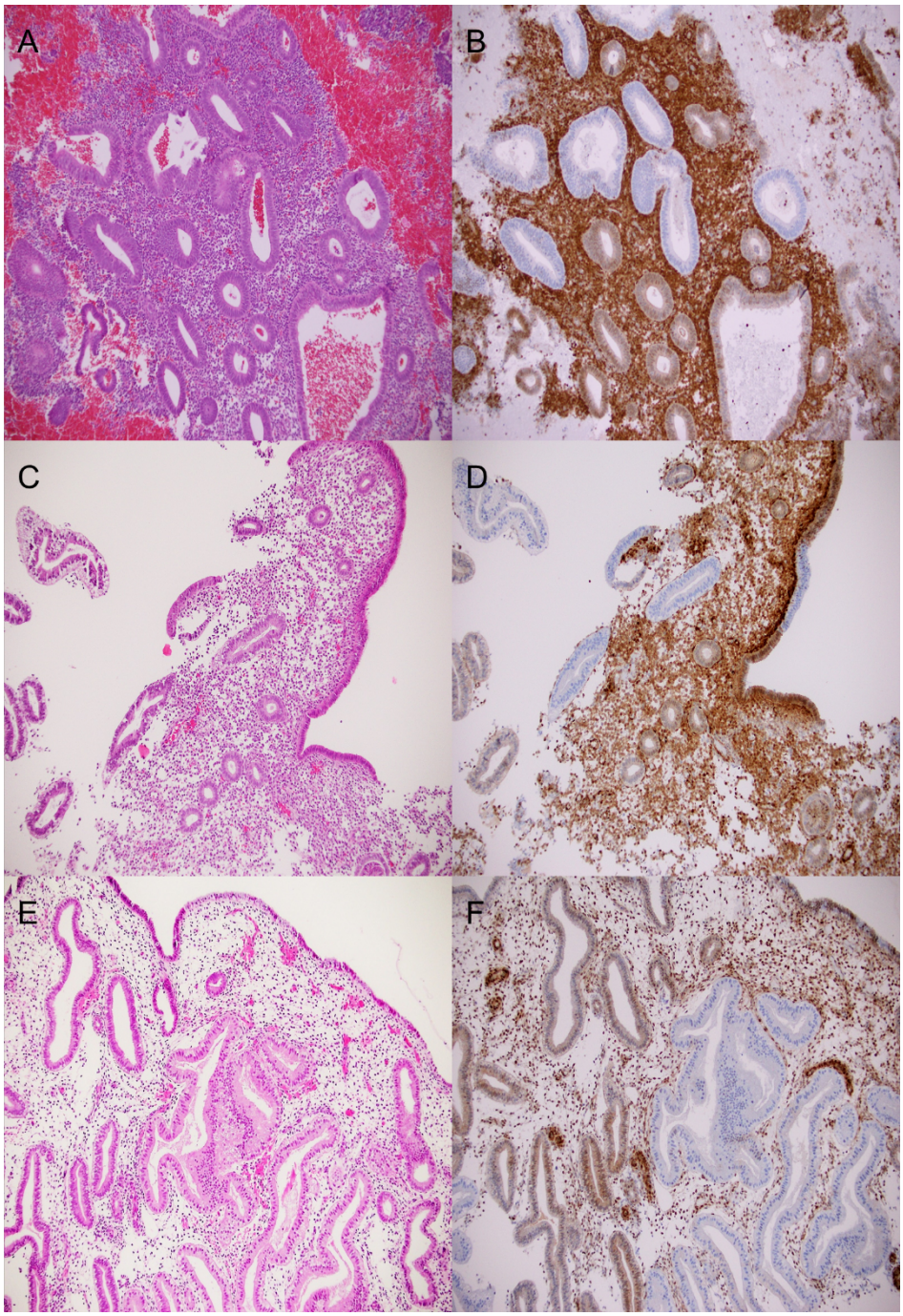

Figure 4.5: PTEN IHC studies of Hx specimens showing (A,C,E) regional loss/heterogeneous expression of PTEN in epithelial endometriosis cells and (B,D,F) matching H&E stain.

I performed the Fisher's exact test on the overall rate of somatic events in Hx patients and Bx patients as well as somatic events affecting each individual gene to assess whether the observed rates of cancer-driver events were significantly different between the two cohorts. All tests were two-sided, where a P-value <0.05 was considered to be statistically significant. The *P*-value for each pairwise comparison is shown below in Table 4.3. Although the overall rate of somatic events was not significant (p = 0.1588), PTEN-loss seemed to occur more frequently in Hx patients compared to Bx patients (p = 0.0524).

Table 4.3: Reported P*-values for pairwise comparisons of somatic events in Hx patients and Bx patients.*

Pairwise Comparison	Hx patients affected	Bx patients affected	*P*-value
Total Affected in Hx vs. Bx	17/25	33/66	0.1588
KRAS in Hx vs. Bx	8/25	18/66	0.7954
ERBB2 in Hx vs. Bx	1/25	0/66	0.2747
PIK3CA in Hx vs. Bx	4/25	8/66	0.7302
FGFR2 in Hx vs. Bx	3/25	3/66	0.3404
NRAS in Hx vs. Bx	0/25	2/66	1.0000
AKT1 in Hx vs. Bx	0/25	1/66	1.0000
CTNNB1 in Hx vs. Bx	0/25	1/66	1.0000
PTEN-loss in Hx vs. Bx	10/25	12/66	0.0524
ARID1A-loss in Hx vs. Bx	0/25	0/66	1.0000

*Note: Because of the exploratory nature of this study and because the number of comparisons was small, I did not adjust the *P*-value for multiple comparisons.

4.3.4 Multiple Sampling Analysis in Hysterectomy Cases

As mentioned, two FFPE blocks containing endometrial tissue were obtained from each Hx patient. With the exception of Patient Hx25 (wherein the anatomical sites where samplings were obtained from are not specified), we collected anterior and posterior endometrial tissue samplings from each patient. The presence of specific point mutations in the anterior versus posterior uterine samplings is outlined in Fig. 4.6 and Table 4.4. Forty-four percent of Hx patients (11 of 25) harboured ≥1 point mutation between two endometrial samplings. Of patients with ≥1 point mutation, 90.9% (10 of 11) had

different/discordant point mutations in their two samplings, whereas only 9.1% (1 of 11) had the same/concordant point mutations in both samplings. Interestingly, the anatomical location of the uterus where samplings were obtained from is not known in the case with concordant mutations in both samplings (Patient Hx_25; Table 4.4).

Note: This analysis does not include IHC findings since the specific molecular event resulting in loss of protein expression cannot be inferred (i.e. if PTEN-loss is observed in both anterior and posterior samplings, we do not know if this is caused by the same point mutation/deletion or two separate events).

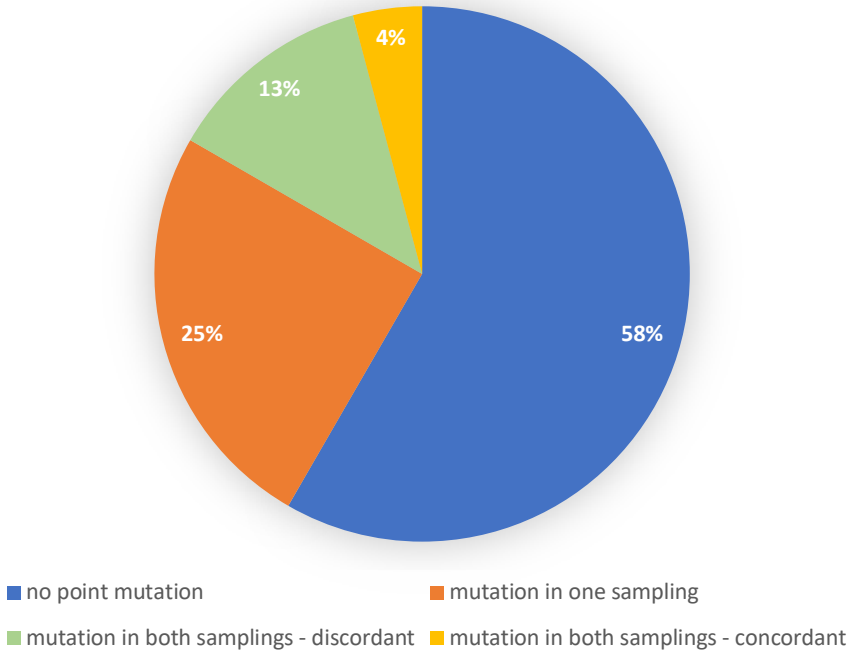

Figure 4.6: Concordance and discordance of point mutations observed among both samplings obtained from Hx patients.

Table 4.4: Specific point mutations observed in samplings obtained from Hx patients. The VAF determined by targeted sequencing and ddPCR are provided. Data for patients listed correspond to the colours in the legend key in Figure 4.6.

Identifier	Site of Uterus Sampled	Driver Gene Mutation	VAF (%) - Targeted Sequencing	VAF (%) - ddPCR
Hx_2A	anterior	none identified		
Hx_2B	posterior	ERBB2 S310F	0.974	0.792
Hx_6A	anterior	KRAS G12V	2.654	1.63
Hx_6B	posterior	KRAS G12A	1.408	1.08
Hx_9A	anterior	none identified		
Hx_9B	posterior	KRAS G13D	2.16	pending
Hx_12A	anterior	PIK3CA R88Q	1.337	1.23
Hx_12B	posterior	none identified		
Hx_13A	posterior	PIK3CA H1047R	2.497	3.36
		KRAS G12C	1.036	0.538
Hx_13B	anterior	none identified		
Hx_16A	anterior	KRAS G12V	1.079	1.06
		PIK3CA E542K	1.015	0.897
Hx_16B	posterior	PIK3CA H1047R	2.402	1.92
Hx_18A	anterior	FGFR2 K659E	5.505	7.77
		KRAS G12V	1.551	1.24
Hx_18B	posterior	none identified		
Hx_21A	anterior	KRAS G12D	5.587	4.71
		PIK3CA M1043I	2.39	pending
Hx_21B	posterior	KRAS G12V	6.112	pending
		PIK3CA H1047R	2.373	276.00%
		FGFR2 S252W	1.889	pending
Hx_23A	ant	none identified		
Hx_23B	post	KRAS G12D	11.866	pending
Hx_24A	ant	none identified		
Hx_24B	post	FGFR2 S252W	1.769	pending
Hx_25A	N/A	KRAS G12A	1.584	1.6
Hx_25B	N/A	KRAS G12A	1.67	1.0

4.3.5 Relationship Between Age and Presence of Somatic Cancer-Driver Events in Endometrial Biopsy Cases

To assess the relationship between age and presence of somatic cancer-driver events, I generated a logistic regression model based on 66 Bx specimens wherein the dependent variable is a binary variable: patients either harboured somatic events in their endometrial tissue (regardless of the specific number of events) or they did not harbour somatic events (based on our analysis). The designed logistic regression model is shown below in Figure 4.7. Despite our small sample size, the likelihood of harbouring a somatic event in an endometrial biopsy appears to increase by age (OR = 1.05, 95% CI = 0.99– 1.11, p = 0.06, Wald test).

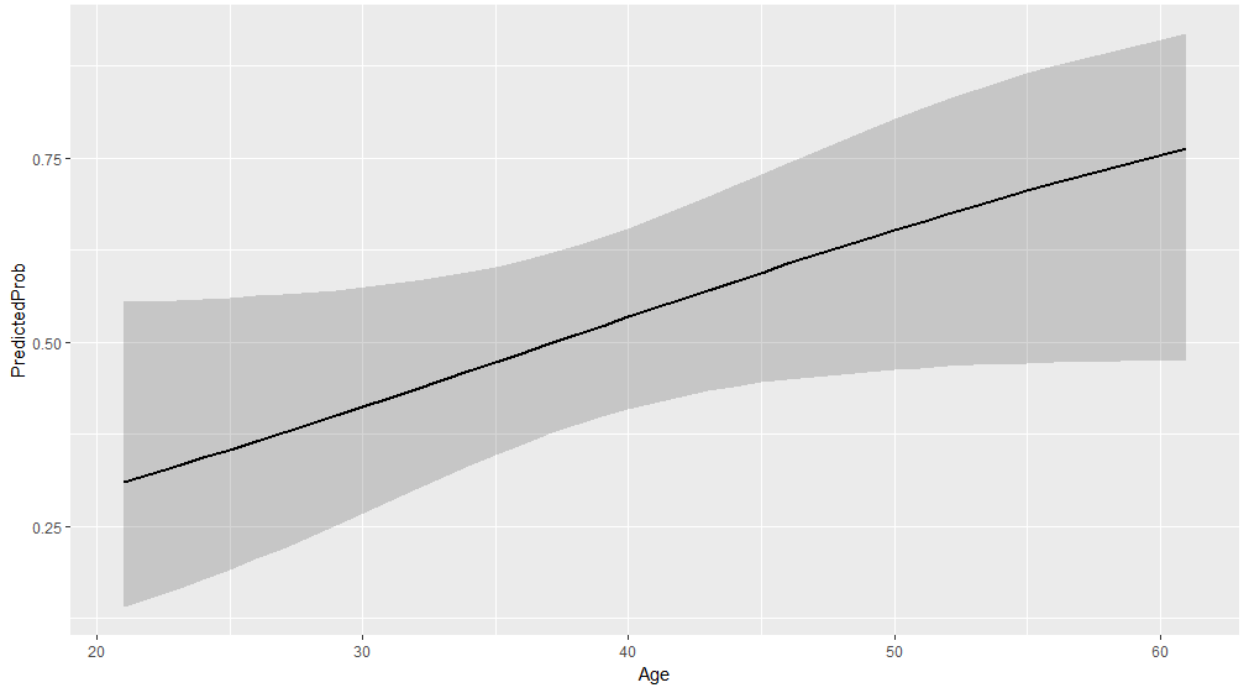

Figure 4.7: Logistic regression model depicting the correlation between age and presence of somatic cancer-driver events in Bx patients. The shaded regions represent the 95% confidence interval for the likelihood of harbouring somatic cancer-driver events at a given age.

Since we determined the phase of the endometrium (proliferative phase or secretory phase), I also generated a model considering both age and the phase of the endometrium,

as illustrated below in Figure 4.8. In this model, the likelihood of harbouring a somatic event is demonstrated to increase significantly with age (OR = 1.06, 95% CI = 1.00 – 1.12, p = 0.048, Wald test). Endometrial tissue in secretory phase is associated with nearly five times the likelihood of observing a somatic event compared to the proliferative phase (OR = 4.86, 95% CI = 1.67 – 15.6, p = 0.0051, Wald test). Details on the somatic-cancer driver alterations observed in Bx patients are provided in Table 4.5.

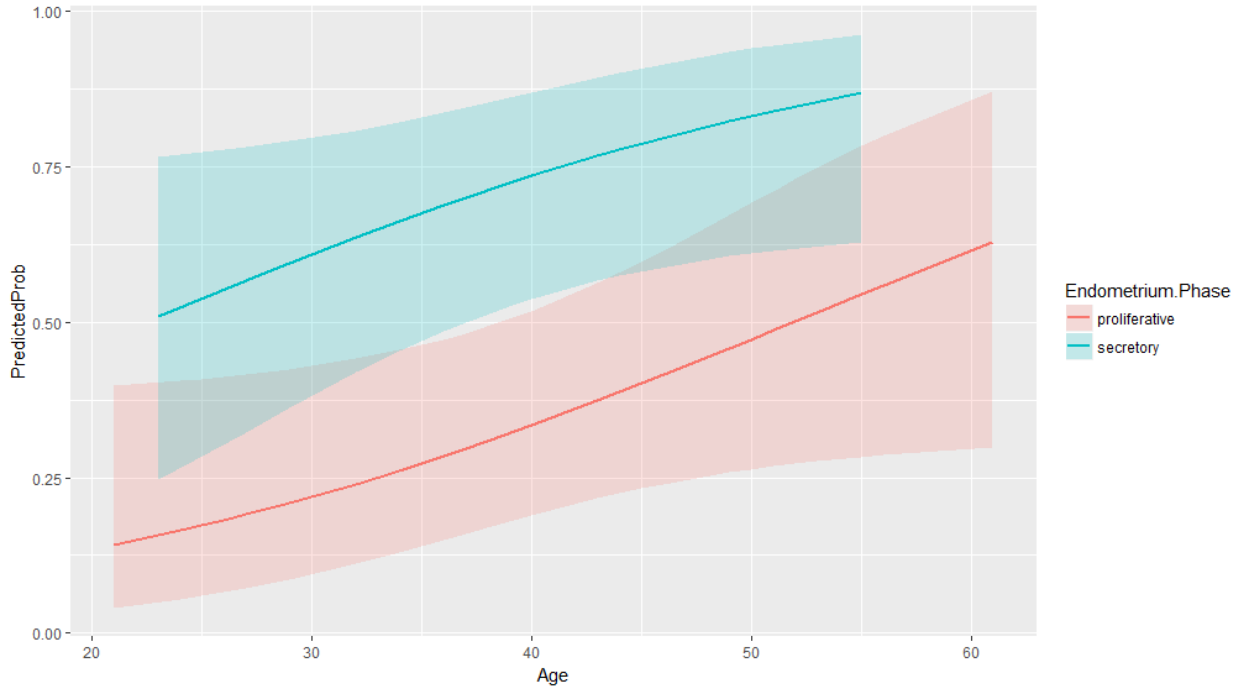

Figure 4.8: Logistic regression model depicting the correlation between age and presence of somatic cancer-driver events in Bx patients with endometrium samplings with respect to the phase of the endometrium. The shaded regions represent the 95% confidence interval for the likelihood of harbouring somatic cancer-driver events at a given age.

Table 4.5: Somatic cancer-driver mutations detected in Bx patients. The age, phase of endometrium, and VAF as determined by means of targeted panel sequencing and corresponding ddPCR assays are presented.

Identifier	Age (years)	Endometrium Phase	Driver Gene Mutation	VAF (%) - Targeted Sequencing	VAF (%) - ddPCR
Bx_3	38	proliferative	KRAS G12A	2.529	2.41
Bx_5	45	proliferative	PIK3CA H1047R	1.536	1.71
Bx_6	32	secretory	KRAS G12C	0.872	pending
			KRAS G12D	1.675	pending
Bx_8	49	secretory	FGFR2 S252W	1.177	pending
Bx_9	44	secretory	KRAS G12D	6.43	pending
Bx_12	29	secretory	KRAS G12V	2.437	2.65
			PIK3CA H1047R	0.806	1.1
Bx_13	29	secretory	KRAS G12D	1.158	pending
Bx_15	34	secretory	KRAS G12V	1.162	1.12
Bx_16	40	secretory	NRAS G13D	3.064	1.46
			PIK3CA E545K	1.456	1.35
Bx_18	34	secretory	KRAS G12D	5.554	pending
Bx_21	37	secretory	KRAS G12V	1.424	1.05
			NRAS Q61R	10.232	pending
Bx_22	43	secretory	KRAS G12D	3.546	pending
Bx_23	29	secretory	FGFR2 S252W	1.889	pending
Bx_35	29	proliferative	AKT1 E17K	1.193	pending
Bx_37	29	secretory	KRAS G12D	1.281	pending
Bx_40	34	proliferative	KRAS G12A	1.973	pending
Bx_46	43	late secretory	FGFR2 S252W	1.18	pending
			PIK3CA E542K	0.994	pending
			PIK3CA H1047R	1.084	pending
Bx_50	44	secretory	PIK3CA G1049S	0.983	pending
Bx_51	46	proliferative	PIK3CA H1047R	2.927	pending
Bx_52	46	secretory	KRAS G12D	1.464	pending
Bx_53	49	inactive	KRAS G12D	1.505	pending
			PIK3CA E545K	1.453	pending
			PIK3CA R88Q	0.965	pending
Bx_58	51	proliferative	PIK3CA H1047R	1.014	pending
Bx_60	51	secretory	KRAS G12V	1.686	pending
Bx_61	52	proliferative	KRAS G12D	9.421	pending
Bx_64	55	secretory	KRAS G12D	1.031	pending
Bx_65	55	proliferative	CTNNB1 T41I	0.825	pending
			KRAS G12V	1.018	pending
Bx_67	61	proliferative	KRAS G12D	1.131	pending

4.4 Discussion

In Chapter 3, I observed that somatic cancer-driver events are a common feature of endometriosis. The goal of this chapter was to assess the presence of such events in the histologically unremarkable, eutopic endometrium of women lacking evidence of gynecologic malignancy. Analyzing 25 Hx cases and 66 Bx cases, I observed high rates of somatic cancer-driver events (68% and 50% respectively) including *KRAS* and *PIK3CA* gain-of-function mutations and loss of PTEN protein. The differences in observed rates of somatic events likely result from my analysis of two samplings per case for Hx cases but only one sampling per case for Bx cases. Nevertheless, these rates are comparable to the rates of somatic alterations we observed in benign forms of endometriosis (27.5% in IE and 36.1% in DE) in Chapter 3. In addition, many Hx patients and Bx patients remarkably harboured multiple mutations in their endometrial samplings (Fig. 4.2). Although the biological function/impact of these somatic cancer-driver events remains unclear, I have demonstrated that these alterations pre-exist in the eutopic endometrium prior to the development of endometriosis or associated malignancies.

Consistent with my observations of PTEN loss in endometriotic glands in Chapter 3 as well as other studies focusing on PTEN-null glands in endometrial specimens[70,73], I found that cases always exhibited regional PTEN-loss in a small cluster of glands within a section of endometrial tissue (Fig. 4.5). I sought to clarify whether other somatic mutations I observed in the eutopic endometrium were present in a localized area or whether such mutations existed at low allelic frequencies throughout the uterus. In our analysis of Hx patients, I selected one anterior and posterior endometrial sampling per case to ensure that I was analyzing endometrium from spatially separated areas of the uterus. Nearly all Hx patients wherein I detected at least one somatic cancer-driver alteration harboured discordant mutations in their anterior and posterior endometrial samplings (> 90%). Only one patient harboured concordant *KRAS* G12A mutations in both endometrial samplings, however the distortion of the uterus in this patient made it impossible to determine the location of the uterus in which samplings were obtained from (and thus whether they were spatially separated). Although my analysis represents a gross snapshot of the localization of these mutations and does not exclude the possibility that somatic mutations may span a large area of the uterus (yet uncommonly so large as

to be detected in both an anterior and posterior sampling), they are consistent with the localization of somatic events to small clonal patches within the uterus as previously observed with *PTEN*-null glands[70,73].

A prominent question I sought to investigate was whether somatic cancer-driver events reflect the aging of women and thus their endometrial tissue. Somatic mutations have been described in normal tissue including blood[91], skin[92] , and peritoneal washings[90] from patients and seemingly reflect tissue aging even in the absence of cancer[73]. Moreover, Monte et al. (2010) found loss of PAX2 and PTEN proteins to be common events in normal endometrial tissue occurring in 36% and 49% of cases respectively and their occurrence increased significantly with age[73]. Analyzing endometrial biopsy specimens obtained from 66 women ranging from 21-61 years of age, I observed that increasing age appears to be associated with an increased likelihood of harbouring somatic cancer-driver events in normal, eutopic endometrial tissue. An increase of age by one year is associated with an increase in likelihood of harbouring such alterations by approximately 6% ($p = 0.048$). Interestingly, however, at a given age endometrial tissue in the secretory phase is more likelihood to harbour detectable somatic alterations compared to tissue in the proliferative phase ($p = 0.0051$). Generally, women go in for endometrial biopsies according to their own schedules, and thus the phase at which women have a biopsy is random. However, certain conditions influence the observance of secretory or proliferative phases at the time of biopsy – for instance, women with polycystic ovarian syndrome have continuous estrogen stimulation and are therefore constantly in proliferative phase[93], therefore it is likely that the population of women who receive biopsies in proliferative versus secretory phases may be slightly different. Additionally, this association with endometrial phase may be a product of high rates of proliferation as endometrial gland cells transition from proliferative phase to late secretory phase[94], which could allow glandular epithelial cells harbouring somatic events to clonally expand to levels (VAFs) detectable by our targeted sequencing assay. Overall, regardless of the specific mechanism resulting in the observed differences, the phase of the endometrium should be considered in the analysis of somatic events affecting the eutopic endometrium.

5. Concluding Chapter

5.1 Overview of Findings

Beyond the association of endometriosis and ovarian cancer, endometriosis is an understudied disease as its origin remains contentious and molecular pathogenesis poorly understood. Despite the high prevalence of endometriosis in women across the world, millions of women continue to live with endometriosis and its associated morbidities for years before formal diagnosis and receiving appropriate medical treatment. In a large multicenter, cross-sectional study of over 1,400 women, women with endometriosis were found to have a significantly reduced physical health-related quality of life compared to unaffected women and experienced a loss on average of 10.8 hours of work weekly[95]. With consideration of direct health care costs and indirect costs (predominated by productivity loss), the estimated cost of endometriosis in the United States in 2009 totaled roughly $69.4 billion USD[96], thereby bringing to attention the importance of studying endometriosis. Expanding recent finding of somatic molecular alterations across endometriosis types stands to benefit endometriosis classification and may lead to a novel and more biologically informative system of classification. Widespread knowledge on the prevalence of mutations may highlight common pathway dysfunction. Even with difficulties in targeting the RAS pathway[97] and potential toxicities related to PI3K-Akt pathway inhibitors[98], molecular characterization may justify the use of targeted therapies in select circumstances and will undoubtedly drive innovation for novel intervention strategies.

The overall goal of my study was to explore the prevalence of somatic cancer-driver mutations in forms of endometriosis unlikely to progress to malignancy as well as the eutopic endometrium. In Chapter 3, I addressed the question: “Does incisional endometriosis harbour somatic cancer-driver mutations?” Comparing the mutation profiles of IE and DE, I observed comparable rates of somatic cancer-driver events in both forms of endometriosis (affecting 27.5% and 36.1% of cases respectively). The somatic events largely affected the MAPK/RAS and PI3K-Akt signalling pathways, thereby suggesting that these pathways may play a key role in the pathogenesis of endometriosis even outside of the context of cancer. Interestingly, all somatic events

affected only the epithelial component of endometriosis lesions. Similar rates and mutation profiles of IE and DE are consistent with a uterine origin of endometriosis (which is likely facilitated by retrograde menstruation in endogenously-occurring forms of endometriosis). Consequently, I sought to determine if somatic cancer-driver mutations can be traced back to the eutopic endometrium. In Chapter 4, I addressed the question: "Are somatic cancer-driver mutations present in the eutopic endometrium and if so, does their presence correlate with increasing age?" Analyzing either Hx or Bx specimens from women lacking evidence of endometrial hyperplasia or gynecologic malignancy, I determined that somatic cancer-drivers are at least as prevalent in the eutopic endometrium as they are in benign forms of endometriosis – occurring in roughly half of all patients – and similarly affect canonical components of the MAPK/RAS (*KRAS*, *ERBB2*, *FGFR2*, or *NRAS*) and PI3K-Akt (*PIK3CA* or *PTEN*) signalling pathways. Additionally, these mutations appear to affect distinct regions of the uterus and the likelihood of finding somatic events increases with age. (It is important to note, however, that alterations are more commonly observed in secretory phase endometrium compared to proliferative phase endometrium.)

Conventionally, somatic cancer-driver mutations are regarded as early events in malignant transformation, however my findings demonstrate that cancer-drivers can be found in endometriosis not at-risk for malignant transformation and even in the eutopic endometrium. Roughly 10% of women are believed to be affected by endometriosis, yet approximately half of women unaffected by endometriosis or malignancy harbour somatic cancer-drivers in their eutopic endometrium. This mutation damage likely accumulates overtime as a product of aging of this tissue (DNA replication errors) and environmental exposures (such as dioxin or diethylstilboestrol). Whether endometrial cells harbouring cancer-driver mutations are implanted at an ectopic site or these mutations arise *de novo* within endometriotic lesions themselves, driver mutations (even if present in a small fraction of epithelial cells within endometriotic lesions) may confer a survival advantage to such lesions and enable their persistence ectopically. For instance, several studies have suggested endometriosis expresses high levels of VEGF and BCL-2 or BCL-xL, mediating angiogenesis and resistance to apoptosis respectively [60,99-101]. Likewise, KRAS-transformed epithelial cell have been shown to upregulate VEGF and other pro-

angiogenic factors[102,103]. Additionally, the expression of oncogenic Ras results in the upregulation of BCL-xL in colon cancer cells, and the upregulation of both BCL-2 and BCL-xL in hematopoietic cells *in vitro*[104,105]. While these specific mechanisms have not been linked to *KRAS* alteration in endometriosis, Cheng et al. (2011) were able to develop a mouse model of endometriosis by transplanting endometrium from *KRAS*$^{G12V/+}$ donor mice into subcutaneous, abdominal pockets of immunocompetent recipient mice. In this model, oncogenic *KRAS* promoted the formation of endometriosis and enabled the prolonged survival of endometriotic lesions but does not result in malignant transformation[106]. In combination with other factors including the accumulation of more mutations or epigenetic events, hormone influence (particularly high levels of estrogen), cell-organ interactions contributing to the local microenvironment, and immune or inflammatory interactions, endometriotic lesions may undergo malignant transformation (see Figure 5.1). Cancer risk is also dependent on the form of endometriosis: ovarian endometriosis is associated with the highest risk, whereas DE is associated with the lowest risk[47].

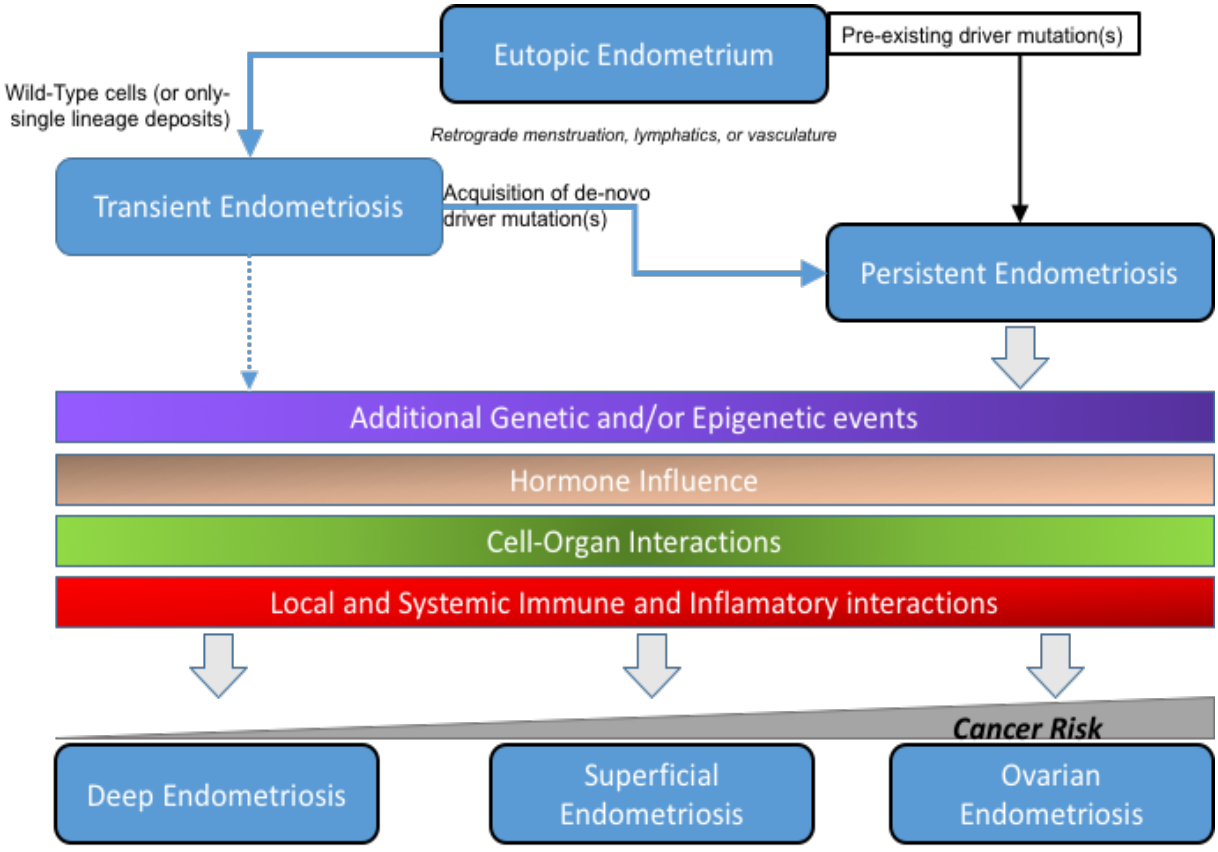

Figure 5.1: A revised model of the pathogenesis of endometriosis lesions. Cancer-driver mutations arise spontaneously in endometriotic cells or in the eutopic endometrium prior to seeding at an ectopic site and confer a survival advantage to cells, thereby allowing for the persistence of endometriotic lesions. Additional factors such as further genetic or epigenetic events, hormone influence, cell-organ interactions, and immune or inflammatory interactions contribute to progression to malignancy.

5.2 Limitations

It is crucial to note several limitations in my analyses, which are listed below:

1. Even though I have described somatic cancer-driver events in the tissues analyzed using the FIND IT^{TM} version 3.4 assay, there remains challenges in ultra-low input sequencing from FFPE tissue. Orthogonal validation by means of ddPCR resulted in our empirical determination of a targeted sequencing VAF cut-off of 0.8% for macrodissected FFPE tissue – it is possible that I failed to detect and report real mutations in endometriosis or endometrial tissue existing at lower VAFs.
2. We only conducted targeted panel sequencing for hotspot mutations in 33 genes in addition to PTEN IHC and ARID1A IHC. It is possible that whole genome or exome sequencing, or epigenetic analysis may uncover additional somatic cancer-driver alterations missed by our methods.
3. Exploration of the relationship between age and the presence of somatic alterations in endometrial tissue is limited by my relatively small sample size of n = 66 (note that despite this, we found increased age to be correlated with an increased likelihood of harbouring mutation (p = 0.048). This is particularly problematic if we want to simultaneously consider several variables (including menstrual state) in our logistic regression model.
4. Because of the descriptive nature of my study, the functional roles of identified mutations within the context of endometriosis remain unclear and causality cannot be established.
5. My study was also a retrospective, cross-sectional study by design. The associated risks for development of malignancy if an endometriotic lesion harbours somatic alterations or the development of endometriosis if somatic alterations are

present in the eutopic endometrium remain undetermined by this study. Furthermore, whether specific somatic alterations in the eutopic endometrium persist over time or disappear and emerge over the course of many menstrual cycles, as previously observed by Mutter et al. (2014) in PTEN-null endometrial glands[72], is also unclear.

5.3 Future Directions

The findings in my study give rise to more questions than those that were clarified in the process. Firstly, the mutations I have identified in women with IE and DE (as well as the eutopic endometrium) are commonly mutated in clear cell and endometrioid ovarian cancers[107,108], and therefore study of the prevalence of such mutations in endometriomas, which are most commonly linked to malignancy, is warranted. In contrast to my studies on IE and DE, a recent targeted sequencing study including many of the genes we analyzed in our sequencing panel (such as *KRAS*, *PIK3CA*, and *PTEN*) identified somatic mutations in only 3 of 101 (3%) ovarian endometriosis samples[67]. The sampling methods used to enrich for endometriosis within tissue specimens are not explicitly stated in this study, and therefore we are unsure whether such low frequencies of somatic alterations in ovarian endometriosis are truly reflective of a reduced burden compared to benign forms of endometriosis or whether endometriosis was insufficiently enriched for to be detected by targeted sequencing. Analyzing ovarian endometriosis with methods consistent with my study will help clarify this contention and determine the relative mutation burden in this form of endometriosis.

Regarding my analysis of eutopic endometrium, the distribution of glands harbouring somatic cancer-driven mutations is unknown aside that they are rarely ubiquitous throughout the uterus or span from one side of the uterus to the opposite site (i.e. from anterior to posterior). PTEN IHC revealed PTEN-null glands exist in small clonal patches among many normally-expressing glands. I suspect that the same is true for somatic mutations such as *KRAS* or *PIK3CA* driver mutations. For the most part, mutation-specific antibodies such as those designed to target *KRAS* are unable to reliably distinguish mutant/aberrant versions of these proteins from wildtype (the exception is

BRAF, wherein an antibody achieving great sensitivity and specificity has been designed)[109,110]. To clarify this matter, novel base-specific *in situ* hybridization may be an optimal mechanism to specifically indentify affected cells. The *BaseScope* assay (Advanced Cellular Diagnostics), is an RNA *in situ* hybridization assay based on the design of unique 'Z' probes which recognize RNA sequences of interest, followed by signal amplification (Fig. 5.2)[111] . Ultimately, this technique can discriminate between alterations as small as a single nucleotide change and enable the visualization of mutant subpopulations within archival tissue specimens while preserving morphological context[111]. The *BaseScope* assay has been used successfully to precisely map the spatial and morphological context of subclones harbouring common point mutations in *BRAF*, *KRAS*, and *PIK3CA* in archival colorectal cancer specimens[111] as well as splice junction visualization in metastatic castration-resistant prostate cancer[112].

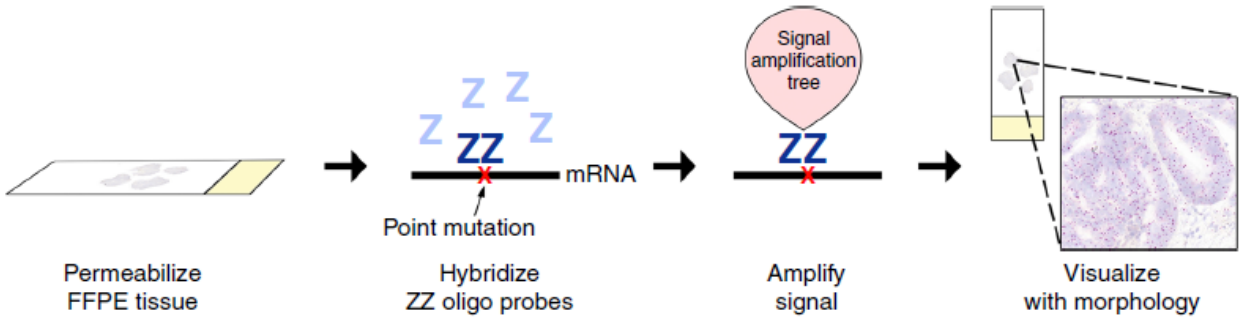

Figure 5.2: Schematic of the BaseScope assay. Two custom-designed 'Z' probes recognize and bind to target mRNA sequence. This binding allows for signal amplification followed by visualization of the point mutation of interest while preserving spatial context and cellular morphology of FFPE tissue. [Figure adapted from Baker et al., 2007[111].]

Additionally, probes can be designed in various colours, therefore enabling the simultaneous visualization of cell populations harbouring different point mutations yet within the same FFPE tissue specimen (via multiplexing). As noted in the overview of somatic events observed in eutopic endometrium in Fig. 4.2, several Hx and Bx cases exhibited multiple somatic point mutations. It is unclear whether mutations observed in the same tissue specimen affect different clusters of glands, thereby representing

independent events, or whether affected glands overlap to some extent – the latter scenario would imply the accumulation of cellular damage.

My study is consistent with a uterine origin of endometriosis – operating under this premise implies that EAOCs ultimately arise from the eutopic endometrium. The eutopic endometrium can also give rise to endometrial cancers[113]. Oral contraceptive pill (OCP) use is known to reduce the incidence of both ovarian cancers[114] and endometrial cancers[115,116]. Lin et al. (2009) observed a significantly reduced frequency of latent precancers (defined as endometrial glands exhibiting PTEN-loss) in women with a history of OCP or non-hormonal intra-uterine device use and hypothesized that these glands may be targets of endometrial cancer risk modulating exposures [71]. Consequently, in my analysis of the relationship between age and the presence of somatic cancer-drivers in the eutopic endometrium, a possible confounding variable is OCP use. OCP use should be assessed for significance in its association with the presence of somatic drivers in the endometrium and possibly included in a future, more comprehensive logistic regression model.

5.4 Significance of Study

In short, despite the unclear role of somatic cancer-driver mutations outside the context of cancer, such mutations commonly exist in both endometriosis and eutopic endometrium. Therefore, my findings have profound implications for basic researchers and society at large.

I discovered that somatic cancer-driver mutations are not restricted to specific anatomical forms of endometriosis – DE and IE harbour similar mutation profiles and therefore appear to be biologically equivalent despite differing mechanisms of dissemination. The development of animal models for *in vivo* endometriosis research presents many challenges, particularly because endometriosis occurs spontaneously only in humans and some non-human primates[117]. Ectopic rat and mouse models of endometriosis have been developed, however the usefulness of such models is contentious because these models represent induced disease in species that do not

naturally develop endometriosis [117]. Our findings serve as additional validation for the use of these ectopic animal models in endometriosis research since iatrogenically-caused endometriosis (IE) is similar to endogenously-occurring disease (DE) even on a molecular level.

Perhaps the most important message from my study is that the mutational burden caused by the emergence of a single cancer-driver event in ectopic or eutopic endometrial tissue is clearly insufficient for malignant transformation and it is likely other additional events must occur for the development of EAOCs (or endometrial cancers). Liquid biopsies represent exciting tools for the clinical management of disease – especially in the early, non-invasive detection of a variety of cancers and monitoring treatment response or residual disease following medical invention[118]. Recently, Wang et al. (2018) reported on the detection of ovarian and endometrial cancers based on the genetic analysis (incorporating assays for mutation detection in 18 genes and an assay for aneuploidy) of DNA recovered from fluids obtained during routine Papanicolaou (Pap) tests[119]. 33% of ovarian cancer patients and 81% of endometrial cancer patients had positive Pap brush samples, whereas only 1.4% of women without cancer had positive results – when sampling with a Tao brush instead, the percentage of false positive women fell to 0%[119]. Alongside findings of genetic abnormalities in uterine lavage samples[88] and peritoneal washings[89], my findings contradict these observations that somatic cancer-driver mutations nearly exclusively occur in cancer cases. Indeed, the study by Wang et al. is deeply flawed as its control group were dissimilar to the patient population in a key way, age. Specifically, the age of the control cohort was younger – the mean age of the control cohort for Pap brush and Tao brush analysis was 34 and 29 years respectively, whereas the mean age of cancer patients was 61 years[119] – and therefore this study and its conclusions are not interpretable provided my own findings of high rates of somatic driver mutations in the eutopic endometrium, which increases with age. This contention should be resolved if liquid biopsies based on somatic mutations detected in material obtained from Pap smears or other similar sources containing uterine material are to be used clinically.

References

1. Eskenazi B, Warner ML. Epidemiology of endometriosis. *Obstet Gynecol Clin North Am*. 1997;24(2):235-258. doi: S0889-8545(05)70302-8 [pii].

2. Vercellini P, Vigano P, Somigliana E, Fedele L. Endometriosis: Pathogenesis and treatment. *Nat Rev Endocrinol*. 2014;10(5):261-275. doi: 10.1038/nrendo.2013.255 [doi].

3. Giudice LC. Clinical practice. endometriosis. *N Engl J Med*. 2010;362(25):2389-2398. doi: 10.1056/NEJMcp1000274 [doi].

4. Adamson GD, Kennedy SH, Hummelshoj L. Creating solutions in endometriosis: Global collaboration through the world endometriosis research foundation. *J Endometriosis*. 2010;2(1):3-6.

5. Guo SW. Recurrence of endometriosis and its control. *Hum Reprod Update*. 2009;15(4):441-461. doi: 10.1093/humupd/dmp007 [doi].

6. Hudelist G, Keckstein J, Wright JT. The migrating adenomyoma: Past views on the etiology of adenomyosis and endometriosis. *Fertil Steril*. 2009;92(5):1536-1543. doi: 10.1016/j.fertnstert.2008.08.086 [doi].

7. Seydel AS, Sickel JZ, Warner ED, Sax HC. Extrapelvic endometriosis: Diagnosis and treatment. *Am J Surg*. 1996;171(2):8. doi: S0002-9610(97)89557-8 [pii].

8. Matalliotakis M, Goulielmos GN, Kalogiannidis I, Koumantakis G, Matalliotakis I, Arici A. Extra pelvic endometriosis: Retrospective analysis on 200 cases in two different countries. *Eur J Obstet Gynecol Reprod Biol*. 2017;217:34-37. doi: S0301-2115(17)30389-5 [pii].

9. Ceccaroni M, Clarizia R, Placci A. Pericardial, pleural, and diaphragmatic endometriosis. *J Thorac Cardiovasc Surg*. 2010;140(5):1189-1190. doi: 10.1016/j.jtcvs.2010.07.064 [doi].

10. Bourgioti C, Preza O, Panourgias E, et al. MR imaging of endometriosis: Spectrum of disease. *Diagn Interv Imaging*. 2017;98(11):751-767. doi: S2211-5684(17)30149-3 [pii].

11. Gunes M, Kayikcioglu F, Ozturkoglu E, Haberal A. Incisional endometriosis after cesarean section, episiotomy and other gynecologic procedures. *J Obstet Gynaecol Res*. 2005;31(5):471-475. doi: JOG322 [pii].

12. Chapron C, Fauconnier A, Dubuisson JB, Barakat H, Vieira M, Breart G. Deep infiltrating endometriosis: Relation between severity of dysmenorrhoea and extent of disease. *Hum Reprod*. 2003;18(4):760-766.

13. American Society for Reproductive Medicine. Revised american society for reproductive medicine classification of endometriosis: 1996. *Fertil Steril*. 1997;67(5):817-821. doi: S001502829781391X [pii].

14. Johnson NP, Hummelshoj L, Adamson GD, et al. World endometriosis society consensus on the classification of endometriosis. *Hum Reprod*. 2017;32(2):315-324. doi: 10.1093/humrep/dew293 [doi].

15. Haas D, Chvatal R, Habelsberger A, Wurm P, Schimetta W, Oppelt P. Comparison of revised american fertility society and ENZIAN staging: A critical evaluation of classifications of endometriosis on the basis of our patient population. *Fertil Steril*. 2011;95(5):1574-1578. doi: 10.1016/j.fertnstert.2011.01.135 [doi].

16. Adamson GD, Pasta DJ. Endometriosis fertility index: The new, validated endometriosis staging system. *Fertil Steril*. 2010;94(5):1609-1615. doi: 10.1016/j.fertnstert.2009.09.035 [doi].

17. Vercellini P, Fedele L, Aimi G, Pietropaolo G, Consonni D, Crosignani PG. Association between endometriosis stage, lesion type, patient characteristics and severity of pelvic pain symptoms: A multivariate analysis of over 1000 patients. *Hum Reprod*. 2007;22(1):266-271. doi: del339 [pii].

18. Leng J, Lang J, Guo L, Li H, Liu Z. Carcinosarcoma arising from atypical endometriosis in a cesarean section scar. *Int J Gynecol Cancer*. 2006;16(1):432-435. doi: IJG199 [pii].

19. Medeiros F, Araujo AR, Erickson-Johnson MR, et al. HMGA1 and HMGA2 rearrangements in mass-forming endometriosis. *Genes Chromosomes Cancer*. 2010;49(7):630-634. doi: 10.1002/gcc.20772 [doi].

20. Bulun SE. Endometriosis. *N Engl J Med*. 2009;360(3):268-279. doi: 10.1056/NEJMra0804690 [doi].

21. Ryan IP, Taylor RN. Endometriosis and infertility: New concepts. *Obstet Gynecol Surv*. 1997;52(6):365-371.

22. Barnhart K, Dunsmoor-Su R, Coutifaris C. Effect of endometriosis on in vitro fertilization. *Fertil Steril*. 2002;77(6):1148-1155. doi: S0015028202031126 [pii].

23. Berkley KJ, Dmitrieva N, Curtis KS, Papka RE. Innervation of ectopic endometrium in a rat model of endometriosis. *Proc Natl Acad Sci U S A*. 2004;101(30):11094-11098. doi: 10.1073/pnas.0403663101 [doi].

24. Burney RO, Giudice LC. Pathogenesis and pathophysiology of endometriosis. *Fertil Steril*. 2012;98(3):511-519. doi: 10.1016/j.fertnstert.2012.06.029 [doi].

25. Sanfilippo JS, Wakim NG, Schikler KN, Yussman MA. Endometriosis in association with uterine anomaly. *Am J Obstet Gynecol*. 1986;154(1):39-43. doi: 0002-9378(86)90389-3 [pii].

26. Ulukus M, Arici A. Immunology of endometriosis. *Minerva Ginecol*. 2005;57(3):237-248.

27. Martin JD, Hauck AE. Endometriosis in the male. *Am Surg*. 1985;51(7):426-430.

28. Jabr FI, Mani V. An unusual cause of abdominal pain in a male patient: Endometriosis. *Avicenna J Med*. 2014;4(4):99-101. doi: 10.4103/2231-0770.140660 [doi].

29. Dinulescu DM, Ince TA, Quade BJ, Shafer SA, Crowley D, Jacks T. Role of K-ras and pten in the development of mouse models of endometriosis and endometrioid ovarian cancer. *Nat Med*. 2005;11(1):63-70. doi: nm1173 [pii].

30. Simpson JL, Elias S, Malinak LR, Buttram VC. Heritable aspects of endometriosis. I. genetic studies. *Am J Obstet Gynecol*. 1980;137(3):327-331. doi: 0002-9378(80)90917-5 [pii].

31. Treloar SA, O'Connor DT, O'Connor VM, Martin NG. Genetic influences on endometriosis in an australian twin sample. sueT@qimr.edu.au. *Fertil Steril*. 1999;71(4):701-710. doi: S0015028298005408 [pii].

32. Treloar SA, Wicks J, Nyholt DR, et al. Genomewide linkage study in 1,176 affected sister pair families identifies a significant susceptibility locus for endometriosis on chromosome 10q26. *Am J Hum Genet*. 2005;77(3):365-376. doi: S0002-9297(07)63018-3 [pii].

33. Uno S, Zembutsu H, Hirasawa A, et al. A genome-wide association study identifies genetic variants in the CDKN2BAS locus associated with endometriosis in japanese. *Nat Genet*. 2010;42(8):707-710. doi: 10.1038/ng.612 [doi].

34. Pagliardini L, Gentilini D, Vigano' P, et al. An italian association study and meta-analysis with previous GWAS confirm WNT4, CDKN2BAS and FN1 as the first identified susceptibility loci for endometriosis. *J Med Genet*. 2013;50(1):43-46. doi: 10.1136/jmedgenet-2012-101257 [doi].

35. Nyholt DR, Low SK, Anderson CA, et al. Genome-wide association meta-analysis identifies new endometriosis risk loci. *Nat Genet*. 2012;44(12):1355-1359. doi: 10.1038/ng.2445 [doi].

36. Painter JN, Anderson CA, Nyholt DR, et al. Genome-wide association study identifies a locus at 7p15.2 associated with endometriosis. *Nat Genet*. 2011;43(1):51-54. doi: 10.1038/ng.731 [doi].

37. Sapkota Y, Steinthorsdottir V, Morris AP, et al. Meta-analysis identifies five novel loci associated with endometriosis highlighting key genes involved in hormone metabolism. *Nat Commun*. 2017;8:15539. doi: 10.1038/ncomms15539 [doi].

38. Parazzini F, Chiaffarino F, Surace M, et al. Selected food intake and risk of endometriosis. *Hum Reprod*. 2004;19(8):1755-1759. doi: 10.1093/humrep/deh395 [doi].

39. Missmer SA, Chavarro JE, Malspeis S, et al. A prospective study of dietary fat consumption and endometriosis risk. *Hum Reprod*. 2010;25(6):1528-1535. doi: 10.1093/humrep/deq044 [doi].

40. Mayani A, Barel S, Soback S, Almagor M. Dioxin concentrations in women with endometriosis. *Hum Reprod*. 1997;12(2):373-375.

41. Goldberg JM, Falcone T. Effect of diethylstilbestrol on reproductive function. *Fertil Steril*. 1999;72(1):1-7. doi: S0015-0282(99)00153-3 [pii].

42. Taniguchi F. New knowledge and insights about the malignant transformation of endometriosis. *J Obstet Gynaecol Res*. 2017;43(7):1093-1100. doi: 10.1111/jog.13372 [doi].

43. Sampson JA. Endometrial carcinoma of the ovary arising in endometrial tissue in that organ. *American Journal of Obstetrics & Gynecology*. 1925;9(1):111-114. http://dx.doi.org/10.1016/S0002-9378(25)90949-0. doi: 10.1016/S0002-9378(25)90949-0.

44. Brinton LA, Gridley G, Persson I, Baron J, Bergqvist A. Cancer risk after a hospital discharge diagnosis of endometriosis. *Am J Obstet Gynecol*. 1997;176(3):572-579. doi: S0002-9378(97)70550-7 [pii].

45. Pearce CL, Templeman C, Rossing MA, et al. Association between endometriosis and risk of histological subtypes of ovarian cancer: A pooled analysis of case-control studies. *Lancet Oncol*. 2012;13(4):385-394. doi: 10.1016/S1470-2045(11)70404-1 [doi].

46. Merritt MA, De Pari M, Vitonis AF, Titus LJ, Cramer DW, Terry KL. Reproductive characteristics in relation to ovarian cancer risk by histologic pathways. *Hum Reprod*. 2013;28(5):1406-1417. doi: 10.1093/humrep/des466 [doi].

47. Saavalainen L, Lassus H, But A, et al. Risk of gynecologic cancer according to the type of endometriosis. *Obstet Gynecol*. 2018;131(6):1095-1102. doi: 10.1097/AOG.0000000000002624 [doi].

48. Sieh W, Salvador S, McGuire V, et al. Tubal ligation and risk of ovarian cancer subtypes: A pooled analysis of case-control studies. *Int J Epidemiol*. 2013;42(2):579-589. doi: 10.1093/ije/dyt042 [doi].

49. Shen H, Fridley BL, Song H, et al. Epigenetic analysis leads to identification of HNF1B as a subtype-specific susceptibility gene for ovarian cancer. *Nat Commun*. 2013;4:1628. doi: 10.1038/ncomms2629 [doi].

50. Phelan CM, Kuchenbaecker KB, Tyrer JP, et al. Identification of 12 new susceptibility loci for different histotypes of epithelial ovarian cancer. *Nat Genet*. 2017;49(5):680-691. doi: 10.1038/ng.3826 [doi].

51. Anglesio MS, Yong PJ. Endometriosis-associated ovarian cancers. *Clin Obstet Gynecol*. 2017;60(4):711-727. doi: 10.1097/GRF.0000000000000320 [doi].

52. Jiang X, Hitchcock A, Bryan EJ, et al. Microsatellite analysis of endometriosis reveals loss of heterozygosity at candidate ovarian tumor suppressor gene loci. *Cancer Res*. 1996;56(15):3534-3539.

53. Goumenou AG, Arvanitis DA, Matalliotakis IM, Koumantakis EE, Spandidos DA. Microsatellite DNA assays reveal an allelic imbalance in p16(Ink4), GALT, p53, and

APOA2 loci in patients with endometriosis. *Fertil Steril*. 2001;75(1):160-165. doi: S0015-0282(00)01663-0 [pii].

54. Sato N, Tsunoda H, Nishida M, et al. Loss of heterozygosity on 10q23.3 and mutation of the tumor suppressor gene PTEN in benign endometrial cyst of the ovary: Possible sequence progression from benign endometrial cyst to endometrioid carcinoma and clear cell carcinoma of the ovary. *Cancer Res*. 2000;60(24):7052-7056.

55. Prowse AH, Manek S, Varma R, et al. Molecular genetic evidence that endometriosis is a precursor of ovarian cancer. *Int J Cancer*. 2006;119(3):556-562. doi: 10.1002/ijc.21845 [doi].

56. Gounaris I, Charnock-Jones DS, Brenton JD. Ovarian clear cell carcinoma--bad endometriosis or bad endometrium? *J Pathol*. 2011;225(2):157-160. doi: 10.1002/path.2970 [doi].

57. Mandai M, Yamaguchi K, Matsumura N, Baba T, Konishi I. Ovarian cancer in endometriosis: Molecular biology, pathology, and clinical management. *Int J Clin Oncol*. 2009;14(5):383-391. doi: 10.1007/s10147-009-0935-y [doi].

58. Wiegand KC, Shah SP, Al-Agha OM, et al. ARID1A mutations in endometriosis-associated ovarian carcinomas. *N Engl J Med*. 2010;363(16):1532-1543. doi: 10.1056/NEJMoa1008433 [doi].

59. Anglesio MS, Papadopoulos N, Ayhan A, et al. Cancer-associated mutations in endometriosis without cancer. *N Engl J Med*. 2017;376(19):1835-1848. doi: 10.1056/NEJMoa1614814 [doi].

60. Taylor RN, Lebovic DI, Mueller MD. Angiogenic factors in endometriosis. *Ann N Y Acad Sci*. 2002;955:406.

61. Kavallaris A, Kohler C, Kuhne-Heid R, Schneider A. Histopathological extent of rectal invasion by rectovaginal endometriosis. *Hum Reprod*. 2003;18(6):1323-1327.

62. Chene G, Ouellet V, Rahimi K, Barres V, Provencher D, Mes-Masson AM. The ARID1A pathway in ovarian clear cell and endometrioid carcinoma, contiguous endometriosis, and benign endometriosis. *Int J Gynaecol Obstet*. 2015;130(1):27-30. doi: 10.1016/j.ijgo.2015.02.021 [doi].

63. Samartzis EP, Samartzis N, Noske A, et al. Loss of ARID1A/BAF250a-expression in endometriosis: A biomarker for risk of carcinogenic transformation? *Mod Pathol*. 2012;25(6):885-892. doi: 10.1038/modpathol.2011.217 [doi].

64. Strom SP. Current practices and guidelines for clinical next-generation sequencing oncology testing. *Cancer Biol Med*. 2016;13(1):3-11. doi: 10.28092/j.issn.2095-3941.2016.0004 [doi].

65. Vestergaard AL, Thorup K, Knudsen UB, et al. Oncogenic events associated with endometrial and ovarian cancers are rare in endometriosis. *Mol Hum Reprod*. 2011;17(12):758-761. doi: 10.1093/molehr/gar049 [doi].

66. Kim MS, Yoo NJ, Hwang H, Kim MR, Lee SH. Absence of KRAS hotspot mutations in endometriosis of korean patients. *Histopathology*. 2018;73(2):357-360. doi: 10.1111/his.13524 [doi].

67. Zou Y, Zhou JY, Guo JB, et al. The presence of KRAS, PPP2R1A and ARID1A mutations in 101 chinese samples with ovarian endometriosis. *Mutat Res*. 2018;809:1-5. doi: S0027-5107(17)30206-3 [pii].

68. Li X, Zhang Y, Zhao L, et al. Whole-exome sequencing of endometriosis identifies frequent alterations in genes involved in cell adhesion and chromatin-remodeling complexes. *Hum Mol Genet*. 2014;23(22):6008-6021. doi: 10.1093/hmg/ddu330 [doi].

69. Wilbur MA, Shih IM, Segars JH, Fader AN. Cancer implications for patients with endometriosis. *Semin Reprod Med*. 2017;35(1):110-116. doi: 10.1055/s-0036-1597120 [doi].

70. Lacey JV, Mutter GL, Ronnett BM, et al. PTEN expression in endometrial biopsies as a marker of progression to endometrial carcinoma. *Cancer Res*. 2008;68(14):6014-6020. doi: 10.1158/0008-5472.CAN-08-1154 [doi].

71. Lin MC, Burkholder KA, Viswanathan AN, Neuberg D, Mutter GL. Involution of latent endometrial precancers by hormonal and nonhormonal mechanisms. *Cancer*. 2009;115(10):2111-2118. doi: 10.1002/cncr.24218 [doi].

72. Mutter GL, Monte NM, Neuberg D, Ferenczy A, Eng C. Emergence, involution, and progression to carcinoma of mutant clones in normal endometrial tissues. *Cancer Res*. 2014;74(10):2796-2802. doi: 10.1158/0008-5472.CAN-14-0108 [doi].

73. Monte NM, Webster KA, Neuberg D, Dressler GR, Mutter GL. Joint loss of PAX2 and PTEN expression in endometrial precancers and cancer. *Cancer Res*. 2010;70(15):6225-6232. doi: 10.1158/0008-5472.CAN-10-0149 [doi].

74. Turashvili G, Yang W, McKinney S, et al. Nucleic acid quantity and quality from paraffin blocks: Defining optimal fixation, processing and DNA/RNA extraction techniques. *Exp Mol Pathol*. 2012;92(1):33-43. doi: 10.1016/j.yexmp.2011.09.013 [doi].

75. Forbes SA, Beare D, Boutselakis H, et al. COSMIC: Somatic cancer genetics at high-resolution. *Nucleic Acids Res*. 2017;45(D1):D783. doi: 10.1093/nar/gkw1121 [doi].

76. Do H, Dobrovic A. Sequence artifacts in DNA from formalin-fixed tissues: Causes and strategies for minimization. *Clin Chem*. 2015;61(1):64-71. doi: 10.1373/clinchem.2014.223040 [doi].

77. Borrelli GM, Abrao MS, Taube ET, et al. (Partial) loss of BAF250a (ARID1A) in rectovaginal deep-infiltrating endometriosis, endometriomas and involved pelvic sentinel lymph nodes. *Mol Hum Reprod*. 2016;22(5):329-337. doi: 10.1093/molehr/gaw009 [doi].

78. Khalique S, Naidoo K, Attygalle AD, et al. Optimised ARID1A immunohistochemistry is an accurate predictor of ARID1A mutational status in gynaecological cancers. *J Pathol Clin Res*. 2018. doi: 10.1002/cjp2.103 [doi].

79. Djordjevic B, Hennessy BT, Li J, et al. Clinical assessment of PTEN loss in endometrial carcinoma: Immunohistochemistry outperforms gene sequencing. *Mod Pathol*. 2012;25(5):699-708. doi: 10.1038/modpathol.2011.208 [doi].

80. Karnezis AN, Leung S, Magrill J, et al. Evaluation of endometrial carcinoma prognostic immunohistochemistry markers in the context of molecular classification. *J Pathol Clin Res*. 2017;3(4):279-293. doi: 10.1002/cjp2.82 [doi].

81. Kaloo P, Reid G, Wong F. Caesarean section scar endometriosis: Two cases of recurrent disease and a literature review. *Aust N Z J Obstet Gynaecol*. 2002;42(2):218-220.

82. Nominato NS, Prates LF, Lauar I, Morais J, Maia L, Geber S. Caesarean section greatly increases risk of scar endometriosis. *Eur J Obstet Gynecol Reprod Biol*. 2010;152(1):83-85. doi: 10.1016/j.ejogrb.2010.05.001 [doi].

83. Rahmioglu N, Fassbender A, Vitonis AF, et al. World endometriosis research foundation endometriosis phenome and biobanking harmonization project: III. fluid biospecimen collection, processing, and storage in endometriosis research. *Fertil Steril*. 2014;102(5):1233-1243. doi: 10.1016/j.fertnstert.2014.07.1208 [doi].

84. Ludbrook J. Multiple comparison procedures updated. *Clin Exp Pharmacol Physiol*. 1998;25(12):1032-1037.

85. Zhang W, Liu HT. MAPK signal pathways in the regulation of cell proliferation in mammalian cells. *Cell Res*. 2002;12(1):9-18. doi: 10.1038/sj.cr.7290105 [doi].

86. Cully M, You H, Levine AJ, Mak TW. Beyond PTEN mutations: The PI3K pathway as an integrator of multiple inputs during tumorigenesis. *Nat Rev Cancer*. 2006;6(3):184-192. doi: nrc1819 [pii].

87. Yamaguchi K, Mandai M, Toyokuni S, et al. Contents of endometriotic cysts, especially the high concentration of free iron, are a possible cause of carcinogenesis in

the cysts through the iron-induced persistent oxidative stress. *Clin Cancer Res*. 2008;14(1):32-40. doi: 10.1158/1078-0432.CCR-07-1614 [doi].

88. Risques RA, Kennedy SR. Aging and the rise of somatic cancer-associated mutations in normal tissues. *PLoS Genet*. 2018;14(1):e1007108. doi: 10.1371/journal.pgen.1007108 [doi].

89. Nair N, Camacho-Vanegas O, Rykunov D, et al. Genomic analysis of uterine lavage fluid detects early endometrial cancers and reveals a prevalent landscape of driver mutations in women without histopathologic evidence of cancer: A prospective cross-sectional study. *PLoS Med*. 2016;13(12):e1002206. doi: 10.1371/journal.pmed.1002206 [doi].

90. Krimmel JD, Schmitt MW, Harrell MI, et al. Ultra-deep sequencing detects ovarian cancer cells in peritoneal fluid and reveals somatic TP53 mutations in noncancerous tissues. *Proc Natl Acad Sci U S A*. 2016;113(21):6005-6010. doi: 10.1073/pnas.1601311113 [doi].

91. Jacobs KB, Yeager M, Zhou W, et al. Detectable clonal mosaicism and its relationship to aging and cancer. *Nat Genet*. 2012;44(6):651-658. doi: 10.1038/ng.2270 [doi].

92. Martincorena I, Roshan A, Gerstung M, et al. Tumor evolution. high burden and pervasive positive selection of somatic mutations in normal human skin. *Science*. 2015;348(6237):880-886. doi: 10.1126/science.aaa6806 [doi].

93. Bromer JG, Aldad TS, Taylor HS. Defining the proliferative phase endometrial defect. *Fertil Steril*. 2009;91(3):698-704. doi: 10.1016/j.fertnstert.2007.12.066 [doi].

94. Ferenczy A, Bertrand G, Gelfand MM. Proliferation kinetics of human endometrium during the normal menstrual cycle. *Am J Obstet Gynecol*. 1979;133(8):859-867. doi: 0002-9378(79)90302-8 [pii].

95. Nnoaham KE, Hummelshoj L, Webster P, et al. Impact of endometriosis on quality of life and work productivity: A multicenter study across ten countries. *Fertil Steril*. 2011;96(2):373.e8. doi: 10.1016/j.fertnstert.2011.05.090 [doi].

96. Simoens S, Dunselman G, Dirksen C, et al. The burden of endometriosis: Costs and quality of life of women with endometriosis and treated in referral centres. *Hum Reprod*. 2012;27(5):1292-1299. doi: 10.1093/humrep/des073 [doi].

97. Samatar AA, Poulikakos PI. Targeting RAS-ERK signalling in cancer: Promises and challenges. *Nat Rev Drug Discov*. 2014;13(12):928-942. doi: 10.1038/nrd4281 [doi].

98. Engelman JA. Targeting PI3K signalling in cancer: Opportunities, challenges and limitations. *Nat Rev Cancer*. 2009;9(8):550-562. doi: 10.1038/nrc2664 [doi].

99. Beliard A, Noel A, Foidart JM. Reduction of apoptosis and proliferation in endometriosis. *Fertil Steril*. 2004;82(1):80-85. doi: 10.1016/j.fertnstert.2003.11.048 [doi].

100. Braun DP, Ding J, Shaheen F, Willey JC, Rana N, Dmowski WP. Quantitative expression of apoptosis-regulating genes in endometrium from women with and without endometriosis. *Fertil Steril*. 2007;87(2):263-268. doi: S0015-0282(06)03192-X [pii].

101. Pylayeva-Gupta Y, Grabocka E, Bar-Sagi D. RAS oncogenes: Weaving a tumorigenic web. *Nat Rev Cancer*. 2011;11(11):761-774. doi: 10.1038/nrc3106 [doi].

102. Matsuo Y, Campbell PM, Brekken RA, et al. K-ras promotes angiogenesis mediated by immortalized human pancreatic epithelial cells through mitogen-activated protein kinase signaling pathways. *Mol Cancer Res*. 2009;7(6):799-808. doi: 10.1158/1541-7786.MCR-08-0577 [doi].

103. Wang ZD, Wei SQ, Wang QY. Targeting oncogenic KRAS in non-small cell lung cancer cells by phenformin inhibits growth and angiogenesis. *Am J Cancer Res*. 2015;5(11):3339-3349.

104. Kinoshita T, Yokota T, Arai K, Miyajima A. Regulation of bcl-2 expression by oncogenic ras protein in hematopoietic cells. *Oncogene*. 1995;10(11):2207-2212.

105. Okamoto K, Zaanan A, Kawakami H, Huang S, Sinicrope FA. Reversal of mutant KRAS-mediated apoptosis resistance by concurrent noxa/bik induction and bcl-2/bcl-xL antagonism in colon cancer cells. *Mol Cancer Res*. 2015;13(4):659-669. doi: 10.1158/1541-7786.MCR-14-0476 [doi].

106. Cheng CW, Licence D, Cook E, et al. Activation of mutated K-ras in donor endometrial epithelium and stroma promotes lesion growth in an intact immunocompetent murine model of endometriosis. *J Pathol*. 2011;224(2):261-269. doi: 10.1002/path.2852 [doi].

107. Committee on the State of the Science in Ovarian Cancer Research, Board on Health Care Services, Institute of Medicine, National Academies of Sciences, Engineering. Ovarian cancers: Evolving paradigms in research and care. . 2016. doi: 10.17226/21841 [doi].

108. Wang YK, Bashashati A, Anglesio MS, et al. Genomic consequences of aberrant DNA repair mechanisms stratify ovarian cancer histotypes. *Nat Genet*. 2017;49(6):856-865. doi: 10.1038/ng.3849 [doi].

109. Wang Q, Chaerkady R, Wu J, et al. Mutant proteins as cancer-specific biomarkers. *Proc Natl Acad Sci U S A*. 2011;108(6):2444-2449. doi: 10.1073/pnas.1019203108 [doi].

110. Piton N, Borrini F, Bolognese A, Lamy A, Sabourin JC. KRAS and BRAF mutation detection: Is immunohistochemistry a possible alternative to molecular biology in colorectal cancer? *Gastroenterol Res Pract*. 2015;2015:753903. doi: 10.1155/2015/753903 [doi].

111. Baker AM, Huang W, Wang XM, et al. Robust RNA-based in situ mutation detection delineates colorectal cancer subclonal evolution. *Nat Commun*. 2017;8(1):5. doi: 10.1038/s41467-017-02295-5 [doi].

112. Zhu Y, Sharp A, Anderson CM, et al. Novel junction-specific and quantifiable in situ detection of AR-V7 and its clinical correlates in metastatic castration-resistant prostate cancer. *Eur Urol*. 2018;73(5):727-735. doi: S0302-2838(17)30695-4 [pii].

113. Merritt MA, Cramer DW. Molecular pathogenesis of endometrial and ovarian cancer. *Cancer Biomark*. 2010;9(1-6):287-305. doi: 10.3233/CBM-2011-0167 [doi].

114. Collaborative Group on Epidemiological Studies of Ovarian Cancer, Beral V, Doll R, Hermon C, Peto R, Reeves G. Ovarian cancer and oral contraceptives: Collaborative reanalysis of data from 45 epidemiological studies including 23,257 women with ovarian cancer and 87,303 controls. *Lancet*. 2008;371(9609):303-314. doi: 10.1016/S0140-6736(08)60167-1 [doi].

115. Gierisch JM, Coeytaux RR, Urrutia RP, et al. Oral contraceptive use and risk of breast, cervical, colorectal, and endometrial cancers: A systematic review. *Cancer Epidemiol Biomarkers Prev*. 2013;22(11):1931-1943. doi: 10.1158/1055-9965.EPI-13-0298 [doi].

116. Mueck AO, Seeger H, Rabe T. Hormonal contraception and risk of endometrial cancer: A systematic review. *Endocr Relat Cancer*. 2010;17(4):263. doi: 10.1677/ERC-10-0076 [doi].

117. Grummer R. Animal models in endometriosis research. *Hum Reprod Update*. 2006;12(5):641-649. doi: dml026 [pii].

118. Diaz LA, Bardelli A. Liquid biopsies: Genotyping circulating tumor DNA. *J Clin Oncol*. 2014;32(6):579-586. doi: 10.1200/JCO.2012.45.2011 [doi].

119. Wang Y, Li L, Douville C, et al. Evaluation of liquid from the papanicolaou test and other liquid biopsies for the detection of endometrial and ovarian cancers. *Sci Transl Med*. 2018;10(433):10.1126/scitranslmed.aap8793. doi: eaap8793 [pii].

120. Heim LJ. Evaluation and differential diagnosis of dyspareunia. *Am Fam Physician*. 2001;63(8):1535-1544.

121. Yong PJ, Williams C, Yosef A, et al. Anatomic sites and associated clinical factors for deep dyspareunia. *Sex Med*. 2017;5(3):e195. doi: S2050-1161(17)30039-9 [pii].

122. Denny E, Mann CH. Endometriosis-associated dyspareunia: The impact on women's lives. *J Fam Plann Reprod Health Care*. 2007;33(3):189-193. doi: 10.1783/147118907781004831 [doi].

123. Yu J, Francisco AMC, Patel BG, et al. Interleukin-1beta stimulates BDNF production in eutopic endometriosis stromal cell cultures A model for cytokine regulation of neuroangiogenesis. *Am J Pathol*. 2018. doi: S0002-9440(18)30097-X [pii].

124. Williams C, Hoang L, Yosef A, et al. Nerve bundles and deep dyspareunia in endometriosis. *Reprod Sci*. 2016;23(7):892-901. doi: 10.1177/1933719115623644 [doi].

125. Scholl B, Bersinger NA, Kuhn A, Mueller MD. Correlation between symptoms of pain and peritoneal fluid inflammatory cytokine concentrations in endometriosis. *Gynecol Endocrinol*. 2009;25(11):701-706. doi: 10.3109/09513590903159680 [doi].

126. Neziri AY, Bersinger NA, Andersen OK, Arendt-Nielsen L, Mueller MD, Curatolo M. Correlation between altered central pain processing and concentration of peritoneal fluid inflammatory cytokines in endometriosis patients with chronic pelvic pain. *Reg Anesth Pain Med*. 2014;39(3):181-184. doi: 10.1097/AAP.0000000000000068 [doi].

127. Woolf CJ, Allchorne A, Safieh-Garabedian B, Poole S. Cytokines, nerve growth factor and inflammatory hyperalgesia: The contribution of tumour necrosis factor alpha. *Br J Pharmacol*. 1997;121(3):417-424. doi: 10.1038/sj.bjp.0701148 [doi].

128. Cui J, Liu Y, Wang X. The roles of glycodelin in cancer development and progression. *Front Immunol*. 2017;8:1685. doi: 10.3389/fimmu.2017.01685 [doi].

129. Okumura T, Ericksen RE, Takaishi S, et al. K-ras mutation targeted to gastric tissue progenitor cells results in chronic inflammation, an altered microenvironment, and progression to intraepithelial neoplasia. *Cancer Res*. 2010;70(21):8435-8445. doi: 10.1158/0008-5472.CAN-10-1506 [doi].

130. Okumura T, Ericksen RE, Takaishi S, et al. K-ras mutation targeted to gastric tissue progenitor cells results in chronic inflammation, an altered microenvironment, and progression to intraepithelial neoplasia. *Cancer Res*. 2010;70(21):8435-8445. doi: 10.1158/0008-5472.CAN-10-1506 [doi].

131. Boutin AT, Liao WT, Wang M, et al. Oncogenic kras drives invasion and maintains metastases in colorectal cancer. *Genes Dev*. 2017;31(4):370-382. doi: 10.1101/gad.293449.116 [doi].

Appendices

Appendix A: Summary of clinical data for women with IE.

Source	Patient ID	Age (years)	Diagnosis	Affected Site	Interval (years)	Number of IE Blocks Analyzed	Surgical History	Additional Notes
VGH	IE_1	37	incisional EMS	subcutaneous	11	2	surgical abortion	
VGH	IE_2	36	incisional EMS	subcutaneous	n/a	1	no prior surgery identified	
VGH	IE_3	37	incisional EMS	subcutaneous	3	2	TAH-BSO	
VGH	IE_4	31	incisional EMS	subcutaneous	n/a	1	c-section	
VGH	IE_5	45	incisional EMS	fascia	17	1	surgical abortion	eutopic endometrium sampling available
VGH	IE_6	32	incisional EMS	subcutaneous	4	1	c-section	
VGH	IE_7	28	umbilical EMS	subcutaneous	n/a	2	no prior surgery identified	
VGH	IE_8	48	umbilical EMS	subcutaneous	3	2	laparoscopy	
VGH	IE_9	44	umbilical EMS	subcutaneous	n/a	1	no prior surgery identified	
VGH	IE_10	49	incisional EMS	abdominal wall	1 month[a]	4	c-section (earlier timepoint); laparoscopy	eutopic endometrium sampling available
VGH	IE_11	37	incisional EMS	abdominal wall	4	2	c-section	
VGH	IE_12	41	incisional EMS	abdominal wall	6	3	c-section	eutopic endometrium sampling available
Mannheim	IE_13	34	incisional EMS	recto-uterine pouch	n/a	3	n/a	
Mannheim	IE_14	29	post c-section EMS	abdominal wall	n/a	1	c-section	

Source	Patient ID	Age (years)	Diagnosis	Affected Site	Interval (years)	Number of IE Blocks Analyzed	Surgical History	Additional Notes
Mannheim	IE_15	30	post c-section EMS	abdominal wall	n/a	2	c-section	
Mannheim	IE_16	28	post c-section EMS	abdominal wall	n/a	1	c-section	
Mannheim	IE_17	38	post c-section EMS	abdominal wall	n/a	2	c-section	
Mannheim	IE_18	32	post c-section EMS	abdominal wall	n/a	1	c-section	
Mannheim	IE_19	40	post c-section EMS	abdominal wall	n/a	1	c-section	
Mannheim	IE_20	38	post c-section EMS	abdominal wall	n/a	1	c-section	
Mannheim	IE_21	32	umbilical EMS	subcutaneous	n/a	1	n/a	
Mannheim	IE_22	36	post c-section EMS	abdominal wall	n/a	1	c-section	
Tuebingen	IE_23	39	incisional EMS	n/a	9[a]	3	c-section	
Tuebingen	IE_24	41	incisional EMS	n/a	12	1	c-section via vertical laparotomy	
Tuebingen	IE_25	43	incisional EMS	n/a	2	1	c-section	
Tuebingen	IE_26	35	incisional EMS	n/a	5	2	c-section	
Tuebingen	IE_27	37	umbilical EMS	n/a	3[a]	2	c-section (earlier timepoint); umbilical hernia	hx of endometriosis
Tuebingen	IE_28	39	incisional EMS	n/a	3	1	c-section	eutopic endometrium sampling available
Tuebingen	IE_29	45	umbilical EMS	n/a	1	1	laparoscopic supracervical hysterectomy	hx of endometriosis

Source	Patient ID	Age (years)	Diagnosis	Affected Site	Interval (years)	Number of IE Blocks Analyzed	Surgical History	Additional Notes
Tuebingen	IE_30	40	incisional EMS	n/a	10	2	c-section	
Tuebingen	IE_31	28	umbilical EMS	n/a	4	1	diagnostic laparoscopy	
Tuebingen	IE_32	38	umbilical EMS	n/a	1	1	laparoscopy	
Tuebingen	IE_33	30	umbilical EMS	n/a	2	1	adnexectomy	hx of endometriosis
Tuebingen	IE_34	36	incisional EMS	n/a	13	1	c-section	hx of endometriosis
Tuebingen	IE_35	30	incisional EMS	n/a	4[a]	1	c-section (earlier timepoint); c-section	
Tuebingen	IE_36	36	incisional EMS	n/a	5	1	c-section	hx of endometriosis
Tuebingen	IE_37	41	incisional EMS	n/a	4	1	c-section	hx of endometriosis
VUMC	IE_38	33	post c-section EMS	abdominal wall	2	1	c-section	
VUMC	IE_39	31	post c-section EMS	abdominal wall	3	1	c-section	
VUMC	IE_40	35	post c-section EMS	abdominal wall	3	1	c-section	

[a] Patients IE_10, IE_23, and IE_35 had multiple documented surgeries prior to resection of incisional endometriosis – the reported time interval between suspected inciting surgery and resection of endometriosis in these women reflect the time of the most recent surgery.

Appendix B: Summary of clinical data for women with DE.

Source	Patient ID	Age (years)	Clinical Stage (r-ASRM)	Block ID and Descriptor	Anatomical Site	Additional Notes
BC Women's	DE_1	41	IV	A: index	peri-ureter	
BC Women's	DE_2	50	IV	A: index	recto-uterine	
BC Women's	DE_3	29	II	A: index	uterosacral ligament	MFPE tissue
BC Women's	DE_4	28	IV	A: index	sigmoid colon	MFPE tissue
BC Women's	DE_5	25	III	A: index	uterosacral ligament	MFPE tissue
BC Women's	DE_6	34	IV	A: index	rectovaginal	MFPE tissue
BC Women's	DE_7	41	IV	A: index	rectovaginal	MFPE tissue
BC Women's	DE_8	40	II	A: index	uterosacral ligament	MFPE tissue
BC Women's	DE_9	33	III	A: index	sigmoid colon	MFPE tissue
BC Women's	DE_10	27	III	A: index	posterior cul-de-sac	MFPE tissue
BC Women's	DE_11	27	II	A: index	central cul-de-sac	
				B: separate	left uterosacral	
BC Women's	DE_12	39	IV	A: index	left uterosacral	
				B: separate	bladder peritoneum	
BC Women's	DE_13	26	III	A: index	central cul-de-sac	
				B: separate	left peri-ureteric nodule	
BC Women's	DE_14	22	I	A: index	left uterosacral	
BC Women's	DE_15	49	IV	A: index	right uterosacral	
BC Women's	DE_16	36	IV	A: index	Cul-de-sac	
				B: separate	ovary	

Source	Patient ID	Age (years)	Clinical Stage (r-ASRM)	Block ID and Descriptor	Anatomical Site	Additional Notes
BC Women's	DE_17	32	III	A: index	left ureterosacral area	
BC Women's	DE_18	36	IV	A: index	rectovaginal nodule	
BC Women's	DE_19	38	III	A: index	left ovarian fossa	
				B: separate	bladder peritoneum	
BC Women's	DE_20	45	IV	A: index	posterior cul-de-sac	
BC Women's	DE_21	44	III	A: index	uterosacra right periureteric nodule	
				B: separate	right pararectal	
BC Women's	DE_22	24	III	A: index	left uterosacral	
				B: separate	right uterosacral	
BC Women's	DE_23	35	III	A: index	right vaginal-rectal nodule	
VUMC	DE_24	32	IV	A: index	Colon (rectosigmoid)	
VUMC	DE_25	33	IV	A: index	Colon (rectosigmoid)	
VUMC	DE_26	30	IV	A: index	colon, (rectosigmoid) bladder, left tube, endometriosis cyst (right side)	
VUMC	DE_27	37	IV	A: index	sigmoid colon	
VUMC	DE_28	26	IV	A: index	rectosigmoid	
VUMC	DE_29	35	IV	A: index	sigmoid	
VUMC	DE_30	33	IV	A: index	Colon (rectosigmoid),	

Source	Patient ID	Age (years)	Clinical Stage (r-ASRM)	Block ID and Descriptor	Anatomical Site	Additional Notes
					bladder peritoneum	
VUMC	DE_31	33	II	A: index	posterior bladder wall	
VUMC	DE_32	31	III	A: index	rectosigmoid	
VUMC	DE_33	29	IV	A: index	Bladder (posterior wall)	
VUMC	DE_34	31	IV	A: index	Colon (rectosigmoid), left , right tube	
VUMC	DE_35	43	II	A: index	Bladder (posterior wall)	
VUMC	DE_36	26	IV	A: index	Tubes left & right	

Appendix C: Summary of somatic cancer-driver events in women with IE.

Patient ID	Block ID and Descriptor	Driver Mutation Identified	Material for IHC Staining	PTEN IHC	ARID1A IHC
IE_1	A:index		whole section	+	+
	B: adjacent		whole section	+	+
IE_2	A: index		whole section	+	+
IE_3	A: index		whole section	+	+
	B: adjacent		whole section	+	+
IE_4	A: index		whole section	+	+
IE_5	A: index		whole section	+	+
IE_6	A: index		whole section	+	+
IE_7	A: index		whole section	+	+
	B: adjacent		whole section	+	+
IE_8	A: index	KRAS G12V	whole section	+	+
	B: adjacent	KRAS G12V	whole section	+	+
IE_9	A: index		whole section	+	+
IE_10	A: index		whole section	+	+
	B: adjacent		whole section	+	+
	C: adjacent		whole section	+	+
	D: adjacent		whole section	+	+
IE_11	A: index		whole section	HET	+
	B: adjacent		whole section	+	+
IE_12	A: index		whole section	+	+
	B: adjacent		whole section	+	+
	C: adjacent		whole section	+	+
IE_13	A: index		whole section	HET	+
	B: adjacent		whole section	+	+
	C: adjacent		whole section	+	+

Patient ID	Block ID and Descriptor	Driver Mutation Identified	Material for IHC Staining	PTEN IHC	ARID1A IHC
IE_14	A: index		whole section	+	+
IE_15	A: index		whole section	HET	+
	B: adjacent		whole section	HET	+
IE_16	A: index	ERBB2 S310F	whole section	+	+
IE_17	A: index		whole section	HET	+
	B: adjacent		whole section	HET	+
IE_18	A: index		whole section	+	+
IE_19	A: index	KRAS G12C	whole section	+	+
IE_20	A: index		whole section	+	+
IE_21	A: index		whole section	HET	+
IE_22	A: index		whole section	+	+
IE_23	A: index		whole section	+	+
	B: adjacent		whole section	+	+
	C: adjacent		whole section	+	+
IE_24	A: index		whole section	+	+
IE_25	A: index	PIK3CA H1047R	whole section	+	+
IE_26	A: index		whole section	+	+
	B: adjacent		whole section	+	+
IE_27	A: index		whole section	+	+
	B: adjacent		whole section	+	+
IE_28	A: index		whole section	+	+
IE_29	A: index		whole section	+	+
IE_30	A: index		whole section	+	+
	B: adjacent		whole section	+	+

Patient ID	Block ID and Descriptor	Driver Mutation Identified	Material for IHC Staining	PTEN IHC	ARID1A IHC
IE_31	A: index		n/a	n/a	n/a
IE_32	A: index		whole section	+	+
IE_33	A: index		whole section	+	+
IE_34	A: index		whole section	HET	+
IE_35	A: index		whole section	+	+
IE_36	A: index		whole section	n/a	+
IE_37	A: index		whole section	n/a	+
IE_38	A: index		TMA	+	+
IE_39	A: index		TMA	LOSS	+
IE_40	A: index		TMA	+	+

*“HET” denotes loss of expression in some glands in a section, but not others. “LOSS” indicates loss of expression in all glands. “Adjacent” refers to tissue specimens obtained from a different archival tissue block yet the same anatomical site as the index block.

Appendix D: Summary of somatic cancer-driver events in women with DE.

Patient ID	Block ID and Descriptor	Anatomical Site	Driver Mutation Identified	Material for IHC Staining	PTEN IHC	ARID1A IHC
DE_1	A: index	peri-ureter	CTNNB1 G34V	whole section	+	+
DE_2	A: index	recto-uterine	KRAS G12D	whole section	+	+
DE_3	A: index	uterosacral ligament		whole section	n/a[a]	+
DE_4	A: index	sigmoid colon		whole section	n/a[a]	+
DE_5	A: index	uterosacral ligament	KRAS G12D	whole section	n/a[a]	+
DE_6	A: index	Rectovaginal		whole section	n/a[a]	+
DE_7	A: index	Rectovaginal		whole section	n/a[a]	HET
DE_8	A: index	uterosacral ligament		whole section	n/a[a]	+
DE_9	A: index	sigmoid colon		whole section	n/a[a]	+
DE_10	A: index	posterior cul-de-sac	KRAS G12V	whole section	n/a[a]	+
DE_11	A: index	central cul-de-sac	KRAS G12D	whole section	+	+
	B: separate	left uterosacral		whole section	+	+
DE_12	A: index	left uterosacral		whole section	+	+
	B: separate	bladder peritoneum		whole section	+	+
DE_13	A: index	central cul-de-sac		whole section	HET	+

Patient ID	Block ID and Descriptor	Anatomical Site	Driver Mutation Identified	Material for IHC Staining	PTEN IHC	ARID1A IHC
	B: separate	left peri-ureteric nodule		whole section	+	+
DE_14	A: index	left uterosacral	KRAS G12C	whole section	+	+
DE_15	A: index	right uterosacral	PIK3CA E545A	whole section	HET	+
DE_16	A: index	Cul-de-sac		whole section	+	+
	B: separate	Ovary		whole section	+	+
DE_17	A: index	left ureterosacral area		whole section	HET	+
DE_18	A: index	rectovaginal nodule		whole section	failed	+
DE_19	A: index	left ovarian fossa		whole section	+	+
	B: separate	bladder peritoneum		whole section	+	+
DE_20	A: index	posterior cul-de-sac		whole section	+	+
DE_21	A: index	uterosacra right periureteric nodule		whole section	HET	+
	B: separate	right pararectal	KRAS G12V	whole section	+	+
DE_22	A: index	left uterosacral		whole section	+	+
	B: separate	right uterosacral		whole section	+	+
DE_23	A: index	right vaginal-rectal nodule		whole section	HET	+

Patient ID	Block ID and Descriptor	Anatomical Site	Driver Mutation Identified	Material for IHC Staining	PTEN IHC	ARID1A IHC
DE_24	A: index	Colon (rectosigmoid)		TMA	+	+
DE_25	A: index	Colon (rectosigmoid)		TMA	+	+
DE_26	A: index	colon, (rectosigmoid) bladder, left tube, endometriosis cyst (right side)		n/a	n/a	n/a
DE_27	A: index	sigmoid colon		TMA	+	+
DE_28	A: index	Rectosigmoid		TMA	+	+
DE_29	A: index	Sigmoid		TMA	+	+
DE_30	A: index	Colon (rectosigmoid), bladder peritoneum		TMA	+	+
DE_31	A: index	posterior bladder wall		TMA	+	+
DE_32	A: index	Rectosigmoid	KRAS G12A	TMA	+	+
DE_33	A: index	Bladder (posterior wall)		n/a	n/a	n/a
DE_34	A: index	Colon (rectosigmoid), left , right tube		TMA	+	+
DE_35	A: index	Bladder (posterior wall)		TMA	+	+
DE_36	A: index	Tubes left & right		TMA	+	+

[a] All PTEN staining for MFPE sections (Patients DE_3 to DE_10) failed (no MFPE tissue retained PTEN stain).

*"HET" denotes loss of expression in some glands in a section, but not others. "Separate" refers to specimens obtained from an anatomically distinct site from the index block.

Appendix E: Summary of clinical data for women in Hx cohort.

Patient ID	Age (years)	Reason for surgery	Endometrium Phase	Clinical History / Comments
Hx_1	29	pelvic pain	proliferative	Hx of mature cystic teratoma
Hx_2	29	pelvic pain	proliferative	
Hx_3	30	chronic pelvic pain	proliferative	
Hx_4	31	Chronic pelvic pain	late proliferative	
Hx_5	31	? Leiomyoma	irregular secretory	
Hx_6	32	fibroid	secretory	
Hx_7	33	? (endometrial polyp)	proliferative	
Hx_8	32	fibroid/pain	proliferative	
Hx_9	33	prolapse	??? (branching present...)	
Hx_10	36	? (leios)		
Hx_11	36	sex reassignment	proliferative	
Hx_12	37	fibrods (leios)	proliferative	
Hx_13	38	r/o endometriosis (leios)	secretory	
Hx_14	37	fibroids (leios)	early secretory	
Hx_15	40	bleeding -on Fibristal (leios)	secretory	
Hx_16	44	Fibroid (leios)	secretory	
Hx_17	45	? (leios)	proliferative	adenomyosis present
Hx_18	48	Fibroid (leios)	disordered proliferative	
Hx_19	34	pelvic pain (leios)	proliferative	
Hx_20	35	dysmenorrhea	proliferative	
Hx_21	37	fibroid (leios)	proliferative	
Hx_22	51	fibroids	weakly proliferative	

Patient ID	Age (years)	Reason for surgery	Endometrium Phase	Clinical History / Comments
Hx_23	44	degenerating leiomyoma	proliferative	endometriotic cyst left ovary
Hx_24	49	fibroid	disordered proliferative	
Hx_25	42	leiomyoma	secretory	distortion of uterus

Appendix F: Summary of clinical data for women in Bx cohort.

Patient ID	Age (years)	Clinical History	Endometrium Phase
Bx_1	37	Abnormal uterine bleeding	Proliferative
Bx_2	36	Irregular cycles	Benign proliferative
Bx_3	38		proliferative
Bx_4	32	Abnormal uterine bleeding	Benign proliferative
Bx_5	45	Menorrhagia	proliferative endometrium
Bx_6	32	infertility, polypoid endometrial lining	late secretory
Bx_7	27	1 year history of abnormal bleeding, Mother has endometrial cancer	Proliferative endometrium
Bx_8	49	R/O pathology, dysmenorrhea	Secretory endometrium
Bx_9	44	Irregular bleeding, R/O hyperplasia	Secretory endometrium
Bx_10	34	Menorrhagia	Secretory
Bx_11	29	R/O hyperplasia PCOS	proliferative endometrium
Bx_12	29	Chronic anovulation	secretory endometrium
Bx_13	29	recurrent implant failure	early secretory
Bx_14	38	recurrent implant failure	proliferative
Bx_15	34	Infertility multiple polyps seen on hysteroscopy	late secretory

Patient ID	Age (years)	Clinical History	Endometrium Phase
Bx_16	40	?polyp, menorrhagia	secretory
Bx_17	38		proliferative
Bx_18	34	Abnormal uterine bleeding	secretory
Bx_19	36	submucosal fibroid -> reason for procedure	late secretory
Bx_20	49	menorrhagia	proliferative
Bx_21	37	Irregular bleeding	Irregular secretory
Bx_22	43	Menorrhagia and fibroid uterus	Postovulatory menstrual endometrium
Bx_23	29	Postcoital spotting	secretory endometrium
Bx_24	21	irregular menses, rule out acute pathology	Proliferative type endometrium
Bx_25	23	menorrhagia	secretory
Bx_26	24	Irregular menstrual cycles	Disordered proliferative endometrium
Bx_27	25	Rule out hyperplasia, PCOS	Proliferative endometrium
Bx_28	25	PCOS, R/O hyperplasia	Proliferative endometrium
Bx_29	26	Abnormal uterine bleeding	proliferative
Bx_30	27	menorrhagia	Secretory endometrium
Bx_31	27	Menorrhagia, chronic anovulation	Proliferative endometrium
Bx_32	27		proliferative endometrium

Patient ID	Age (years)	Clinical History	Endometrium Phase
Bx_33	27		proliferative endometrium
Bx_34	27	Abnormal uterine bleeding. R/O hyperplasia or malignancy	Secretory endometrium
Bx_35	29	Menorrhagia, R/O hyperplasia	Menstrual endometrium
Bx_36	29	infertility	progesterone treatment changes
Bx_37	29	Infertility, R/O luteal phase defect	secretory endometrium
Bx_38	29		proliferative endometrium
Bx_39	34	Synechia seen in office hysteroscopy	mid secretory
Bx_40	34	Abnormal bleeding on Estrace plus Lupron	disordered proliferative
Bx_41	35	known fibroids plus menorrhagia	weakly proliferative
Bx_42	39	infertility	late secretory
Bx_43	39	abnormal bleeding and endometrial polyp	inactive
Bx_44	40	Infertility, endometrial synechiae, submucosal fibroid	disordered proliferative
Bx_45	43		Mildly disordered proliferative endometrium
Bx_46	43	menorrhagia	late secretory

Patient ID	Age (years)	Clinical History	Endometrium Phase
Bx_47	43		Irregular secretory endometrium
Bx_48	44		Endometrium showing changes secondary to progestational
Bx_49	44		Secretory endometrium
Bx_50	44	Menorrhagia	Irregular secretory endometrium
Bx_51	46		Proliferative endometrium
Bx_52	46		Menstrual endometrium
Bx_53	49	Abnormal bleeding, fibroids	inactive
Bx_54	50	Abnormal uterine bleeding	Proliferative endometrium
Bx_55	50	Abnormal uterine bleeding	Secretory endometrium
Bx_57	51	Heavy menstrual bleeding	Weakly proliferative
Bx_58	51	Abnormal uterine bleeding, Pretreatment with Ulipristal	proliferative endometrium
Bx_59	51		secretory
Bx_60	51	menorrhagia	irregular secretory
Bx_61	52	menorrhagia	disordered proliferative
Bx_62	53	Postmenopausal bleeding	disordered proliferative endometrium
Bx_63	53	Abnormal bleeding	weakly proliferative
Bx_64	55	Heavy bleeding	late secretory endometrium
Bx_65	55	Perimenopausal bleeding, fibroids	Proliferative endometrium

Patient ID	Age (years)	Clinical History	Endometrium Phase
Bx_66	56	intermenstrual spotting. R/O hyperplasia or malignancy	Proliferative endometrium
Bx_67	61	PMB on HRT	Weakly proliferative

Appendix G: Summary of somatic cancer-driver events in Hx patients.

Patient ID	Block ID and Descriptor	Driver Mutation Identified	PTEN IHC	ARID1A IHC
Hx_1	A:		+	+
	B:		+	+
Hx_2	A: anterior		+	+
	B: posterior	ERBB2 S310F	+	+
Hx_3	A:		+	+
	B:		+	+
Hx_4	A:		H	+
	B:		+	+
Hx_5	A:		H	+
	B:		+	+
Hx_6	A: anterior	KRAS G12V	+	+
	B: posterior	KRAS G12A	+	+
Hx_7	A:		H	+
	B:		+	+
Hx_8	A:		H	+
	B:		H	+
Hx_9	A: anterior		+	+
	B: posterior	KRAS G13D	H	+
Hx_10	A:		+	+
	B:		H	+
Hx_11	A:		+	+
	B:		+	+
Hx_12	A: anterior	PIK3CA R88Q	+	+
	B: posterior	ERBB2 S310F	+	+

Patient ID	Block ID and Descriptor	Driver Mutation Identified	PTEN IHC	ARID1A IHC
Hx_13	A: posterior	PIK3CA H1047R, KRAS G12C	+	+
	B: anterior		+	+
Hx_14	A:		+	+
	B:		+	+
Hx_15	A:		+	+
	B:		+	+
Hx_16	A: anterior	KRAS G12V, PIK3CA E542K	+	+
	B: posterior	PIK3CA H1047R	H	+
Hx_17	A:		+	+
	B:		+	+
Hx_18	A: anterior	FGFR2 K659E, KRAS G12V	+	+
	B: posterior		H	+
Hx_19	A:		+	+
	B:		+	+
Hx_20	A:		+	+
	B:		+	+
Hx_21	A: anterior	KRAS G12D, PIK3CA M1043I	+	+
	B: posterior	KRAS G12V, PIK3CA H1047R, FGFR2 S252W	+	+
Hx_22	A: anterior		H	+

Patient ID	Block ID and Descriptor	Driver Mutation Identified	PTEN IHC	ARID1A IHC
	B: posterior	KRAS G12D	N/A	+
Hx_23	A: anterior		FAILED	+
	B: posterior		+	+
Hx_24	A: anterior	FGFR2 S252W	+	+
	B: posterior		+	+
Hx_25	A: N/A	KRAS G12A	+	+
	B: N/A	KRAS G12A	H	+

Appendix H: Summary of somatic cancer-driver events in Bx patients.

Patient ID	Driver Mutation Identified	PTEN IHC	ARID1A IHC
Bx_1	none identified	+	+
Bx_2	none identified	+	+
Bx_3	KRAS G12A	+	+
Bx_4	none identified	+	+
Bx_5	PIK3CA H1047R	H (min)	+
Bx_6	KRAS G12C, KRAS G12D	+	+
Bx_7	none identified	+	+
Bx_8	FGFR2 S252W	+	+
Bx_9	KRAS G12D	H (min)	+
Bx_10	none identified	H	+
Bx_11	none identified	+	+
Bx_12	KRAS G12V, PIK3CA H1047R	+	+
Bx_13	KRAS G12D	H (min)	+
Bx_14	none identified	+	+
Bx_15	KRAS G12V	+	+
Bx_16	NRAS G13D, PIK3CA E545K	H	+
Bx_17	none identified	+	+
Bx_18	KRAS G12D	+	+
Bx_19	none identified	+	+
Bx_20	none identified	+	+
Bx_21	KRAS G12V, NRAS Q61R	+	+
Bx_22	KRAS G12D	+	+
Bx_23	FGFR2 S252W	+	+
Bx_24	none identified	+	+
Bx_25	none identified	+	+

Patient ID	Driver Mutation Identified	PTEN IHC	ARID1A IHC
Bx_26	none identified	H	+
Bx_27	none identified	+	+
Bx_28	none identified	+	+
Bx_29	none identified	+	+
Bx_30	none identified	+	+
Bx_31	none identified	+	+
Bx_32	none identified	+	+
Bx_33	none identified	+	+
Bx_34	none identified	H	+
Bx_35	AKT1 E17K	+	+
Bx_36	none identified	+	+
Bx_37	KRAS G12D	+	+
Bx_38	none identified	+	+
Bx_39	none identified	+	+
Bx_40	KRAS G12A	+	+
Bx_41	none identified	+	+
Bx_42	none identified	+	+
Bx_43	none identified	H	+
Bx_44	none identified	+	+
Bx_45	none identified	H	+
Bx_46	FGFR2 S252W; PIK3CA E542K; PIK3CA H1047R	+	+
Bx_47	none identified	+	+
Bx_48	none identified	+	+
Bx_49	none identified	H	+
Bx_50	PIK3CA G1049S	H	+
Bx_51	PIK3CA H1047R	+	+

Patient ID	Driver Mutation Identified	PTEN IHC	ARID1A IHC
Bx_52	KRAS G12D	+	+
Bx_53	KRAS G12D; PIK3CA E545K; PIK3CA R88Q	+	+
Bx_54	none identified	H	+
Bx_55	none identified	+	+
Bx_57	none identified	+	+
Bx_58	PIK3CA H1047R	+	+
Bx_59	none identified	+	+
Bx_60	KRAS G12V	+	+
Bx_61	KRAS G12D	H	+
Bx_62	none identified	+	+
Bx_63	none identified	+	+
Bx_64	KRAS G12D	+	+
Bx_65	CTNNB1 T41I; KRAS G12V	+	+
Bx_66	none identified	+	+
Bx_67	KRAS G12D	+	+

Appendix I: Is the Presence of Somatic Cancer-Driver Events in Deep Infiltrating Endometriosis Associated with Deep Dyspareunia?

As discussed in Chapter 1, endometriosis represents a substantial burden to women affected by the disease. Among other symptoms, approximately half of women with DE suffer from deep dyspareunia (defined as pelvic pain with intercourse)[120,121]. Deep dyspareunia has profound negative impact on the quality of life of affected women and relationship with partners (resulting from the avoidance of sexual activity)[122] . However, the phenotype of deep dyspareunia is clinically heterogeneous and is seldom accounted for by endometriosis alone – for instance, one woman with cul-de-sac endometriosis may have severe dyspareunia, whereas another woman with endometriosis at the same site may exhibit minimal/no pain[121]. This heterogeneity may be partly explained by differences in the extent of macrophage infiltration of endometriotic lesions and/or nerve bundle density. A recent study has shown that interleukin (IL)-1B stimulates brain-derived neurotrophic factor (BDNF) production by endometriotic stromal cells *in vitro* – a growth factor known to stimulate nerve growth and angiogenesis[123]. Moreover, compared to women without deep dyspareunia, women with deep dyspareunia have increased local PGP9.5 nerve bundle density around endometriotic lesions[124]. This local nerve bundle density may interact with other biological factors (e.g. inflammation) or psychological factors to produce this heterogeneity in deep dyspareunia among patients. Nevertheless, an understanding of contributing factors to deep dyspareunia and potential therapeutic strategies for such symptoms is still lacking.

In Chapter 3, I found that 36.1% of DE cases examined harboured a somatic cancer-driver event. It is plausible that such somatic alterations could help distinguish/stratify patients with severe deep dyspareunia (which will herein be referred to as “high-pain” patients) and those with minimal or no pain (which will herein be referred to as “low-pain” patients).

Methods

Analyses generally follows the methodology described in Chapter 2 (Methodology) and the additional details described specifically in Chapter 3 (Somatic Cancer-Driver Mutations in Incisional Endometriosis). For the purposes of this appendix, the DE women we studied were classified as follows:

Patient Classification

We identified 28 women with DE (including 20/23 women from the BC Women's cohort described in Chapter 3 (see section 3.1.8)) and collected deep dyspareunia data for each woman based on a self-report pelvic pain questionnaire by The International Pelvic Pain Society or an in-house questionnaire wherein the question regarding deep dyspareunia was similar (referred to as "pain with deep penetration") (see Appendix J). In short, women were asked to rate the extent of deep pain with intercourse from 0 (no pain) – 10 (worse pain imaginable). Initially, women with a pain score ≥ 7 were classified as "high-pain" whereas women with a pain score of ≤ 3 were classified as "low-pain". However, in order to increase the number of cases included in the low-pain cohort, we extended low-pain criteria to a pain score of ≤ 5. The breakdown of the deep dyspareunia classification of women with DE included in this sub-analysis is summarized below in Fig. 1:

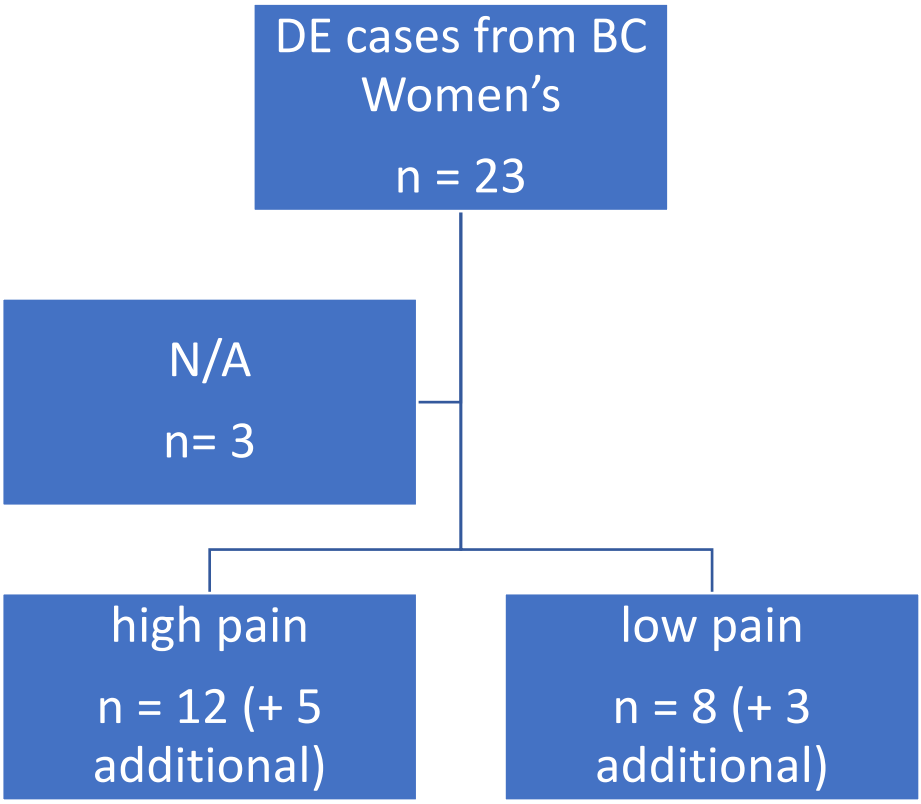

Figure 1: Breakdown of DE cases included in deep dyspareunia study. "N/A" refers to women wherein deep dyspareunia data was unavailable.

Results

Sample Description

As described in Chapter 3, I examined women with DE for somatic cancer-driver events by targeted sequencing (with orthogonal validation by means of ddPCR) as well as ARID1A and PTEN IHC. A summary of clinical data relevant to this study and somatic alterations found is provided below in Table 1. It is important to note that some women had multiple DE lesions at anatomically distinct/separated sites, which were collected and analyzed if available. For the purposes of the deep dyspareunia study, I focused solely on the binary variable (i.e. yes or no) of whether at least one somatic alteration was found, either through hotspot sequencing or inferred from IHC findings, in at least one of the lesions analyzed from a given patient.

Table 1: Summary of clinical data for DE women included in deep dyspareunia study. Mutations noted with (*) have not yet been orthogonally validated by ddPCR.

Patient ID	**Age (years)**	**Clinical Stage (r-ASRM)**	**Deep Dyspareunia Classification**	**Pain Score**	**Somatic Alteration**
DE_1	41	IV	low	4	CTNNB1 G34V
DE_2	50	IV	high	9	KRAS G12D
DE_4	28	IV	high	9	None identified
DE_5	25	III	high	8	KRAS G12D
DE_6	34	IV	high	9	None identified
DE_7	41	IV	low	4	ARID1A – loss
DE_10	27	III	high	10	KRAS G12V
DE_11	27	II	high	9	KRAS G12D
DE_12	39	IV	high	10	None identified
DE_13	26	III	high	8	PTEN – loss
DE_14	22	I	high	8	KRAS G12C
DE_15	49	IV	high	7	PTEN – loss
DE_16	36	IV	high	7	None identified
DE_17	32	III	low	0	PTEN – loss
DE_18	36	IV	high	9	None identified
DE_19	38	III	low	0	None identified
DE_20	45	IV	low	1	None identified
DE_21	44	III	low	0	KRAS G12V; PTEN – loss
DE_22	24	III	low	0	None identified
DE_23	35	III	low	0	PTEN – loss
DE_37	35	IV	high	8	None identified

DE_38	43	II	high	10	KRAS G12D*; PTEN – loss
DE_40	36	II	high	10	None identified
DE_42	27	I	high	9	None identified
DE_43	29	III	high	8	None identified
DE_45	25	IV	low	5	None identified
DE_46	39	III	low	4	None identified
DE_47	25	III	low	5	PIK3CA E545K*

The mean age of women with DE in the “low-pain” group is 35.4 years (range: 24-45 years), whereas the mean age of women in the “high-pain” group is 33.5 years (range: 22-50 years) (Table 1; Fig. 2). The mean age of women in these two groups is not statistically different (p = 0.5503, Student’s t-test) (Fig. 2).

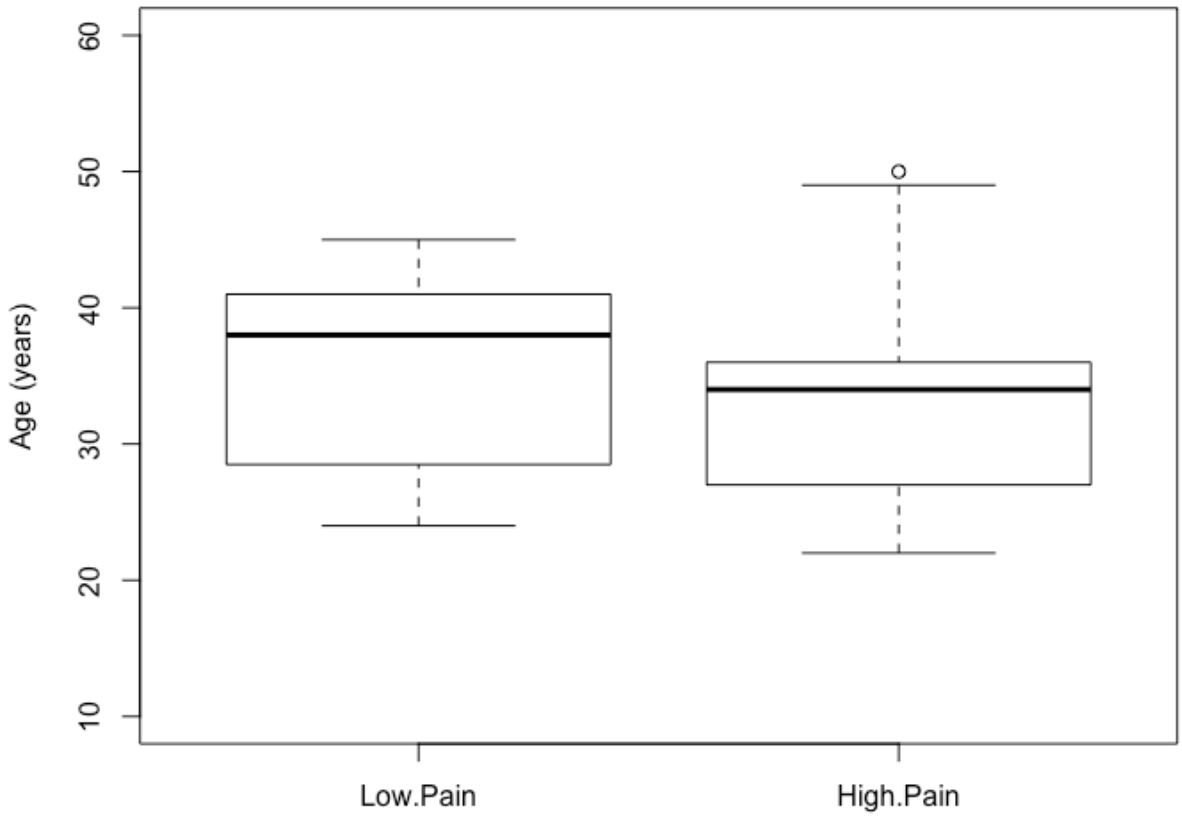

Figure 2: Mean age of DE women included in deep dyspareunia study. The difference in age of women in the low-pain and high-pain groups is not statistically significant (p = 0.5503, Student's t-test).

The clinical stage of endometriosis (according to r-ASRM) was provided for women with DE included in this study. The stage of endometriosis is also independent of whether patients experienced high or low pain in regards to deep dyspareunia (p = 0.13252, Fisher's exact test).

Mutation Rates According to Deep Dyspareunia Severity

Overall, 47.1% (8/17) high-pain and 54.5% (6/11) low-pain patients harboured a somatic alteration within their DE lesions (Fig. 3). The breakdown of mutations according to gene affected is provided in Fig. 3 (note that alterations in PTEN and ARID1A were determined *via* IHC findings).

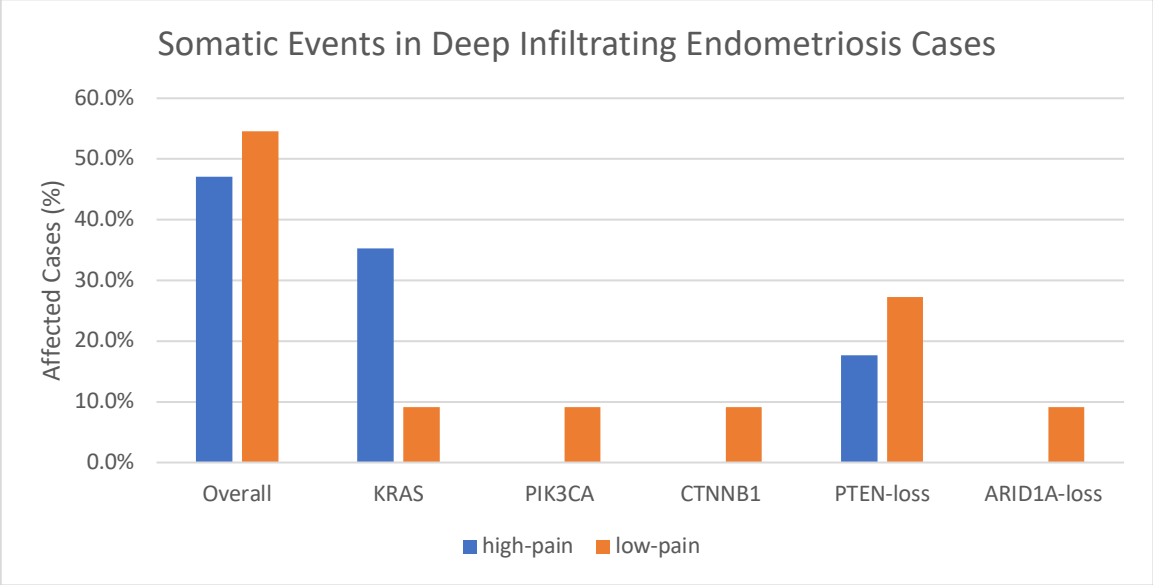

Figure 3: Breakdown of rates of somatic cancer-driver events by gene for high-pain and low-pain patients.

To determine whether overall somatic events or gene-specific somatic events were associated with either high-pain or low-pain groups, I performed Fisher's exact tests on each pairwise comparison of interest. All tests were two-sided, where a *P*-value <0.05 was considered to be statistically significant. The *P*-value for each pairwise comparison is shown below in Table 2.

Table 2: Reported P-values for pairwise comparisons of somatic events affecting specific genes in patients with high-pain and low-pain.

Pairwise Comparison	high pain patients affected	low pain patients affected	*P*-value
Overall Affected	8/17	6/11	1.0000
KRAS	6/17	1/11	0.1914
PIK3CA	0/17	1/11	0.3929
CTNNB1	0/17	1/11	0.3929
PTEN-loss	3/17	3/11	0.6525
ARID1A-loss	0/17	1/11	0.3929

As shown in Table 2, all P-values were > 0.05 and therefore the rates of somatic events (both overall and affecting each gene specifically) did not significantly differ among high-pain or low-pain patients. *KRAS* mutations appear to be more common in high-pain patients (occurring in 6/17 high-pain patients compared to 1/11 low-pain patients), however this observation is not statistically significant given our small sample size (p = 0.1914).

To better assess the relationship between the likelihood of harbouring a somatic alteration (regardless of gene since sample sizes are insufficiently large for gene-specific mutational analysis) in DE lesions and deep dyspareunia pain scores, I performed a logistic regression analysis with pain scores as a continuous variable (rather than as discrete high-pain and low-pain groups) (see Figure 4 below). Given our sample sizes, the likelihood of harbouring a somatic alteration does not appear to be associated with pain scores (p = 0.71, Wald Test).

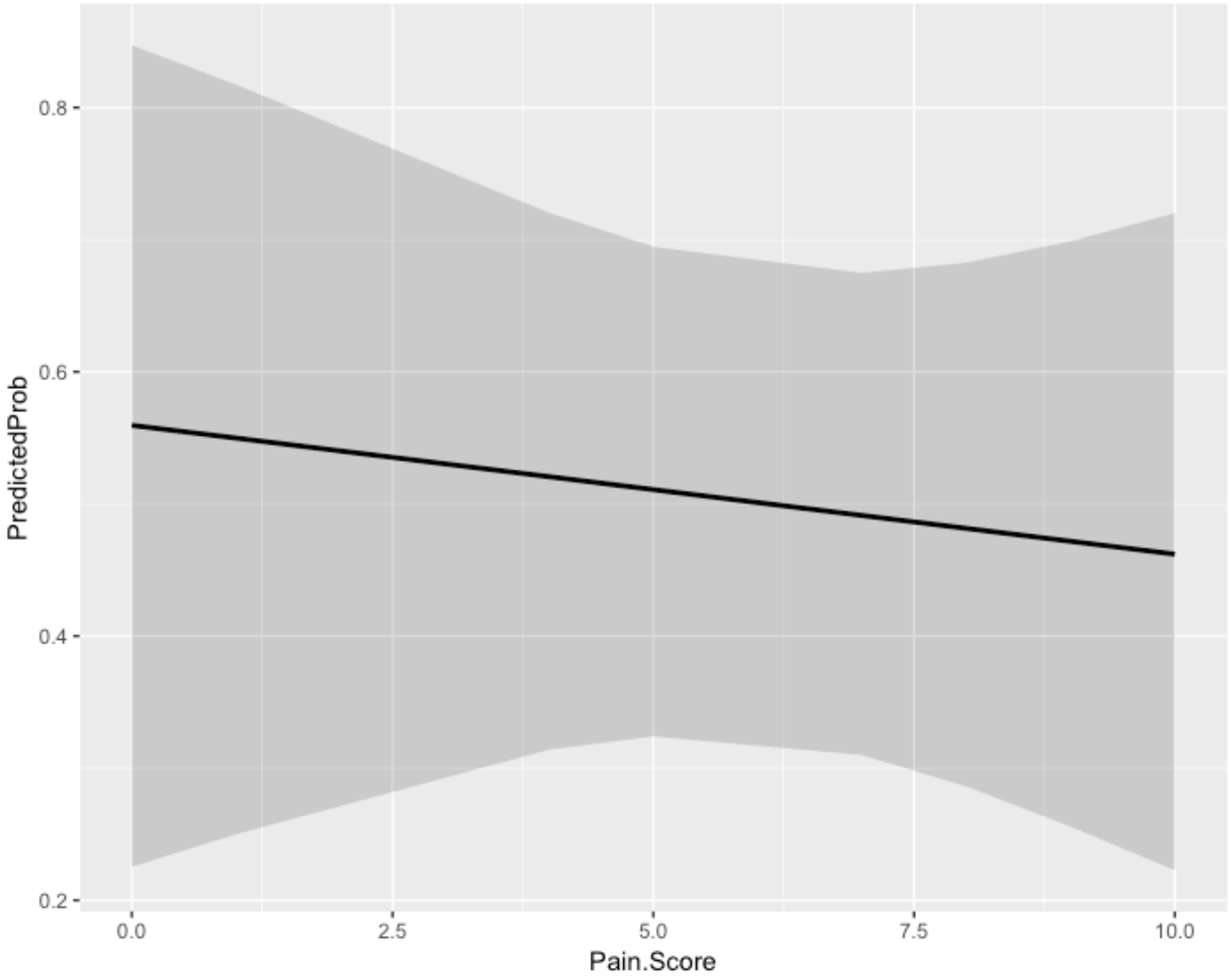

Figure 4: Logistic regression model illustrating the likelihood of harbouring a somatic cancer-driver alteration in DE lesions given self-reported deep dyspareunia pain scores. The shaded regions represent 95% confidence intervals for the likelihood of harbouring somatic cancer-driver events at each pain score.

Discussion

The analysis in Chapter 3 revealed that overall one-third of DE patients harboured detectable somatic cancer-driver events within their endometriotic lesions. This observation prompts speculation over the role of such alterations within endometriosis. Specifically, are there any phenotypic differences between patients harbouring such somatic events in endometriosis? Exploring such questions may enhance our understanding of endometriosis pathophysiology and are potentially useful for the clinical

management of disease (*via* targeted therapies). Deep dyspareunia continues to be a prevailing issue for women with DE – greatly affecting one's self-esteem and relationship with others. In this exploratory sub-analysis, I sought to interrogate whether the presence of somatic cancer-driver events within DE lesions could be used to distinguish patients with severe deep dyspareunia ("high-pain") from those with minimal/no pain ("low-pain").

With consideration of our small sample sizes with respect to patients with high-pain (17 women) and low-pain (11 women), no somatic event was significantly enriched in either the high-pain or low-pain groups. Note that this exploratory sub-analysis is intended to be hypothesis-generating and a larger, prospectively collected cohort with detailed clinicopathological data is being collected and has recruited over 250 women. Based on this sub-analysis, of all genes wherein somatic mutations have been detected, *KRAS* appears to be the most enriched in the high-pain group (p = 0.1914), with 6/17 (47.1%) of high-pain patients and 1/11 (9.1%) of low-pain patients harbouring a *KRAS* mutation in their DE lesions. Evidence suggests that there is a correlation between elevated concentration of inflammatory cytokines (especially TNF-α and glycodelin) and daily/chronic pain in endometriosis patients as well as greater central sensitization[125,126] – such cytokines may enhance local nerve growth and angiogenesis, thereby potentially contributing to deep dyspareunia[127,128]. Oncogenic *KRAS* may influence inflammatory cytokine production in endometriosis as this has been observed in early progression models of other diseases including pancreatic cancer and gastric cancer (wherein *KRAS* mutations are frequently observed)[129,130] . In support of this hypothesis, Cheng et al. (2011) developed an immunocompetent mouse model of endometriosis by transplanting endometrium from *KRAS*$^{G12V/+}$ donor mice into subcutaneous, abdominal pockets of immunocompetent recipient mice and observed numerous leukocytes and macrophages around endometriotic lesions (which would contribute to inflammatory cytokine production including TNF-α)[106]. Oncogenic *KRAS* may also contribute to deep dyspareunia directly by causing a greater depth of invasion of local tissue by endometriotic lesions. Although this has not been studied in endometriosis, studies suggest that oncogenic *KRAS* drives invasion in colorectal cancer[131].

In short, assuming these rates of *KRAS* mutation are reflective of the true incidence of *KRAS* mutations among high-pain and low-pain patients (as defined by our pain score cut-offs), then at least 38 high-pain and 38 low-pain patients are required in the prospective study to show a statistical significance in the difference in *KRAS* mutation rates among the two groups at 80% power and a significance level of 0.05.

Appendix J: Pelvic Pain Assessment Form

Patient Label

BC WOMEN'S HOSPITAL & HEALTH CENTRE
An Agency of the Provincial Health Services Authority

Questionnaire # 1
(Initial visit)

Pelvic Pain Questionnaire

BC Women's Centre for Pelvic Pain
& Endometriosis,
Women's Health Centre, D6 – 4500 Oak Street
Vancouver, B.C., V6H 3N1
Phone: (604)875-2445 Fax:(604)875-2569

Date : _____

Please describe the pain you have been experiencing?

_____

_____

_____

Please shade areas of pain and write a number from 1-10 at the site(s) of pain
(10 = most severe pain imaginable)

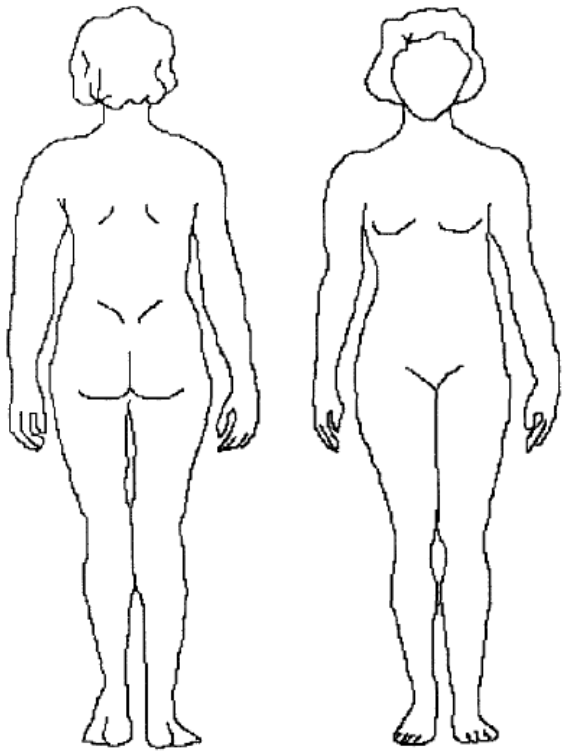

Left Right Right Left

Pain History:

How old were you when you first experienced pelvic pain? _____

Did the pelvic pain become worse at some point? No ☐ Yes ☐

If yes; when? _____

If yes; what triggered it? _____

Have you **ever** had **painful menstrual cramps when bleeding**?

No ☐ Yes ☐

If **Yes**, how **painful** were your **menstrual cramps when bleeding**?

Least pain	0	1	2	3	4	5	6	7	8	9	10
Average pain	0	1	2	3	4	5	6	7	8	9	10
Worst pain	0	1	2	3	4	5	6	7	8	9	10

1. Check **any** of the following health care providers you have seen in the past for this pain:

☐ Anesthesiologist ☐ Gynecologist ☐ Gastroenterologist
☐ General surgeon ☐ Urologist ☐ Neurosurgeon
☐ Rheumatologist ☐ Psychiatrist ☐ Psychologist/Counsellor
☐ Psychotherapist ☐ Rehabilitation Medicine specialist

2. Check **any** of the Complementary Medicine providers you have seen in the past for this pain:

☐ Homeopathic medicine ☐ Naturopathic medicine ☐ Biofeedback
☐ Massage therapist ☐ Physical therapy / physiotherapy
☐ Acupuncturist ☐ Chiropractor ☐ Hypnosis

3. Which of the following diagnosis, if any, have you been given for your pain (check all that apply)?

☐ Endometriosis
☐ Pelvic Adhesions
☐ Pelvic Infection/vaginal infection
☐ Irritable Bowel Syndrome
☐ Bladder Pain/ Interstitial Cystitis
☐ Vestibulitis/vulvodynia
☐ Vaginismus/pelvic floor muscle problem
☐ Other muscle problem
☐ Nerve entrapment
☐ Stress/ anxiety
☐ Depression
☐ None of the above

4. Medical treatments

- Column 1: lists available medical treatments for pelvic pain
- Column 2: Check the treatments that you tried before, but didn't help
- Column 3: Check the treatments that you tried before, but had problems with side-effects
- Column 4: Check the treatments that you have tried before and did help
- Column 5: Check the treatments that you are trying now
- Column 5: Check the treatments that you would like to try
- Column 6: Check the treatments that you do not want to try
- Column 7: Check if you don't know what the treatment is
- Column 8: Circle how confident are you that the treatment will help your pelvic pain. (If you don't know what the treatment is, you can skip this step.)

[Can choose more than one]

1	2	3	4	5	6	7	8	9
Treatments for pelvic pain	**Tried before but did NOT help**	**Tried before but side effects**	**Tried before and did help**	**Trying now**	**I would like to try**	**I would NOT like to try**	**I don't know what this is**	**How confident are you this treatment will help your pain? 0……10 Not at all Strongly confident**
Tylenol, Advil, other anti-inflammatories (e.g. Ponstan, Voltaren)								0 1 2 3 4 5 6 7 8 9 10
Opioids/narcotics (e.g. Tylenol #3, Tramacet, oxycodone, morphine)								0 1 2 3 4 5 6 7 8 9 10
Birth control pill or patch or ring (w/ monthly period)								0 1 2 3 4 5 6 7 8 9 10
Hormone treatment to stop periods:								
Continuous birth control pill or patch or ring								0 1 2 3 4 5 6 7 8 9 10
Progestin (Depo Provera, Norlutate, Visanne)								0 1 2 3 4 5 6 7 8 9 10
Mirena IUD								0 1 2 3 4 5 6 7 8 9 10
GnRH agonist (Lupron, Synarel)								0 1 2 3 4 5 6 7 8 9 10
Other treatments:								
Vaginal medications (e.g. danazol, diazepam)								0 1 2 3 4 5 6 7 8 9 10
Nerve medications (e.g. nortriptyline, gabapentin/Neurontin, pregabalin/Lyrica)								0 1 2 3 4 5 6 7 8 9 10
Surgery								0 1 2 3 4 5 6 7 8 9 10
Physiotherapy								0 1 2 3 4 5 6 7 8 9 10
Trigger point injections with local anesthetic								0 1 2 3 4 5 6 7 8 9 10
Nerve blocks								0 1 2 3 4 5 6 7 8 9 10

Botox injections								0 1 2 3 4 5 6 7 8 9 10
Dry needling or intra-muscular stimulation (IMS)								0 1 2 3 4 5 6 7 8 9 10
Neuro-prolotherapy								0 1 2 3 4 5 6 7 8 9 10
Small groups (Mindfulness, cognitive-behavioral therapy)								0 1 2 3 4 5 6 7 8 9 10
Individual counselling (Mindfulness, cognitive-behavioral therapy)								0 1 2 3 4 5 6 7 8 9 10
Education session (online)								0 1 2 3 4 5 6 7 8 9 10
Education session (in-person, i.e. "Meet the Team" session								0 1 2 3 4 5 6 7 8 9 10
Other _____								0 1 2 3 4 5 6 7 8 9 10

5. If you have had **surgery** in the past, please check all surgeries that apply and how many times:

	Laparoscopy (scope)	Laparotomy (open cut/incision)
Diagnostic only (no treatment)	#/dates	#/dates
Cautery of endometriosis	#/dates	#/dates
Excision of endometriosis	#/dates	#/dates
Lysis (cutting) of adhesions	#/dates	#/dates
Removal of ovarian cysts	#/dates	#/dates
Hysterectomy (removal of uterus)	date	date
Removal of right ovary	date	date
Removal of left ovary	date	date
Removal of both ovaries (at same time)	date	date

Please rate your pain from: **0 (no pain) to 10 (worst pain imaginable)**

1) **IN THE PAST 3 MONTHS**, about how many days have you had menstrual (vaginal) bleeding?

0 1-10 10-20 20-40 40-60 60-80 >80

2) **IN THE PAST 3 MONTHS**, how **painful** were your **menstrual cramps when bleeding**?

No bleeding ☐

Least pain	0	1	2	3	4	5	6	7	8	9	10
Average pain	0	1	2	3	4	5	6	7	8	9	10
Worst pain	0	1	2	3	4	5	6	7	8	9	10

[Least/average/worst amount of pain with menstrual cramps when bleeding]

3) **IN THE PAST 3 MONTHS**, how **painful** was **deep penetration** during sexual activity?

No penetration ☐

Least pain	0	1	2	3	4	5	6	7	8	9	10
Average pain	0	1	2	3	4	5	6	7	8	9	10
Worst pain	0	1	2	3	4	5	6	7	8	9	10

4) **IN THE PAST 3 MONTHS**, how **painful** was **initial penetration (entry)** during sexual activity? ☐

No penetration

Least pain	0	1	2	3	4	5	6	7	8	9	10
Average pain	0	1	2	3	4	5	6	7	8	9	10
Worst pain	0	1	2	3	4	5	6	7	8	9	10

5) **IN THE PAST 3 MONTHS**, how **painful** were **bowel movements**?

Least pain	0	1	2	3	4	5	6	7	8	9	10
Average pain	0	1	2	3	4	5	6	7	8	9	10
Worst pain	0	1	2	3	4	5	6	7	8	9	10

6) **IN THE PAST 3 MONTHS**, how painful was **other pelvic pain** (***that is, pelvic pain when not bleeding, not during sexual activity, and not during bowel movements)***

Least pain	0	1	2	3	4	5	6	7	8	9	10
Average pain	0	1	2	3	4	5	6	7	8	9	10
Worst pain	0	1	2	3	4	5	6	7	8	9	10

Where is this other pelvic pain located? Right ☐ Left ☐ Both sides ☐

Not applicable ☐

Does this other pelvic pain get **worse at certain times of your menstrual cycle**?

Yes ☐ No ☐ Not applicable ☐

7) **IN THE PAST 3 MONTHS**, have you had **back pain**?

Least pain	0	1	2	3	4	5	6	7	8	9	10
Average pain	0	1	2	3	4	5	6	7	8	9	10
Worst pain	0	1	2	3	4	5	6	7	8	9	10

Where is this back pain located? Right ☐ Left ☐ Both sides ☐

Not applicable ☐

Does this back pain get **worse at certain times of your menstrual cycle**?

Yes ☐ No ☐ Not applicable ☐

Does your pain have one or more of the following characteristics?

Burning	Yes ☐	No ☐
Painful cold	Yes ☐	No ☐
Electric shocks	Yes ☐	No ☐

Is your pain associated with one or more of the following symptoms in the same area?

Tingling	Yes ☐	No ☐
Pins and needles	Yes ☐	No ☐
Numbness	Yes ☐	No ☐
Itching	Yes ☐	No ☐

In trying to deal with your pain, in the **PAST 3 MONTHS**, how many times have you:

1. Been to a physician's office (other than this clinic)? _____
2. Been to the emergency room? _____

<u>Bowels</u>

Do you have pain or discomfort (at least 3 days of the month, for at least 3 months, starting at least 6 months before this visit) that is associated with the following:

Change in frequency of bowel movement?	Yes ☐	No ☐
Change in appearance of stool or bowel movement?	Yes ☐	No ☐
Does your pain improve after completing a bowel movement?	Yes ☐	No ☐
Do these symptoms get worse at certain times of your menstrual cycle?	Yes ☐	No ☐

Bladder

Do you have an unpleasant sensation (e.g. pain, pressure, discomfort) that seems related to the bladder (lasting at least 6 weeks)?	Yes ☐	No ☐
Does the pain worsen as your bladder fills up?	Yes ☐	No ☐
Does the pain improve when you urinate?	Yes ☐	No ☐
Do you have a strong need (urge) to urinate because of the pain?	Yes ☐	No ☐
Do you urinate more often than in the past?	Yes ☐	No ☐
Do these symptoms get worse at certain times your menstrual cycle?	Yes ☐	No ☐